UNLOADING OF INTERCEPTED SNOW IN CONIFER FORESTS

A thesis submitted to the
College of Graduate Studies and Research
in partial fulfillment of the requirements for the
degree of Master of Science
in the Department of Geography & Planning
University of Saskatchewan
Saskatoon

By

James P MacDonald

PERMISSION TO USE

In presenting this thesis in partial fulfillment of the requirements for a Master's of Science degree from the University of Saskatchewan, I agree that the libraries of this University may make it freely available for inspection. I further agree that the permission for copying of this thesis in any manner, in whole or in part, for scholarly purposes may be granted by the professor who supervised my thesis work or, in their absence, by the Head of Department or the Dean of the College in which my thesis work was done. It is understood that any copying or publication or use of this thesis or parts thereof for financial gain shall not be allowed without my written permission. It is also understood that due recognition shall be given to me and to the University of Saskatchewan in any scholarly use which may be made of any material in my thesis.

DISCLAIMER

Reference in this thesis to any specific commercial products, process, or service by trade name, trademark, manufacturer, or otherwise, does not constitute or imply its endorsement, recommendation, or favouring by the University of Saskatchewan. The views and opinions of the author expressed herein do not state or reflect those of the University of Saskatchewan, and shall not be used for advertising or product endorsement purposes.

Requests for permission to copy or to make other uses of materials in this thesis in whole or part should be addressed to:

Head of the Department of Geography & Planning
University of Saskatchewan
Saskatoon, Saskatchewan S7N 5C8
Canada

ABSTRACT

Snowfall interception is particularly important to the hydrology of forested cold regions. Unloading of intercepted snow controls the snow available for interception loss due to sublimation from that held in the canopy. This thesis seeks to determine the factors that affect the magnitude and timing of unloading at the forest-stand scale. A field program was established that measured interception and unloading at a forest-stand scale using a series of hanging lysimeters and a 7 m tall spruce tree suspended, *in-situ*, on a load-cell. Meteorological conditions including snowfall, wind speed, air temperature, and incoming radiation were recorded above and below the forest canopy. Unloading did not behave as described by current unloading models. It was observed to be triggered by occurrences of wind gusts or melt conditions within the canopy but no trends were found in the measurements that could be used to predict the onset of unloading from gusts or air temperature alone. An association between intercepted snow sublimation and unloading was found and this relationship was further found to be an exponential function of air temperature. An expression based on this empirical model can be used to calculate unloading as a function of sublimation rate in hydrological models or to calculate unloading directly as a function of canopy snow load and air temperature.

ACKNOWLEDGEMENTS

The success of my thesis is largely attributed to the continued support and of banter with my scientific mentor and supervisor, John Pomeroy. Not once would he let me give in to frustration, but made me pursue a solution to every road block. Also in need of mention, are the many friends and co-workers who helped me along the way. Notably, is Michael Solohub for his hours put in alongside or in my absence, in the backcountry, as well as the hours we spent deliberating over my field site and scientific process. It was a long and windy road, but I wanted to maximize my experience.

TABLE OF CONTENTS

PERMISSION TO USE **1**

ABSTRACT **2**

ACKNOWLEDGEMENTS **3**

TABLE OF CONTENTS **4**

LIST OF TABLES **6**

LIST OF FIGURES **6**

LIST OF SYMBOLS **8**

1.0 INTRODUCTION **10**

2.0 LITERATURE REVIEW **12**

2.1 Interception Processes 12
2.2 Unloading of Intercepted Snow 17
2.3 Resuspension of intercepted snow: missing quantities? 18
2.4 Forest Parameters 18
2.5 Current Interception and Unloading Models 20
2.6 Research Gap 26

3.0 RESEARCH OBJECTIVES **28**

3.1 Objectives 28
3.2 Hypotheses 28

4.0 EXPERIMENTAL DESIGN **30**

4.1 Experimental Site 30
4.2 Data Collection 35
4.3 Evaluation of Model Performance 41

5.0 RESULTS **43**

5.1 Data Survey 43
5.2 Unloading Events 49

6.0 ANALYSIS **52**

6.1 Interception evaluation 52
6.2 Unloading Model Intercomparison 55
6.3 Unloading in Marmot Creek Research Basin 62
6.4 Model performance of the $\Sigma U/\Sigma S$ ratio 74

7.0 SUMMARY & CONCLUSIONS **78**

8.0 REFERENCES **81**

APPENDIX A – INSTRUMENT CALIBRATIONS **85**

APPENDIX B – UNLOADING MODEL INTERCOMPARISON DATA **87**

LIST OF TABLES

Table 4.1 Instrument locations and heights..... 34
Table 5.1 Winter 06/07 and 07/08 snowfall unloading event data..... 51
Table 6.1 Hedstrom and Pomeroy (1998) model output for unloading events..... 58
Table 6.2 Bartlett et al. (2006) modeled unloading..... 60
Table 6.3 Linear relationship between ΣU and ΣS for unloading events..... 69
Table 6.4 Unloading model output comparative statistics..... 77

LIST OF FIGURES

Figure 1.1 Interception losses in the boreal forest of Prince Albert National Park..... 11

Figure 2.1 Forest Snowfall Interception process displayed as a control volume..... 15

Figure 4.1 Marmot Creek Research Basin (MCRB) forest canopy unloading site..... 31

Figure 4.2 Upper Forest study site..... 33

Figure 4.3 Processing of hemispherical photos for the Gap Light Analyzer (GLA)..... 36

Figure 4.4 Upper Clearing study site..... 37

Figure 4.5 Hanging lysimeter apparatus..... 39

Figure 4.6 Calibration of hanging-tree lysimeter canopy load measurements..... 41

Figure 5.1 Upper Forest characteristics..... 44

Figure 5.2 Snow accumulation, winter 06/07 (a) and 07/08 (b)..... 46

Figure 5.3 Winter 06/07 (a) and 07/08 (b) average daily temperature and wind speed..... 47

Figure 5.4 Sub-canopy snowfall and snowfall in Marmot Creek Research Basin..... 48

Figure 5.5 Snowfall interception event February 18, 2007..... 49

Figure 5.6 Unloading of intercepted snow: March 20-22, 2007..... 52

Figure 6.1 Interception (a) and net interception (interception-unloading) (b) compared to snowfall during the winters of 06/07 and 07/08..... 53

Figure 6.2 Unloading versus canopy load in MCRB..... 54

Figure 6.3. Subcanopy snow accumulation at the three subcanopy hanging-lysimeters in MCRB winter 06/07 (a) and 07/08 (b)..... 55

Figure 6.4 Interception model comparison to observations..... 57

Figure 6.5 Relationship of forest albedo to canopy load at MCRB (SWE)..... 59

Figure 6.6 Bartlett et al. (2006) cumulative unloading model output for a 07/08 event..... 61

Figure 6.7 Unloading time series using the Roesch et al. model for a 07/08 event..... 63

Figure 6.8 Unloading as a function of average-daily canopy air temperature..... 64

Figure 6.9 Relationship between unloading and canopy air temperature..... 65

Figure 6.10 Relationship between unloading and wind speeds..... 66

Figure 6.11 Relationship between unloading and storage time in canopy..... 66

Figure 6.12 Estimation of sublimation loss in MCRB during 07/08 unloading event..... 68

Figure 6.13 Cumulative unloading versus cumulative sublimation..... 69

Figure 6.14 ΣU/ΣS as a function of time since interception has occurred..... 70

Figure 6.15 ΣU/ΣS as a function of wind speed..... 70

Figure 6.16 Relationship between ΣU/ΣS and canopy air temperature..... 71

Figure 6.17 Correlation between the independent variables..... 73

Figure 6.18 Performance of the ΣU/ΣS ratio for event based unloading estimates..... 76

Figure 6.19 Comparison of unloading model performance..... 78

Figure A.1 Geonor T-200B catch efficiency curve..... 86

Figure A.2 Load cell calibration coefficients..... 86

Figure A.3 Upper Forest synthetic wind speed generation based on 06/07 values..... 87

Figure B.1 Hedstrom and Pomeroy (1998) modeled unloading time series..... 88

Figure B.2 Roesch et al. (2002) modeled unloading time series..... 91

LIST OF SYMBOLS

dL/dt	change in canopy load with time (kg m^{-2} s^{-1})
dI/dt	change in interception with time (kg m^{-2} s^{-1})
E_t^i	sublimation loss from Gelfan *et al.* (2002)
I	interception (mm SWE)
I^*	interception efficiency (%)
I_N	net interception (mm SWE)
K	proportionality constant
LAI	Leaf Area Index
LAI'	effective Leaf Area Index
L	canopy load (mm SWE)
L^*	maximum canopy load (mm SWE)
L_0	canopy load before snowfall (mm SWE)
L_1	canopy load at time of unloading (mm SWE)
L_m	melt unloading rate (kg m^{-2} s^{-1})
p	significance value
P	snowfall (mm SWE)
P_{SC}	sub-canopy snowfall (mm SWE)
PAI	Plant Area Index
ρ_s	snow density (kg m^{-3})
Q_D	canopy drip (kg m^{-2} s^{-1})
Q_M	mass release (kg m^{-2} s^{-1})
Q_P	snowfall (kg m^{-2} s^{-1})
Q_{Psc}	sub-canopy snow accumulation (kg m^{-2} s^{-1})
Q_S	sublimation (kg m^{-2} s^{-1})
Q_{TF}	throughfall (kg m^{-2} s^{-1})
Q_T	wind transport (kg m^{-2} s^{-1})
Q_U	unloading (kg m^{-2} s^{-1})
r^2	coefficient of determination
RMSE	root mean square error
S	sublimation (mm SWE)
$\overline{S}$	average branch snow collection (m)
S	species loading coefficient (mm SWE)
SVf	Sky View Factor (%)
SWE	Snow Water Equivalent (mm)
t	time (s or hr)

T	temperature (^oC)
T_a	air temperature (^oC)
u	coefficient of unloading (s)
U	unloading (mm SWE)
v	wind speed (m s^{-1})
$\bar{X}$	average value
X_{mod}	modeled value
X_{obs}	observed value
$\bar{X}_{obs}$	average observed value
Ω	clumping factor
ΣU	cumulative unloading (mm SWE)
ΣS	cumulative sublimation (mm SWE)

CHAPTER 1

INTRODUCTION

In Canada, snowfall is of particular importance because it represents over one third of annual precipitation (Bailey *et al.,* 1997). In fact over 50% of the days in Canada that see precipitation see it in the form of snow (Goodison *et al.,* 1998). Snow can act as either an input or a storage term in the water balance, depending on time-scale, which makes the hydrological response vastly different in cold regions compared to low altitudes or latitudes. With greater than two thirds of Canada covered by forest (Bailey *et al.,* 1997) the interaction between forest and snowfall is critical to understanding Canada's hydrology. The primary impact of forests on hydrological processes in cold regions is the reduction in snow accumulation (Pomeroy and Brun, 2001). This reduction in snow accumulation is a result of the interception loss of snowfall as it passes through the forest canopy (Fig. 1.1). Interception is defined as the difference between snowfall at the top of the canopy and snow falling on the forest floor. Limited research has been done on the interception process leading Lundberg and Halldin (1999) to consider it the least known term in the winter water balance.

Interception is a rate with respect to the reduction in snowfall as it passes through the canopy, but also a mass when considering the cumulative amount of snow intercepted. Intercepted snow can be lost through sublimation as it is stored within the forest canopy. Sublimation rates in the canopy can exceed 20 times that of snow on the ground due to a rougher surface and higher available radiation (US Army, 1956). Sublimation is responsible for the interception loss in forests. Seasonal interception losses, due to sublimation, range from 30 - 60% of total snowfall (Suzuki and Nakai, 2008; Lundberg and Koivusalo, 2003; and Pomeroy *et al.,* 1998).

Experiments with canopy removal in forests have shown that snow cover is inversely proportional to Leaf Area Index (LAI). Through canopy removal, different harvesting techniques have been found to enhance the snow accumulation in forests by altering LAI, surface roughness and airflow patterns (Troendle *et al.,* 1988 and Woods *et al.,* 2006).

It is not unexpected that interception rate varies with tree species (Pomeroy and Brun, 2001), and is virtually negligible in deciduous stands (Pomeroy *et al.*, 1998). Studies of coniferous stands and nearby stands of mixed forest, including aspen revealed that the introduction of deciduous tree species decreased interception to less than 15% of interception on average (Pomeroy *et al.*, 1998). Variations of interception rate within the forest are attributed to differences in canopy and branch structure between coniferous species. It is important to gain a better understanding of the losses caused by the interception process given the high percentage of coniferous species in Canada's boreal and mountain forest compositions.

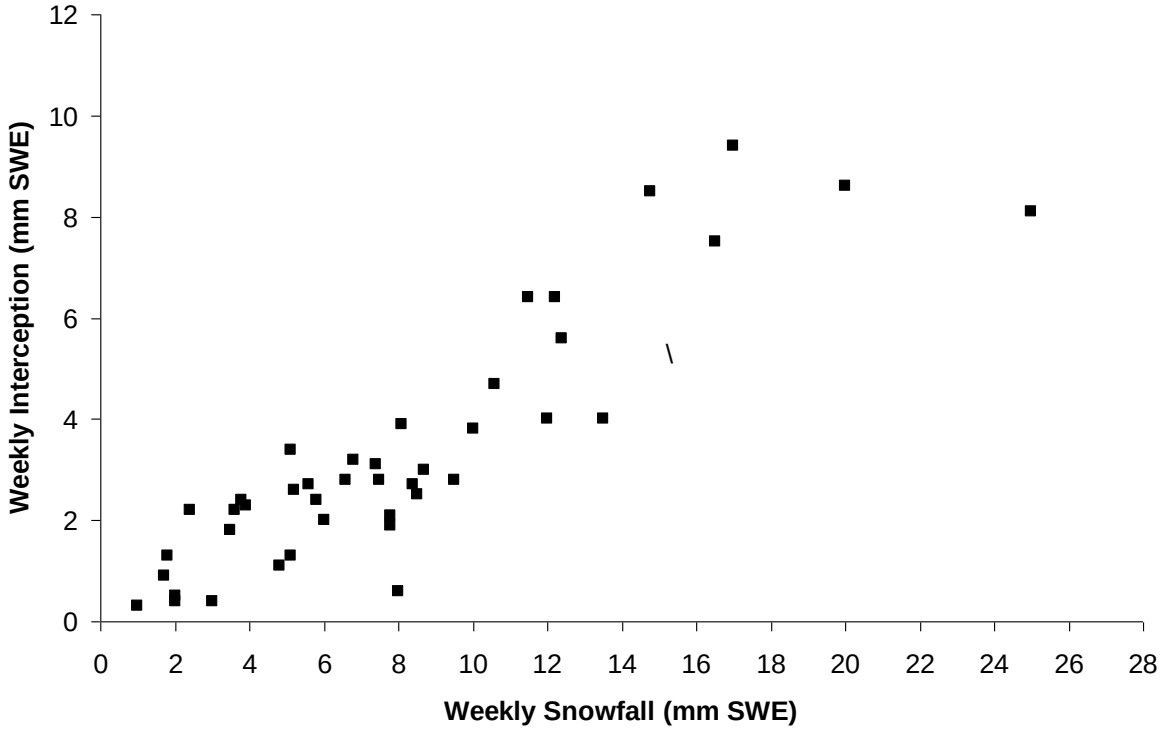

Figure 1.1. Snow interception losses in the boreal forest of Prince Albert National Park. From Hedstrom and Pomeroy (1998).

Also controlling the magnitude and timing of the interception loss is the process of unloading. Unloading is the mechanism for changing the canopy snow load from storage of snowfall into subcanopy snow accumulation by removing the snow from the

canopy where it is highly susceptible to sublimation losses. Unloading may occur in two situations: i) the release of snow clumps from the branches, or ii) as meltwater dripping from the intercepted snow. There are very few studies focused on interception and a very small percentage of these focus primarily on unloading. Hedstrom and Pomeroy (1998) were the first researchers to include a physically based model for unloading and suggested a time-decay function to describe the rate of unloading. This function is still one of the most widespread and commonly used algorithm for unloading (Essery *et al.*, 2003; and Gelfan *et al.*, 2004). The Hedstrom and Pomeroy (1998) function based on the intercepted mass is explained in detail in a later section (section 2.5).

A recent snow model intercomparison project for forest snow processes (SnowMIP2) suggests that interception is a very important process and needs to be further refined (Rutter *et al.*, 2009). The divergence and convergence of measured and modelled SWE and snow depth in forest model outputs is directly influenced by the partitioning of snow to interception and unloading. Therefore, unloading rates must be better understood if a higher degree of accuracy is attained by forest snow process models. Focusing on the unloading process is important to understanding the reduction in snowpack in forested basins compared to open adjacent areas. Changes in forest composition and forest cover may have dramatic effects on spring runoff. Climate change impacts such as spread of wildfires or mountain pine beetle infestations may decrease the LAI of a forest. This decrease in LAI will, in turn, result in a reduction in interception loss thus increasing snow accumulation. Forest harvesting in mountainous watersheds have shown to increase stream flow generation by reducing the interception loss by as much as 35% (Troendle, 1987 and Woods *et al.*, 2006). A more complete understanding of the interception process and the unloading phenomenon will facilitate more accurate estimations of seasonal snow accumulation. Accurate estimations of snow-forest processes will provide a better understanding of the changes that could occur with climate or land use changes.

CHAPTER 2

LITERATURE REVIEW

Studies on snow interception began in the mid-1900's by Miller (1962) and then Hoover and Leaf (1967). The discovery of a missing quantity in the water balance in forested basins was attributed to snowfall interception (Miller, 1962). Schmidt *et al.* (1988) advanced the understanding of interception in a study of tree-scale interception in artificial conditions. Research by Schmidt and Pomeroy (1990) followed up on the unloading of intercepted snow, by studying the effect of temperature changes on the elasticity of branches. Furthering their research on snowfall interception, Pomeroy and Schmidt (1993) experimented with photographic techniques and a suspended tree in the boreal forest. Research by Lundberg approached interception by installing forest lysimeters under individual trees (Lundberg, 1993; Lundberg and Halldin, 1999; and Lundberg *et al.*, 2004). Storck *et al.* (2002) found that meltwater drip was the dominant form of unloading in the coastal forests or Oregon by using lysimeters.

The literature review will outline the unloading process as a component of interception and current unloading models and their parameters.

2.1 Interception Processes

Interception (dI/dt) is the cumulative interception change over time within a plant canopy and is equal to snowfall (Q_P) less throughfall (Q_{TF}) (Eq. 2.1) (Fig. 2.1). Intercepted snow may be stored, sublimated, wind redistributed, or may subsequently unload or melt and drip to the subcanopy snowpack (Fig. 2.1). Harding and Pomeroy (1996) found much higher rates of sublimation from canopy snow than on the forest floor due to higher net radiation and turbulent transfer in the canopy.

$$\frac{dI}{dt} = Q_P - Q_{TF} \tag{2.1}$$

$$Q_{Psc} = Q_{TF} + Q_U \tag{2.2}$$

$$Q_{Psc} = Q_P - \frac{dI}{dt} + Q_U \quad (2.3)$$

$$Q_U = Q_D + Q_M \quad (2.4)$$

$$Q_U = \frac{dI}{dt} - Q_T - Q_S \quad \text{when} \quad Q_P = 0 \quad (2.5)$$

where:

Q_P is snowfall (kg m^{-2} s^{-1})
Q_{Psc} is sub-canopy snowfall (kg m^{-2} s^{-1})
Q_{TF} is throughfall (kg m^{-2} s^{-1})
Q_U is unloading (kg m^{-2} s^{-1})
Q_M is mass release (kg m^{-2} s^{-1})
Q_D is canopy drip (kg m^{-2} s^{-1})
Q_S is sublimation (kg m^{-2} s^{-1})
Q_T is wind transport of snow (kg m^{-2} s^{-1})
dI/dt is interception rate (kg m^{-2} s^{-1})

In terms of continuity, the rate of sub-canopy snowfall (Q_{Psc}) is equal to throughfall (Q_P) less the interception rate (dI/dt)) plus the rate of unloading (Q_U) (Eqs. 2.2 and 2.3). Unloading consists of canopy drip (Q_D) and mass release (Q_M) (Eq. 2.4). Unloading is then defined as interception less sublimation and wind transport when Q_P = 0 (Eq. 2.5).

2.1.1 Snowfall

Snowfall is the vertical flux of solid precipitation from the atmosphere to the surface. In a forest environment, the boundary between the surface and the atmosphere is at the top of the canopy and not the ground level. Snowfall inputs at the top of the canopy are difficult to observe because canopy-level observation requires the installation of a shielded snowfall gauge on a tower above the canopy. An assumption can be made that snowfall in a nearby forest clearing (diameter = 100 m) is representative of the snowfall above the canopy (Schmidt and Troendle, 1989). This convention was validated by Hedstrom and Pomeroy (1998) and Gelfan *et al.* (2004). The clearing must be large

enough to not be affected by the surrounding forest yet small enough to inhibit blowing snow (Pomeroy and Gray, 1995).

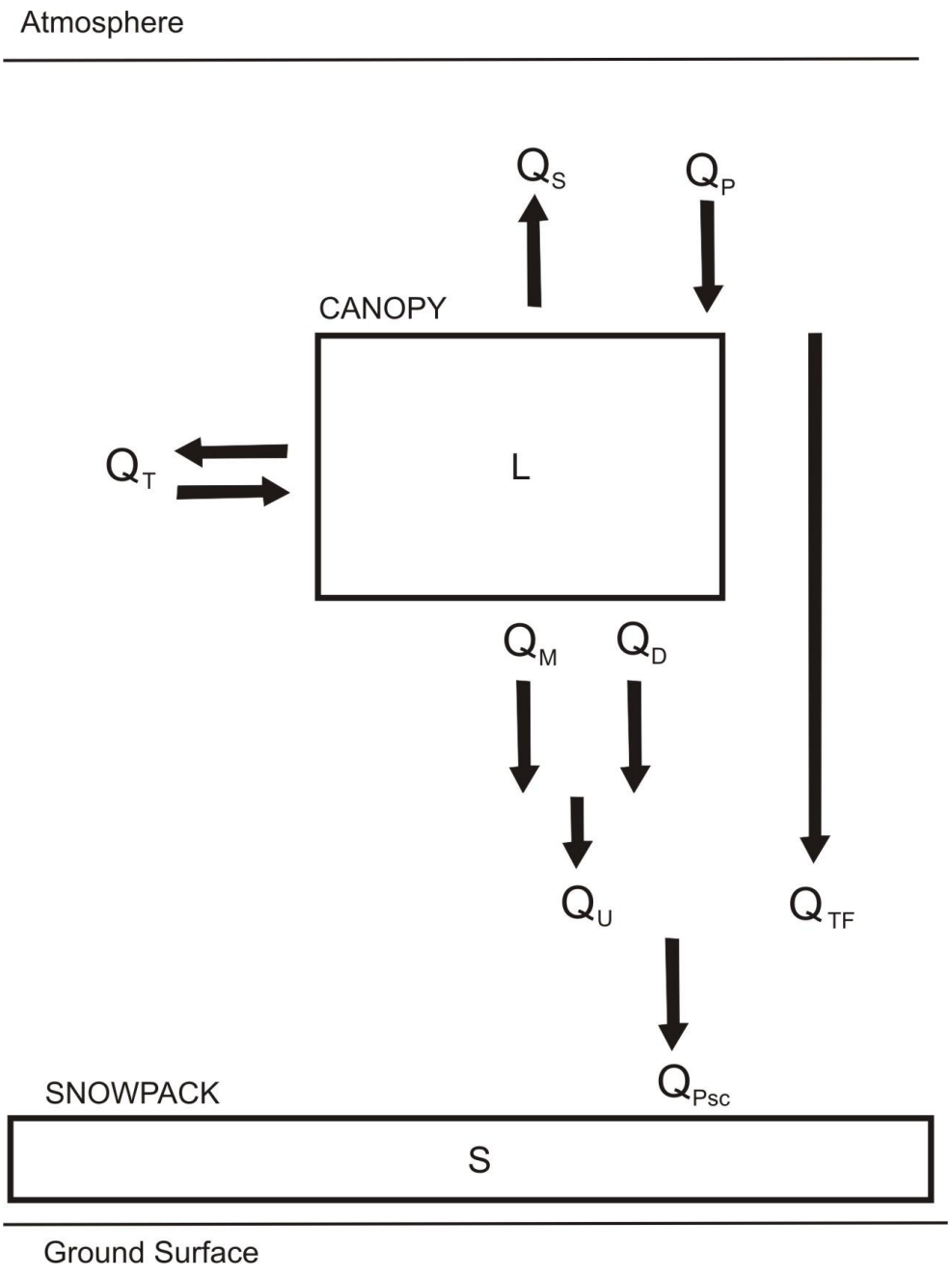

Figure 2.1. Forest Snowfall Interception process displayed as a control volume. Q_{PSC} is sub-canopy snowfall**,** Q_P is snowfall, Q_S is sublimation, Q_U is unloading comprised of: mass release (Q_M) and canopy drip (Q_D), Q_{TF} is throughfall, Q_T is wind transport of snow. Masses (storages) are intercepted load L, and sub-canopy snowpack S.

2.1.2 Throughfall

Throughfall is the rate at which snow falls directly to the sub-canopy snow pack without being intercepted by the canopy. Throughfall is a component of subcanopy snowfall. The literature in this area does not clearly describe whether snow which unloads during snowfall is considered throughfall or unloading. For simplicity, this study will regard any snow which reaches the ground during a snowfall event as throughfall. The reasoning behind this is that the residence time is too short for sublimation losses to be significant.

2.1.3 Canopy Load

The intercepted mass or canopy snow load (L) (Fig. 2.1) is the mass of snow stored in the canopy. This load is the source for sublimation, wind transport and unloading. Hancock and Crowther (1979) and Schmidt and Pomeroy (1990) used measurements of branch strength and deflection to determine load capacity. Branch scale interception was also measured by Schmidt and Gluns (1991) where the snow load on branches was shaken into bags and weighed. The branches were later removed to measure their Leaf Area Index (LAI). Load cells are considered a more effective way of measuring canopy snow load at the tree scale. Schmidt *et al.* (1988) first weighed an artificial tree on an electronic balance to estimate interception losses from a conifer. Following from this was Hedstrom and Pomeroy's (1998) use of a tall tower to hang a full tree to measure interception, which was more natural. Lundberg (1993) and Storck *et al.* (2002) isolated single trees on weighing lysimeter platforms. These two different installations allowed the researchers to continuously measure canopy load. The benefit to the hanging-tree was that it could be situated within the forest in a natural position, whereas the lysimeter platforms were installed in such a way that the natural environment was altered.

Photographic techniques have been used to collect canopy load data by Pomeroy and Schmidt (1993) and Nakai *et al.* (1994). Schmidt and Pomeroy's research analyzed images of snow covered area and found a relationship between it and canopy load through the use of a hanging tree lysimeter. Further data was necessary to conclude that

changes in snow covered area increased linearly with intercepted snow load within the forest canopy.

Albedo changes in the canopy have also been used to infer changes in the canopy load. McKay and Bartlett (2006) have used above canopy radiation measurements to detect the time scales of unloading. This is contrary to the work done by Pomeroy and Dion (1996) where snow in the canopy was not found to affect the surface albedo. The contradictory results may be a result of the Pomeroy and Dion study only having data for small magnitude snowfalls. Determining whether or not there is a detectable albedo change could allow for an estimation of forest-scale unloading from albedo changes.

2.1.4 Interception efficiency

The net reduction in snowfall to the sub-canopy snowpack is the interception loss (I) (Eq. 2.6). Net Interception (I_N) (mm SWE) is the loss due to interception once unloading has occurred and can be quantified by Snowfall (P) (mm SWE) less Sub-canopy Snowfall (P_{SC}) (mm SWE). Interception efficiency (I^*), given as a percent, is the ratio of subcanopy snowfall to snowfall, is controlled by many meteorological and biological factors including: the available vegetated surface for collection in the canopy (Plant Area Index (PAI)), wind speed, air/snow temperature, snow particle size, and snowfall rate/volume/frequency. I^* is the ratio of subcanopy snow fall to snowfall for a snowfall event.

$$I_N = P - P_{SC} \qquad (2.6)$$

Hedstrom and Pomeroy (1998) calculated the maximum canopy load (L*) of the forest based on forest PAI (section 2.4). Maximum canopy snow load is a function of PAI and a species loading coefficient. The species loading coefficient (S) (m) can be estimated as a function of snow density (ρ_s) (kg m^{-3}) and the average snow collected on a branch ($\bar{S}$) (mm SWE) per unit area (Eq. 2.7 & 2.8) (Schmidt and Gluns, 1991). Species loading coefficients for different tree species were developed by Schmidt and Gluns (1991) through extensive manual observations.

$$L^* = S \cdot PAI \tag{2.7}$$

$$S = \bar{S} \cdot (0.27 + \frac{46}{\rho_s}) \tag{2.8}$$

Meteorological factors also have a major control on the interception rates of the canopy. Temperature and particle size greatly affect the ability of snowflakes to bond to the canopy, and also impact the internal structure of the snowpack on branches. Warmer temperatures lead to an increase in snow cohesion and adhesion. During melt the increased moisture content of the snow decreases the cohesion of intercepted snow, resulting in structural failure and unloading (Hedstrom and Pomeroy, 1998). Snowfall during a high winds increases the available surface area for interception due to the increasingly horizontal trajectory of snow particles with increased wind speeds (Hedstrom and Pomeroy, 1998).

2.2 Unloading of Intercepted Snow

Unloading is governed by the failure of the branch and/or snow structure to hold the canopy load. As canopy load increases so do the applied stresses, which cause bending or deflection of the branch. Conifer branch deflection increases proportional to temperature due to the higher modulus of elasticity of warmer branches (Schmidt and Pomeroy, 1990). As well, deflection was found to increase 60% with distance from the trunk, because the diameter of the branch decreases. How temperature variations affect unloading through branch bending or decreased cohesion is not yet known.

The effect of temperature changes on unloading at a branch scale is ambiguous because of metamorphism within the snow structure. Increased temperature within intercepted snow increases the snow's moisture content. As snow becomes moist, snow cohesion increases (Perla and Martinelli, 1976). Once saturation is reached the cohesive strength is lost and structural strength dramatically decreases, thus causing unloading.

Changes within the canopy snow structure may do one of two things. First, warm air temperatures may cause the snow structure to weaken and mass release to occur. Secondly, warming of the snow pack within the canopy creates a layer of moisture at the

interface between the branch and snow (Perla and Martinelli, 1976). This moisture layer can substantially decrease the adhesion between the snow and the branch.

Another form of unloading is meltwater drip, which is produced when conditions for melt are present in the canopy (snow temperature = 0^{o}C). Storck *et al.* (2002) found that meltwater drip contributes a much higher percentage of unloading than mass release in a coastal rain forest. Results from work in the Pacific Northwest showed that 72% of unloading was from meltwater drip while only 28% from mass release (Storck *et al.*, 2002). The maritime forests where these experiments were conducted were dominated by the local meteorological conditions where air temperature was > 0^{o}C and humidity was very high following snowfall. In contrast, the presence of meltwater drip in the boreal forest is uncommon, as air temperatures rarely reach 0^{o}C during winter months. Ultimately, regional differences in meteorological conditions and snowfall regimes require caution when applying the Storck *et al*. model in cold climates.

2.3 Resuspension of intercepted snow: missing quantities?

Resuspension of intercepted snow from the canopy occurs when wind gusts move through the canopy and lift snow into the atmosphere. If the wind gusts are strong enough some of the snow is entrained and carried away from the canopy. Hoover and Leaf (1967) observed large plumes of snow being removed from the canopy in Colorado, much the same as seen on mountain ridges. These observations suggested that the difference in snow accumulation between forests and clearings was due to these plumes. Troendle *et al.* (1988) have shown that these plumes are comprised of very fine snow crystals which are very efficient in scattering visible light ($\approx$ 500 nm diameter) and that, though prominently visible, the mass flux at a forest scale was negligible. Plumes were found to deposit the suspended snow in immediately adjacent trees. The resuspended snow was then vertically redistributed down into the canopy to the forest floor, rather than into adjacent forest clearings (Schmidt and Troendle, 1989).

2.4 Forest Parameters

Linking the unloading processes to biophysical parameters that describe the forest is important if unloading is to be integrated into the interception modules in climate and

hydrology models. Leaf area index (LAI) is often used in forest studies as a parameter for interception because it is easily measured and understood. LAI is defined as the planar area available for transpiration in a plant divided by the projected planar area of the plant (Chen and Black, 1992). However, a more appropriate term needs to be utilized because snow interception studies focus on the total surface area available to collect snowfall. Plant Area Index (PAI) is defined as all surface area capable of intercepting light transmission, including leaf and woody material (Chen, 1996 and Holst *et al.,* 2004).

LAI measurement methods such as the Licor LAI-2000 or hemispherical photograph analysis do not measure LAI directly. Rather, these instruments estimate LAI by quantifying the light transmission and percentage of canopy openness. What is actually measured is an effective LAI (LAI′) (Frazer *et. al.,* 2000), which is a function of the LAI and a clumping factor (Ω) (Eq. 2.9).

$$LAI' = LAI\ \Omega \tag{2.9}$$

Clumping describes a state wherein branches overlap with each other. The clumping factor accounts for irregularities in tree geometry/architecture whereby branches overlap and may not register in LAI analysis. For example, Chen (1996) calculated clumping factors for various coniferous species and found an average value of 0.71 for spruce and 0.6 for pine, with fir being in between.

Chen (1996) outlined the differences in measurement techniques in LAI and defined PAI as what has, in the past, been calculated as LAI in interception studies. Discrepancies were uncovered between what was being represented as LAI and what was being measured as LAI. Transmittance of light through the forest canopy can be blocked by all leafy and non-leafy material. The result of this is that instrumentation using light transmission to estimate LAI is in fact estimating PAI. Therefore, in this thesis, PAI is defined as a function of the LAI′ and a species clumping factor (Chen, 1996) (Eq. 2.10).

$$PAI = LAI' / \Omega \tag{2.10}$$

Canopy gap fraction is also a useful term for describing the density of a forest. Canopy gap fraction or sky view factor (SVf) accounts for the general openness of the forest canopy as a percentage of the sky not obstructed by forest canopy. Canopy closure also quantifies the density of the forest by describing how much of the sky is obstructed by foliage and tree structure. SVf is calculated primarily through digital analysis of hemispherical photographs.

2.5 Current Interception and Unloading Models

The interception model produced by Hedstrom and Pomeroy (1998) is a means for accounting for unloading from intercepted snow (Eq.2.11). Unloading is linked to interception by subtracting unloaded snow from the canopy, where interception over some time interval before unloading is given as:

$$I = (L^{*} - L_0)(1 - e^{-k Q_P}) \tag{2.11}$$

where:

I is interception (kg m^{-2})
L^{*} is maximum canopy load (kg m^{-2})
L_0 is canopy load at start of snowfall (kg m^{-2})
k is a proportionality constant
Q_P is snowfall (kg m^{-2})

It must be noted that in this form the units are in mass although there is an implied time interval for interception and snowfall which effectively makes these terms rates.

Maximum canopy load (L^{*}) is calculated as a function of LAI and the snow load per unit branch area (S) in kg m^{-2}. This is different from Equation 2.7 as LAI was used by Schmidt and Gluns although the argument is that they are synonymous because of instrumentation restrictions.

$$L^{*} = S(LAI) \tag{2.12}$$

Snow load per unit branch area was quantified by Schmidt and Gluns (1991) and is calculated based on an empirical relationship derived from extensive *in-situ* measurements (Eq. 2.13).

$$S = \bar{S}\left(0.27 + \frac{46}{\rho_s}\right) \tag{2.13}$$

where:

$\bar{S}$ *is a species specific loading coefficient (kg m^{-2})*
ρ_s *is the density of freshly fallen snow (kg m^{-3})*

Schmidt and Gluns (1991) suggest values for $\bar{S}$ = 6.6 and 5.9 kg m^{-2} for pine and spruce, respectively. Values for the density of freshly fallen snow can be calculated from the following (US Army, 1956):

$$\rho_s = 67.92 + 51.25\ e^{(T_a / 2.59)} \tag{2.14}$$

where:

T_a *is air temperature (^oC)*

McNay *et al.* (1988) developed an interception model for the forests of coastal British Columbia based on snowfall and SVf. The Pomeroy and Gray (1995) version of the McNay model uses variables of SVf and snowfall to estimate the intercepted mass (Eq. 2.15).

$$I = 1.935 + Q_p\ \ 0.006(1 - SVf) - 0.08 \tag{2.15}$$

A model for unloading was developed by Hedstrom and Pomeroy (1998). The rate of unloading was determined by observed values of interception and interception at time of unloading. Hedstrom and Pomeroy (1998) developed a simple time decay

function (Hedstrom Equation) to represent unloading of intercepted snow in a boreal forest (Eq. 2.16):

$$L = L_1 e^{-ut} \tag{2.16}$$

where:

L is canopy load (kg m^{-2})
L_1 is canopy load at time of unloading (kg m^{-2})
u is an unloading coefficient(day^{-1})
t is time (day^{1})

Application of this model on an annual basis for interception is inappropriate and therefore, smaller time intervals for precipitation on the scale of days or less must be used (Pomeroy *et al.,* 2002).

Inclusion of the unloading process should be paramount to any model that includes interception. Improper characterization of unloading rates may increase the residence time of intercepted snow within the forest canopy allowing sublimation to occur when transfer (unloading) of the snow from the canopy to ground snowpack should occur. The result would be grossly overestimated interception losses. For example, Pomeroy *et al.* (1998) coupled unloading from the Hedstrom Equation within a sublimation model. The coupled model, running on an hourly or shorter time-step, suggests that sublimation losses are incurred by the initial canopy load (L_1) before unloading occurs. L_1 is depleted by sublimation immediately following interception whereas probabilities of unloading increase with time (Pomeroy *et al.,* 1998).

Gelfan *et al.* (2004) uses the Hedstrom equation to derive unloading after sublimation losses during the model time step are accounted for (Eq. 2.16). Gelfan *et al.* (2004) present a general model of unloading (U) as a rate or mass over time (t) (Eq. 2.17). Unloading becomes a function of the time between snowfall events, the intercepted load (I) in mm SWE (or kg m^{-2}), the sublimation losses of intercepted snow over time (E_t^i) in kg m^{-2} and an unloading coefficient (μ) of 0.006467 s^{-1} from Hedstrom and Pomeroy (1998).

$$U = (1 - e^{-ut})(I - E_t^i) \quad (2.17)$$

where:

U is unloading (kg m^{-2})
u is the unloading rate coefficient (s^{-1})
t is time (s^{-1})
I is snow interception in the canopy (kg m^{-2})
E_t^i is sublimation of intercepted snow over elapsed time

Through this model, the humidity and sublimation rate also become important factors in controlling unloading rates. Canopy load in this model is removed by sublimation and unloading. The ice-bulb/wet-bulb temperatures are used as thresholds for sublimation or unloading to occur. Unloading is prevalent when the wet-bulb temperature exceeds 0 ^{o}C for 3 hours, which enables the snowpack to be moist. This model is used in the Cold Regions Hydrological Model (CRHM) (Pomeroy *et al.* 2007)

The Canadian Land Atmosphere Surface Scheme (CLASS) applies the interception/unloading algorithms from Hedstrom and Pomeroy (1998) (unloading coefficient = 0.0969 d^{-1}), but derives a new unloading coefficient of 0.339 d^{-1} (Bartlett *et al.*, 2006). The unloading coefficient was determined from observations of changes in forest albedo from BOREAS (now BERMS) data sets. These sites were characterized by boreal forest coniferous tree species such as *Pinus banksiana* (Jack pine), *Picea mariana* (Black spruce), and *Picea glauca* (White spruce). Bartlett *et al.* (2006) suggest the time scale of unloading in Hedstrom and Pomeroy's model be two days, which increases unloading rates. The results of applying the altered Hedstrom and Pomeroy (1998) algorithm greatly increase the accuracy of the model output by lowering the net interception loss (initial canopy load – unloading), thereby increasing sub-canopy snowpack SWE (Bartlett *et al.*, 2006).

Storck *et al.* (2002) researched the unloading phenomenon in the coastal mountains of Oregon, USA. Their findings show that 70% of unloading occurs as meltwater drip while the remaining 30% is from mass release. A ratio of mass release to meltwater drip equal to 0.4 derived from Storck *et al.* (2002) is applied to canopy unloading in the MOSES2c model (Essery *et al.*, 2003).

The Storck *et al.* (2002) ratio was also applied by Andreadis *et al.* (2009). Andreadis *et al.* (2009) developed their model in a maritime mountainous site in Oregon and validated it within the boreal forest. Discrepancies were reported in their model outputs, which may be explained due to the nature of the Storck *et al.* unloading ratio. That is to say, a model based on the production of meltwater drip may function well in coastal forests as in the Storck *et al.* (2002) research, where rain-on-snow events are frequent and the climate is temperate. Unfortunately, applicability of this model to environments such as the boreal forest or the Rocky Mountains is poor because of the inherent differences in climate and weather patterns.

SnowModel's interception algorithm employs a given melt unloading rate (L_m) of 5 kg m^{-2} d^{-1} K^{-1} based on a temperature function (Eq. 2.18) (Liston and Elder, 2006). Melt unloading rate (L_m) is then a function of air temperature (T_a) and time (t). No unloading is present besides meltwater drip in this model.

$$L_m = 5.8 \times 10^{-5} (T_a - 273.16)\ dt \tag{2.18}$$

ECHAM4 employs a physically based unloading model based on meteorological variables (Roesch *et al.*, 2001). The model is different from the Hedstrom and Pomeroy (1998) model as it includes meteorological factors. The model calculates change in canopy load (dL/dt) as a function of the rate of interception less that which is unloaded due to wind or temperature changes, and less the sublimation rate from the canopy (Eq. 2.19).

$$\frac{dL}{dt} = I - L_1\ f(T_1) + f(v)\ - Q_S \tag{2.19}$$

where:

I is interception rate (kg m^{-2} s^{-1})
L_1 is the initial canopy load (kg m^{-2})
$f(T_1)$ is a function of unloading caused by temperature over a time interval (s^{-1})
f(v) is a function describing wind-induced unloading over a time interval (s^{-1})
Q_S is the rate of sublimation (kg m^{-2} s^{-1})

Roesch *et al.* (2001) suggest a linear function for the influence of air temperature on unloading (Eq. 2.20). A threshold temperature of – 3 ^{o}C must be reached for unloading to occur and at 0 ^{o}C, 50% of the snow load unloads over 12 hours. The threshold is based on the data collected by Yamazaki *et al.* (1996) showing 40% unloading within 12 hrs when air temperature is ≥ 0 ^{o}C.

$$f(T_1) = \frac{c_1 + T_1}{c_2} \tag{2.20}$$

where:

c_1 is a constant of -270.15 (K)
c_2 is a constant of 1.87 x 10^5 (K s)
T_1 is air temperature taken at canopy height (K)

Roesch *et al.* (2001) base their wind speed function on observations that show greater snow load is associated with low wind speeds (< 3 ms^{-1}). This assumption is based on observations of high forest albedo values of 0.30 (meaning a snow covered canopy) corresponding to low wind speeds (Betts and Balls, 1997). Wind speeds of 5 m s^{-1} will empty 50% of the canopy within 6 hr. Wind speed is represented as a linear function described in Equation 2.21:

$$f(v) = \frac{v}{c_3} \tag{2.21}$$

where:

c_3 is a constant of 1.56 x 10^5 (m)
v is wind speed measured at canopy height (m s^{-1})

The use of existing unloading studies within these models can be seen to increase the model accuracy for sub-canopy SWE accumulation. The various models range from the most basic utilization of empirical relationships to more complex algorithms, which consider the influence of temperature and wind speed on unloading. In order for the canopy load to be partitioned between sublimation and unloading, it may be important to

account for meteorological conditions of temperature, wind speed, humidity as well as time since interception occurred.

2.6 Research Gap

There are two main areas that interception/unloading research fail to adequately address: i) lack of process studies that address the unloading phenomenon and investigate its mechanisms and magnitude; ii) scaling of the process from branch to forest-stand scale to predict unloading. These are important to the overall accuracy of hydrological models and estimation of the water balance in forested basins.

First, early research demonstrates that the mechanisms of unloading were poorly understood (Hancock and Crowther, 1979). Furthermore, the application of early unloading studies to unloading of forest stands was unsuccessful (Hancock and Crowther, 1979). The lack of success of these studies may be explained by the dominance of large scale meteorological characteristics on the unloading mechanism at the stand-scale. Hydrometeorological conditions, such as rain-on-snow or Chinook events, are critical to the unloading process. Chinooks, for example are meteorological events that occur in the Rocky Mountains where air masses descend the leeward side of the mountain range. Adiabatic process causes the air to warm and become unsaturated creating high potential for evaporation and melt. These Chinook events often follow periods of high moisture, and have their name originating from myth as "snow eater".

Previous studies were conducted under unnatural and/or artificial conditions that may have compromised the ability to mimic the process in all aspects. For example, in the studies by Schmidt *et al.* (1988); or Montesi *et al.* (2004), the artificial trees used did not have the elasticity or energy exchange properties of a natural tree. Furthermore, studies focusing on individual trees do not describe the unloading process on a forest scale because they lack the overlapping branch structure found in many forests. Conversely, the Hedstrom and Pomeroy study using a tree segment hung from a tower allowed for the natural environment to remain intact. This is an improvement compared to others such as Lundberg (1993), which were not representative of a natural setting. The inadequacies of these studies were found when they were scaled up to the forest

scale where individual small-scale mechanisms are confounded by other factors such as meteorology.

The lack of accurate and repeatable means for capturing unloading events further complicates process studies. Subcanopy snow surveys of depth and density are usually spaced several metres between depth measurements and several tens of metres between density measurements. However, unloading is a very spatially variable process that is concentrated in very small areas near the tree edge. Therefore, there must be more frequent density measurements to capture the changes in subcanopy snowpack accumulation. The snowpack often is compressed by the impact of unloaded snow meaning that density must be measured more frequently when it is prevalent.

The problem is to select an effective and accurate means of quantifying the unloading process from an assortment of methods, many of which have critical flaws, including: i) lack of scaling to the forest stand; ii) an unnatural setting for observations to occur; and iii) lack of focus on the unloading process.

CHAPTER 3

RESEARCH OBJECTIVES

3.1 Objectives

The purpose of this research is to characterize unloading rates of intercepted snow based on environmental conditions. This will be achieved by meeting the following objectives:

I. *gaining a better understanding of the environmental factors that cause unloading of intercepted snow;*
II. *designing a physically-based algorithm that represents the rate of unloading of intercepted snow in forested mountain basins.*

3.2 Hypotheses

Based on the literature reviewed for the interception process and unloading phenomenon the following two hypotheses are proposed. Hypothesis 1 is simply based on Hedstrom and Pomeroy's (1998) model in which the unloading coefficient (U) is measured in days. The Hedstrom and Pomeroy unloading model will be tested for its applicability. It is important to validate the findings of Hedstrom and Pomeroy (1998) within a mountain environment which has dramatic differences in meteorological conditions and apparent unloading mechanisms from their boreal forest site.

H_1: *unloading rates are directly proportional to initial load for time intervals where no there is no snowfall (Eq. 3.1 and 3.2)*

$$Q_U = -u\,L \tag{3.1}$$

Integrating to the following:

$$L = L_0 e^{-u\ t} \tag{3.2}$$

Canopy load (L) after unloading is equal to an exponential decay function of time and an unloading rate which is multiplied by the initial canopy load (L_0). Therefore, the greater the time interval, the greater the unloading.

Hypothesis 2 incorporates the additional effects of meteorological conditions on rates of unloading.

H_2: sublimation contributes to the unloading of canopy snow. The weakened snow structure can then be unloaded by triggers such as wind gust events or melt conditions.

CHAPTER 4

EXPERIMENTAL DESIGN

4.1 Experimental Site

The research was conducted in Marmot Creek Research Basin (MCRB) in the Front Range of the Canadian Rocky Mountains. Approximately 80 km west of Calgary, Alberta, Marmot Creek is a tributary to the Kananaskis River (Fig. 4.1). The basin was the subject of a long-term forest hydrology study that experimented with the effect of variable forest harvesting techniques on snow hydrology and stream flow generation (Swanson, 1977). The forest is an even-aged mature forest comprised of spruce, fir and pine tree species and an undergrowth of moss and lichens.

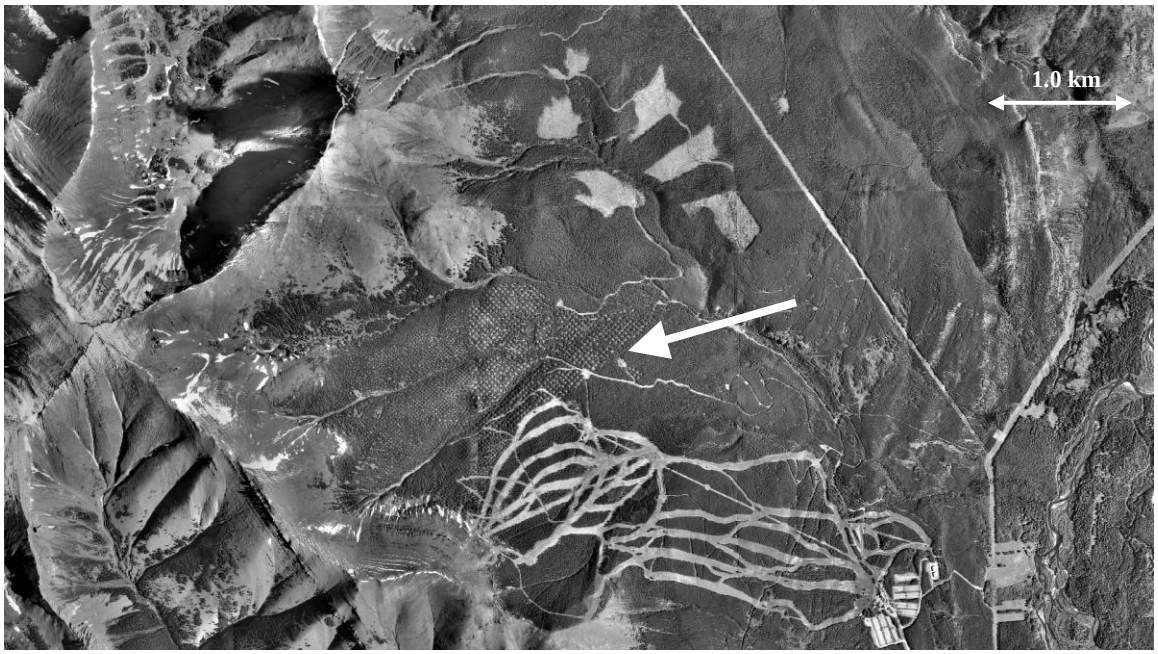

Figure 4.1. Marmot Creek Research Basin (MCRB) forest canopy unloading site.
Locator arrow is identifying the Upper Clearing and Upper Forest study site.

MCRB was chosen as the study site due to the high density of hydro-meteorological stations installed by the University of Saskatchewan Centre for

Hydrology. The research by Swanson (1977) left the basin with infrastructure such as roads and trails that make for reliable access in the winter months. The forest harvesting studies left a variety of forest covers throughout the basin as well as small forest clearings, which could be used as a reference snowfall site.

The experimental area consists of the Upper Clearing and Upper Forest sites as well as the Clearing Tower and Forest Tower. The sites are accessed via Marmot Road. The Upper Forest site (1800 m asl) is located in predominantly *Picea engelmanni* (Engelmann spruce) and *Pseudotsuga menziesii var. glauca* (Douglas fir) while the lower valley (< 1500 m) is *Pinus contorta* var. latifolia (Lodgepole pine) and the upper elevations of the basin transition into alpine species such as *Larix lyallii (*Alpine larch). The Upper Clearing site shows slight regeneration of the forest after harvesting and is comprised of the same species of tree as the Upper Forest (height <2 m). The sites are located within a honeycomb pattern of clear cuts with 30 years of forest regeneration present. These clear cuts have created a patchwork of forest clearings which are approximately 15 m in diameter. Average tree height within the mature forest is > 20 m with maximum heights exceeding 30 m. Understory vegetation is predominantly mosses such as *Ptilium crista-castrensis (*Feather moss), lichens such as *Usnea scabrata* (Old man's beard) and *Bryoria fuscescens (*Horse hair). Deadfall which still remains attached to the tree or is entwined within the canopy also adds to the PAI of the forest at the Upper Forest site.

The honeycomb pattern creates considerable variation in snow accumulation over short distances within the forest. Snow depth may vary by up to an order of magnitude between the clearings and forest stands. The Upper Forest site (Fig. 4.1) is located nearby a clearing that is ≈ 150 m in diameter, which is uniquely large for the honeycomb forest. The Upper Forest site has a dense forest canopy with a PAI = 2.9 as measured by hemispherical photograph analysis. The forest density is highly variable; PAI ranges from 2.4 to 4.0 and Sky View Factor (SVf) from 12.8-23.1%.

The primary requirements of the field program are to: i) capture the amount of snow that is first intercepted and stored within the canopy; ii) capture the flux of unloading snow from the canopy to the snowpack on the forest floor.

The instrumentation was located on 20 m Del-Hi triangular free standing towers at the Forest Tower and Clearing Tower. The Forest Tower was the platform for meteorological instrumentation throughout the forest canopy (Table 4.1) (Fig. 4.2). The hanging-trough lysimeters were situated around the Forest Tower and are described in section 4.2.1. Hanging-tree lysimeters were operated from the Forest Tower to obtain measurements of change in canopy load. The Clearing Tower served as a reference to incoming solar radiation for albedo calculations. Alongside each tower were 3 m tripod meteorological stations which contain instruments for wind speed, air and snow temperature, relative humidity and snow depth (Table 4.1).

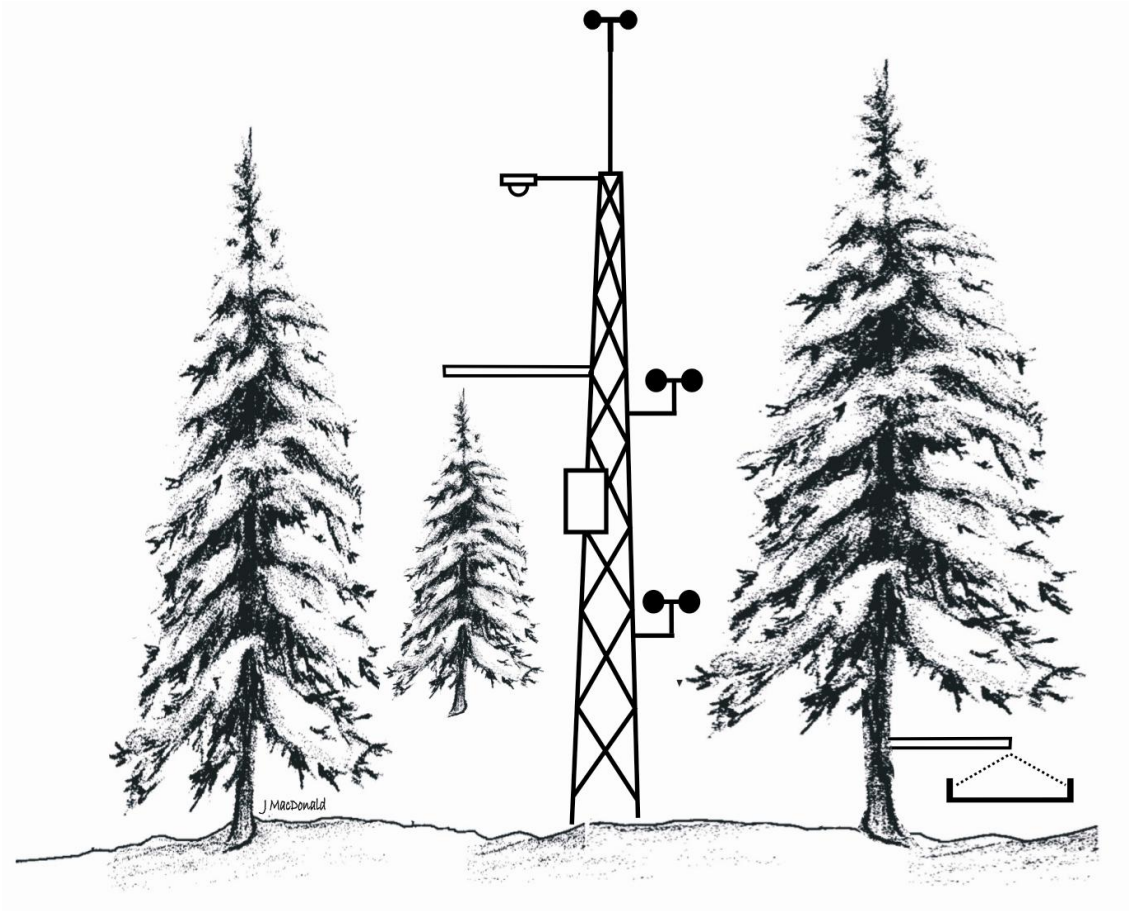

Figure 4.2. Upper Forest study site. The schematic shows the Forest Tower and its situation to the canopy along with the instrumentation levels. Only one hanging-lysimeter is shown to display the relative distance to the hanging-tree lysimeter.

Table 4.1. Instrument locations and heights

	UPPER CLEARING	CLEARING TOWER	UPPER FOREST	FOREST TOWER
ABOVE CANOPY		[20] CM11 radiometer		[25] 2032 anemometer (wind speed) [20] CM5 radiometer [20] SWTC thermocouple (air temp)
CANOPY				
MID				[9.5] 7 m hanging tree (canopy load) [13] 2032 anemometer (wind speed) [18] SWTC thermocouple (air temp) [13] IRTC (canopy temp) [11] FWTC (branch/needle temp)
LOW				[9] HPM45C212 Rh and air [20] temp [9] 2032 anemometer (wind speed) [9] IRTC (canopy temp)
GROUND LEVEL	[2.1] Geonor t-200B w/altershield [1.6] SR50 snow depth [2] 2032 anemometer [2.1] HMP45C212 Rh, air temp		[3.2] RMyoung anemometer [1.7] SR50 snow depth [2.5] HMP45C212 Rh, air temp	[0.65] lys1 hanging lysimeter (SWE) [0.65] lys2 hanging lysimeter (SWE) [0.65] lys3 hanging lysimeter (SWE)

† Heights given in [metres] above ground

4.2 Data Collection

4.2.1 Meteorological Variables

The Forest Tower was equipped with 3 instrumentation levels (Table 4.1). These included above the canopy (above canopy), within the main branch structure (mid canopy) and one at the bottom of the branch structure (below canopy). At each of these levels a HMP45 C212 hygrothermometer was used for recording air temperature and relative humidity and a Weathertronics 2032 3-cup anemometer for wind speed. Canopy temperature was measured throughout the canopy by Exergen infra-red thermocouples (IRTC). Fine scale temperature changes in the canopy were measured at the branch, twig, and needle scale by fine wire thermocouples (FWTC) installed directly on a spruce bough. Above the canopy was a downward looking Kipp and Zonen CM5 solarimeter that recorded the outgoing shortwave radiation from the forest. Gust factor was extrapolated from the wind speed measurements of maximum wind speed (during 15 min interval) and the average wind speed over the same interval. Gust factor is the ratio of maximum wind speed to average wind speed and is a good measure of the turbulence in the canopy (Hsu and Blanchard, 2004).

Instrumentation failure at the above canopy wind speed measurement height caused a gap in the data for winter 07/08. This was corrected by replacing the instrument and gaps in the data were filled using interpolation from the 06/07 data. Linear regression was done on the relationship between wind speeds at the forest floor and the above canopy from winter 06/07 (Figure A.3). Winter 07/08 above canopy wind speeds were then interpolated from this relationship.

The Clearing Tower was 20 m tall and had a Kipp and Zonen CM11 solarimeter mounted on its top measuring the incoming solar radiation. Using the CM11 measurement as incoming shortwave radiation to the forest and the Forest Tower's CM5 outgoing (reflected) shortwave radiation the forest albedo was able to be tracked as the interception and unloading processes occurred.

The change in albedo of the forest canopy has been suggested as a method for tracking unloading rates in the forest (MacKay and Bartlett, 2006). MacKay and Bartlett (2006) presented a adjustment of the Hedstrom and Pomeroy (1998) algorithm by modeling unloading based on changes in albedo.

4.2.2 Forest Characteristics

PAI was obtained from Gap Light Analyzer (GLA) digital image processing software. A Nikon CoolPix 5400 digital camera with a fisheye adaptor lens was used to capture the images that were processed by GLA to produce values for LAI' (Frazer *et. al.,* 2000). PAI was then derived from a function of LAI' and the species clumping factor (Eq. 2.10). An average clumping factor (0.71) was chosen from work done by Chen (1996) in a spruce forest.

PAI was calculated at each of the measurement sites and throughout the forest to obtain an average value for the study site. Hemispherical photographs were taken at each of the hanging-lysimeters (Fig. 4.3), as well as each of the unloading tubs and at 25 points along a sub-canopy snow survey adjacent to the site. SVf was also recorded for each of the locations as a measurement of canopy openness (Frazer *et. al.,* 2000).

Pre-processing of the images was done by registering the image to exclude the ground portion of the hemispherical photograph. The variation in sky and vegetation was differentiated by a pixel threshold and applied to all images (Figure 4.3) (Frazer *et al.,* 2000).

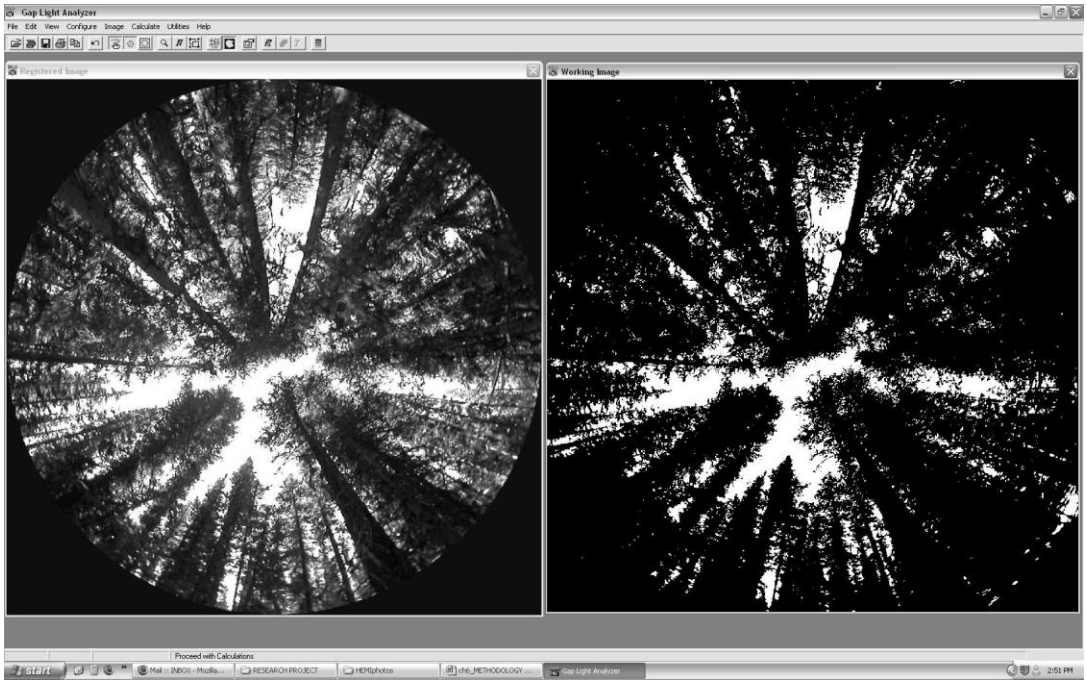

Figure 4.3. Processing of hemispherical photos for the Gap Light Analyzer. Left hand side shows raw hemispherical photograph. Right hand side is processed image with black representing canopy coverage and white showing sky.

4.2.3 Instrumentation

A reference snowfall site was created at the Upper Clearing by an Alter-shield equipped Geonor T-200B precipitation gauge (Figure 4.4). Schmidt and Troendle (1989) used large forest clearings as a substitute for measuring snowfall above the canopy. The clearing must be of sufficient size that it is not overwhelmed by the edge effects of the surrounding trees yet have a small enough fetch to hinder snow relocation and transportation. Measurement of snowfall in a clearing as a proxy value for canopy snowfall was also used by Hedstrom and Pomeroy (1998).

Meteorological observations were recorded by Campbell Scientific CR23x dataloggers. The 30 second readings are temporarily stored and then averaged to record an average observation for 15 minute time intervals. Instrument calibrations were incorporated within the program code to produce output values in units applicable to each variable. Raw mass values were stored as output for the load cells in the hanging-trough and hanging-tree lysimeters. The mass (kg) was used for canopy load measured by the hanging-tree while it could be easily converted to Snow Water Equivalent (SWE) for the hanging-troughs. The conversion from canopy load as a mass (kg) to SWE (mm) is given in section 4.2.4.

Figure 4.4. Upper Clearing study site. Meteorological station with Geonor t-200B precipitation gauge with alter-shield and hydrometeorological instruments.

4.2.4 Capturing interception and canopy load

There is a direct relationship between canopy load and unloading rate as shown by Hedstrom and Pomeroy (1998). Therefore, quantifying both the mass and rate of change in canopy load is paramount to calculating unloading. Two separate methods were employed to quantify interception to verify data accuracy.

First, interception was found as the difference in snowfall above the canopy and below the canopy. Snowfall above the canopy was interpolated from snowfall rates in the Upper Clearing site reference snowfall site (Fig 4.4). For enhanced accuracy, a 2032 3-cup anemometer was installed at the Upper Clearing site to correct the Geonor for undercatch. The Geonor data were corrected using the equation by MacDonald and Pomeroy (2007) (Eq. 4.1) (Figure A.1) based on wind speed (v). The correction provides snowfall data accurate to 0.1 mm SWE.

$$CE = 1.010\ e^{-0.09\ v} \tag{4.1}$$

where:

CE is catch efficiency (%)
v is wind speed (m s^{-1})

Subcanopy snowfall and unloading was observed at the Forest Tower Site where customized hanging-trough lysimeters were installed within the forest (Fig. 4.5). Three forest densities were represented by the hanging-lysimeters: PAI = 3.3 at lysimeter 1, 2.5 at lysimeter 2, and 2.9 at lysimeter 3; and canopy gap fractions of 17.1%, 21.8%, and 18.8% respectively . The hanging-lysimeters are large horse feed troughs which were cut down to a low height (≈ 0.20 m) with an orifice size of 0.81 m^2. The trough was supported from an ARTECH strain-style load cell model # SS20210 with a 40 kg capacity. The hanging-lysimeter load cells have an accuracy of 95.7% and a resolution of 0.1 mm SWE (Appendix A).

Figure 4.5. Hanging-lysimeter apparatus.

A second measurement of interception was also taken in order to verify the accuracy of the hanging-lysimeters. A 7 m tall spruce tree was hung on a load cell from a boom arm extending from the tower. The tree was positioned within the forest canopy in its original position so that the alterations to the environment and canopy structure were minimized. The strain gauge was installed along the cable to the tower apparatus, and had a maximum load of 227 kg. As with the hanging-lysimeters, the load cell was operationally tested *in situ* and shown to have 100 g resolution and 95% accuracy. Accuracy testing of the hanging-lysimeters was conducted at the Upper Forest site using a set of weights and monitoring instrument readings on the data logger. The hanging-tree lysimeter allowed for continuous measurement of canopy snow loss, whether they were from unloading or sublimation. Hanging tree lysimeters have been used in previous studies and provided an accurate and direct measurement of canopy snow load (Schmidt 1990; Hedstrom and Pomeroy, 1998).

Changes in canopy snow load observed by the hanging-tree lysimeter were calibrated to SWE by dividing the mass of snow on the tree by the projected area of the tree crown. When canopy load is calculated in this manner, reductions in canopy load indicating rapid unloading from the hanging-tree deviate from rapid increases in weight of the three hanging-trough lysimeters by an average of 2% with a RMSE = 2.0 mm SWE (Fig. 4.6). This suggests that the

'calibration is robust' and consistent with the forest canopy mass balance for both accumulation and unloading events.

4.2.5 Capturing unloading

Unloading is a process with great spatial variability. Mass release of the intercepted snow causes spatially concentrated changes in SWE, while meltwater drip occurs in a more uniform distribution of snow accumulation under the canopy (if it refreezes). Previous studies have differentiated meltwater drip and mass release, by canopy air temperatures, using a ratio similar to that proposed by Storck *et al.* (2002). This ratio suggests that the ratio of mass release to meltwater drip is 0.4. A measurement technique for quantifying canopy drip as a component of unloading was developed by Calder and Rosier (1976). A network of plastic sheets was installed underneath the canopy to collect unloaded snow in Scotland. All unloaded snow was collected in plastic sheets, which were then heated in order to melt and funnel the snow into a Tipping Bucket Rain Gauge (TBRG) for measurement. The disadvantages of this method are related to the maintenance of the plastic sheeting, which can be easily torn by falling branches, wind or animals and the requirement of a very mild winter climate. Determining the rate and timing of unloading events is difficult because of the time delay caused by the need to first melt and then route the flow of meltwater from unloading into the TBRG.

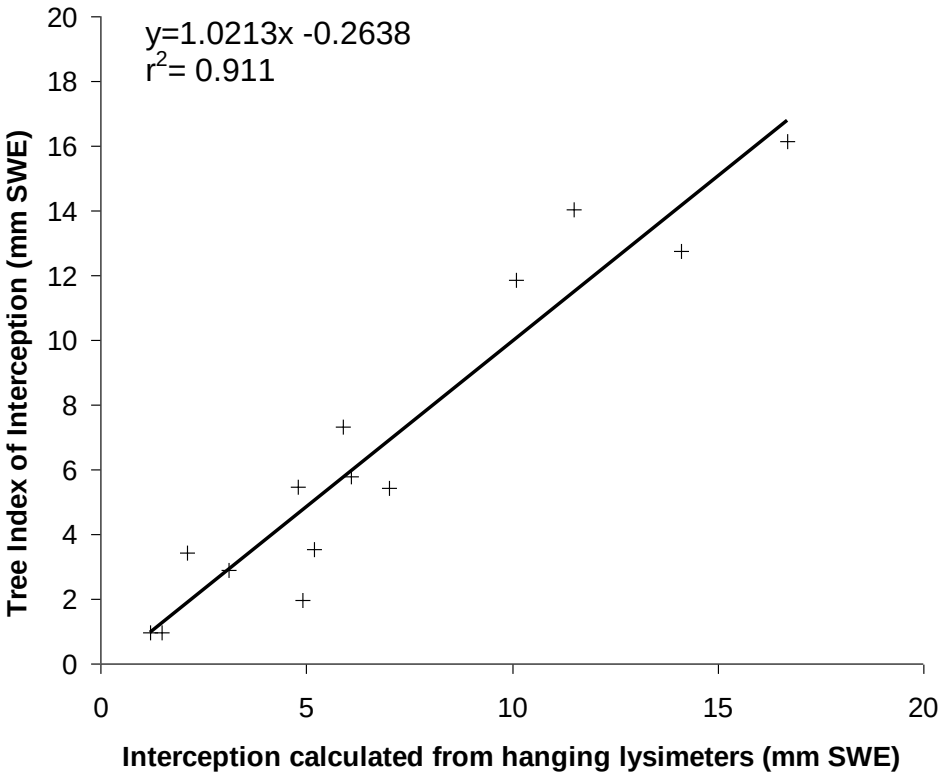

Figure 4.6. Calibration of hanging-tree lysimeter canopy load measurements.

These methods were operationally impossible in MCRB due to a colder climate and the mechanisms in a tipping bucket rain gauge, and the local meteorological conditions were much different than the coastal forests where Stock *et al.* (2002) studied unloading that was characterized by rain on snow events.

The hanging-lysimeters apparatus (Figure 4.5) collected throughfall and unloaded snow from the canopy which had a range in LAI from 2.6 to 4.0 (SVf from 0.128 to 0.231). Each of the hanging lysimeters represented a different forest density, as mentioned previously (section 4.2.2).

The hanging-lysimeters described in section 4.2.1 were installed in varying forest densities (PAI) and were capable of capturing all types of unloading events (Fig. 4.5). These sites were within the immediate vicinity of the hanging-tree lysimeter (within a 15 m radius). Measurements were recorded as mm SWE by taking the observed load (kg) and dividing by the collection area. The hanging-lysimeter apparatus were calibrated for accuracy by using a set of

known weights. The accuracy and resolution of the hanging-lysimeters was satisfactory (95.7% accuracy, 0.1 mm SWE resolution), when compared to that of the Geonor. Hanging-lysimeter output was in 15 min intervals and in mm SWE. This provided the basis for measurement and analysis of unloading rates in the forest stand. The hanging-tree lysimeter used to quantify canopy load was also used to measure unloading of intercepted snow. Decreases in the observed tree weight were interpreted as snow unloading from the canopy or sublimation.

4.2.6 Quantifying sublimation

Sublimation was calculated during the experiment following each snowfall event. A decrease in canopy load which was not recorded as unloading by the hanging-lysimeters was considered sublimation. The possibility of wind transportation accounting for the missing snow quantity was rejected. There were no events in which a decrease in canopy load corresponded to an influx of snowfall to the clearing. All snowfall events recorded in the Forest Clearing site were observed in the Upper Forest site also. This confirms the hypothesis of Troendle *et al.* (1988) that removal of intercepted snow by wind transport is minimal at the stand level. This is contrary to early studies by Hoover and Leaf (1967) that hypothesized that large plumes of canopy snow are responsible for a decrease in canopy snow.

4.3 Evaluation of Model Performance

Model performance was calculated based on model bias (Eq. 4.2) and standard error (Eq. 4.3), Root Mean Square Error (RMSE) (Eq. 4.4), and the coefficient of determination (r^2) (Eq. 4.5) were used to describe the variations within the model output. Model bias describes the level of over or under prediction of the model output and is well suited for hydrological time series data. RMSE and r^2 are used to depict the variation within the model output. These tests were chosen for their simplicity which can be carried out with limited event based data.

$$\text{model bias}\,(\%) = \frac{\text{model output}}{\text{observed data}} \times 100 \qquad \text{(Eq. 4.2)}$$

$$\text{standard error (\%)} = \frac{\text{output}_{\text{observed}} - \text{output}_{\text{model}}}{\text{output}_{\text{observed}}} \times 100 \qquad \text{(Eq. 4.3)}$$

$$\text{RMSE} = \sqrt{\frac{\sum_i (\bar{x} - x_i)^2}{n}} \qquad \text{(Eq. 4.4)}$$

where :

x

x_i

n is the number of samples

$$r^2 = 1 - \left[\frac{\sum_i (x_{obs} - x_{mod})^2}{\sum_i (x_{obs} - \bar{x}_{obs})^2} \right] \qquad \text{(Eq. 4.5)}$$

where :

x_{obs} *is the observed value*

x_{mod} *is the modelled value*

CHAPTER 5

RESULTS

5.1 Data Survey

Marmot Creek Research Basin (MCRB) Upper Forest site has a mixed forest composition (section 4.1). PAI values range from 2.5 – 4.0 with an average value of 3.0. SVf ranges from 0.13 – 0.22 with an average value of 0.19 (Fig. 5.1). An average of the 3 hanging-lysimeter sites was used to depict the sub-canopy snowfall for the entire forest (Fig 5.2).

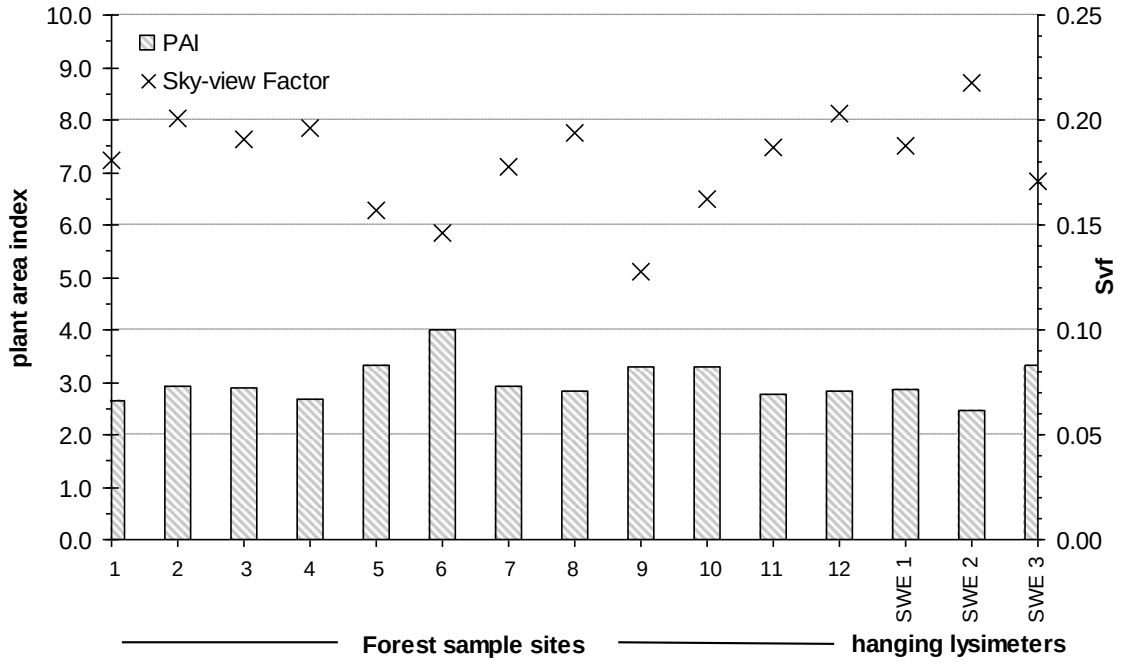

Figure 5.1. Upper Forest characteristics. PAI was measured at 12 sites surrounding the Upper Forest site as well as at the hanging-trough lysimeters (SWE 1-3) in order to obtain an average value for the forest.

The Geonor recorded 134 mm SWE of snowfall between February 14 and April 11 in MCRB during the 06/07 winter (Fig. 5.2a). Forest snow accumulation was 84 mm SWE for the same period due to interception losses. Snowfall in the 07/08 winter was 173 mm SWE between December 2 and April 30 while only 53 mm SWE accumulated on the forest floor (Fig. 5.2b).

Daily averages of above canopy wind speed and air temperature are shown in Figure 5.3. Wind speed was observed above the forest canopy (z = 25 m). Due to errors in the instrumentation program, synthetic wind speed values were generated for winter 07/08. Synthetic wind speeds were interpolated for the Upper Forest site through a linear regression of the 06/07 wind speeds (Appendix A). Maximum average daily wind speeds observed above the forest canopy were 13.1 m s^{-1} in winter 06/07 while the 07/08 winter maximum average daily wind speed was 17.3 m s^{-1}. Winter 06/07 had an average daily wind speed of 3.9 m s^{-1} while the winter of 07/08 average daily wind speed was 3.6 m s^{-1}. Wind speeds from within the forest canopy (13 m) were analyzed to create the unloading model as the impact of wind within the canopy was observed to have more effect on the unloading process than above canopy winds.

Fluctuations in air temperature were recorded just below the top of the canopy (canopy height = 20 m), 18 m above ground level. Snow temperatures within the canopy were not used for the analysis because they closely mimicked changes in air temperature, as a result of the dense forest canopy structure.

The average daily temperature during the snow accumulation period was -5.4 ^{o}C in 06/07 and -6.9 ^{o}C in winter 07/08. Winter 06/07 saw 14 days where melt conditions were present (T_a > 0 ^{o}C) while winter 07/08 had 10 days. The lowest daily temperature in the winter was -19.7 ^{o}C and -30.6 ^{o}C during 06/07 and 07/08 respectively. Average daily air temperature was -5 ^{o}C during the interception events from the 06/07 and 07/08 winters.

a)

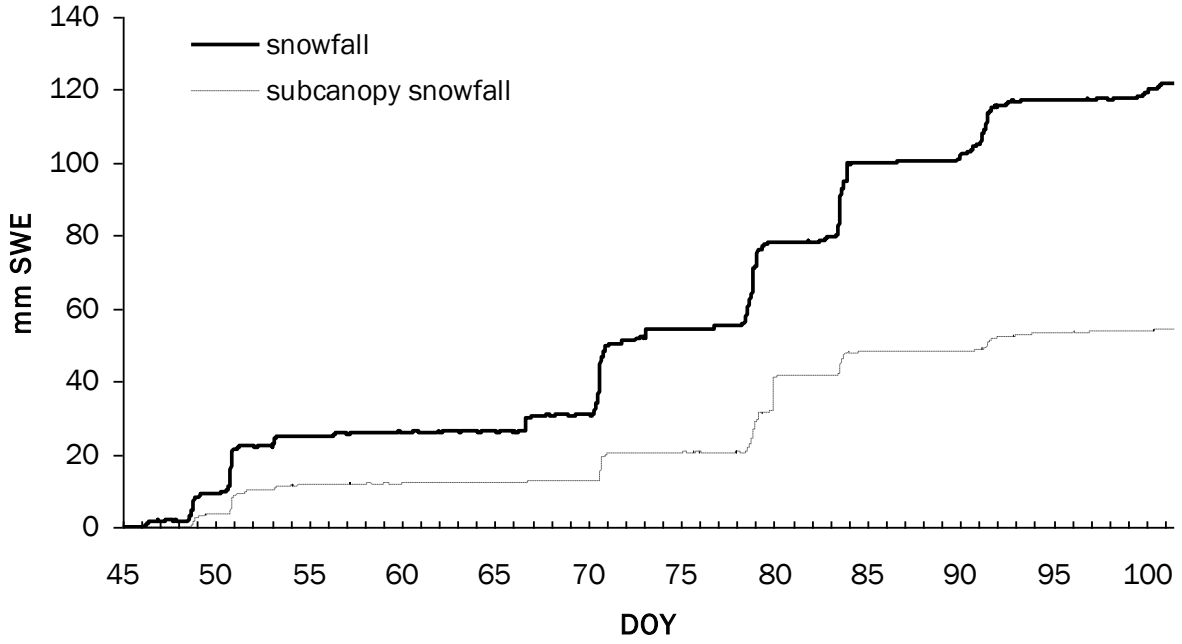

b)

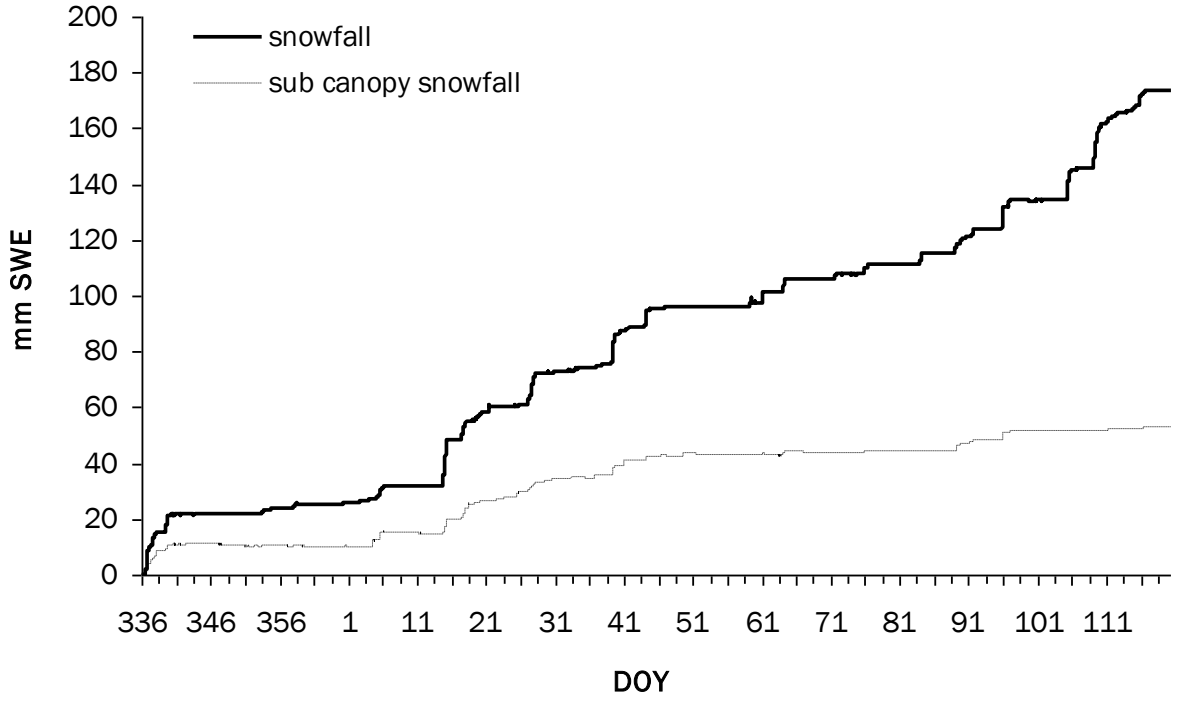

Figure 5.2. Snow accumulation, winter 06/07 (a) and 07/08 (b). Geonor is used for measurement of snowfall, sub canopy snowfall is measured using the hanging-trough lysimeters.

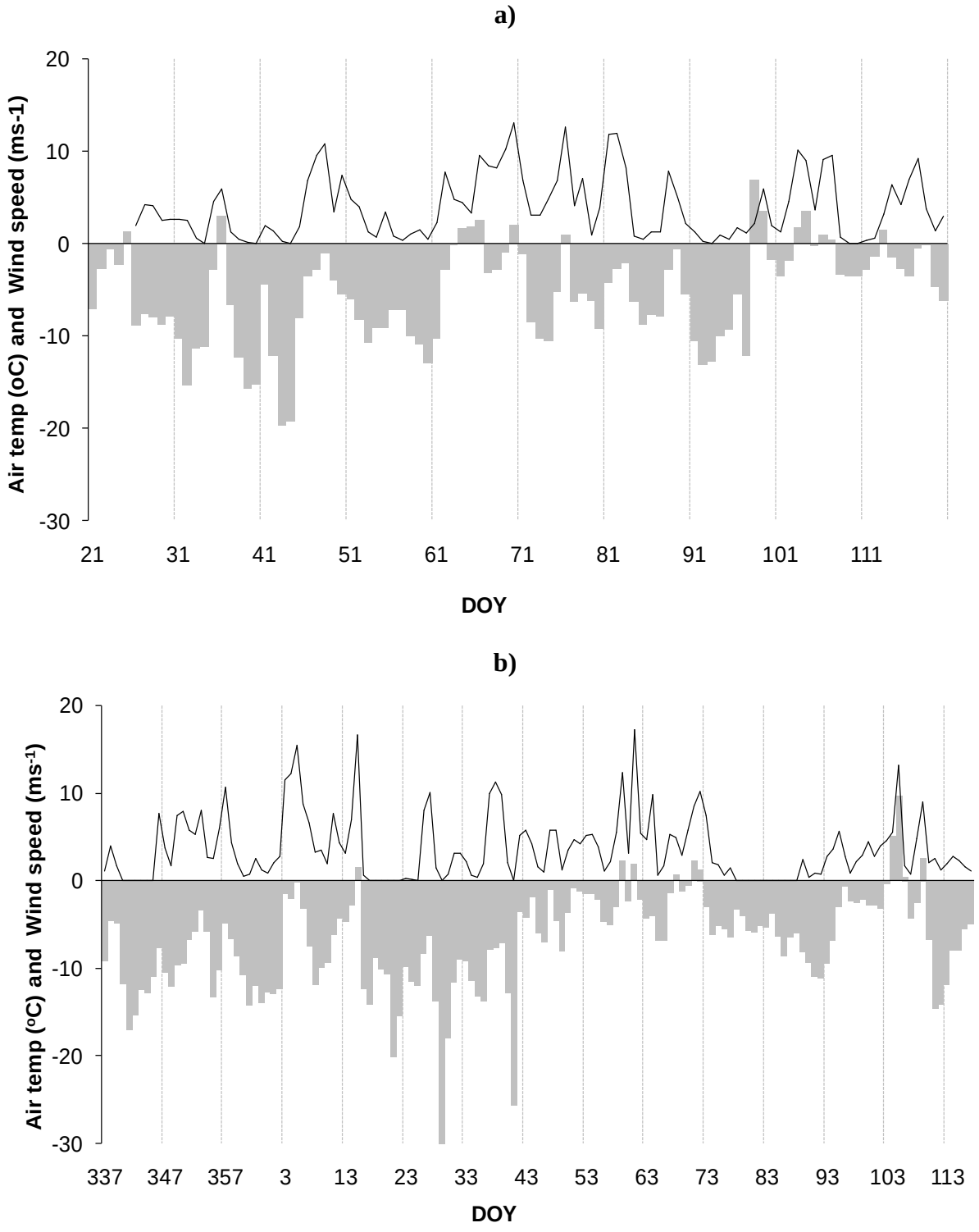

Figure 5.3. Winter 06/07 (a) and 07/08 (b) average daily temperature and wind speed. Wind speeds are depicted by solid line and air temperatures are shown as grey bars.

Interception losses during winter 06/07 and 07/08 were approximately 60% of snowfall (Fig. 5.4). The data points in Figure 5.4 include interception loss measured at each of the hanging-lysimeter sites. Figure 5.4 shows the range in interception losses with forest LAI variability. A typical interception event is shown in Figure 5.5. Snowfall begins at 000 hrs, DOY 49 and is complete at 0915 hrs the same day. Meteorological conditions are shown as daily averages of wind speed and air temperature for each event. There is very little turbulence during the snowfall (wind speed < 2.0 m s^{-1}) and the average temperature during snowfall was -2.0 ^{o}C. There was a lag between the start of snowfall and the appearance of snowfall under the forest canopy. This was unaccounted for and may be the result of the instrument being affected by icing, fallen branches, animals, etc. Furthermore, it can be seen that the sub-canopy snowfall increases as the snowfall increases. The hanging-trough lysimeter, SWE 3 is in the highest density forest and has the longest delay before snowfall reaches the sub-canopy snowpack.

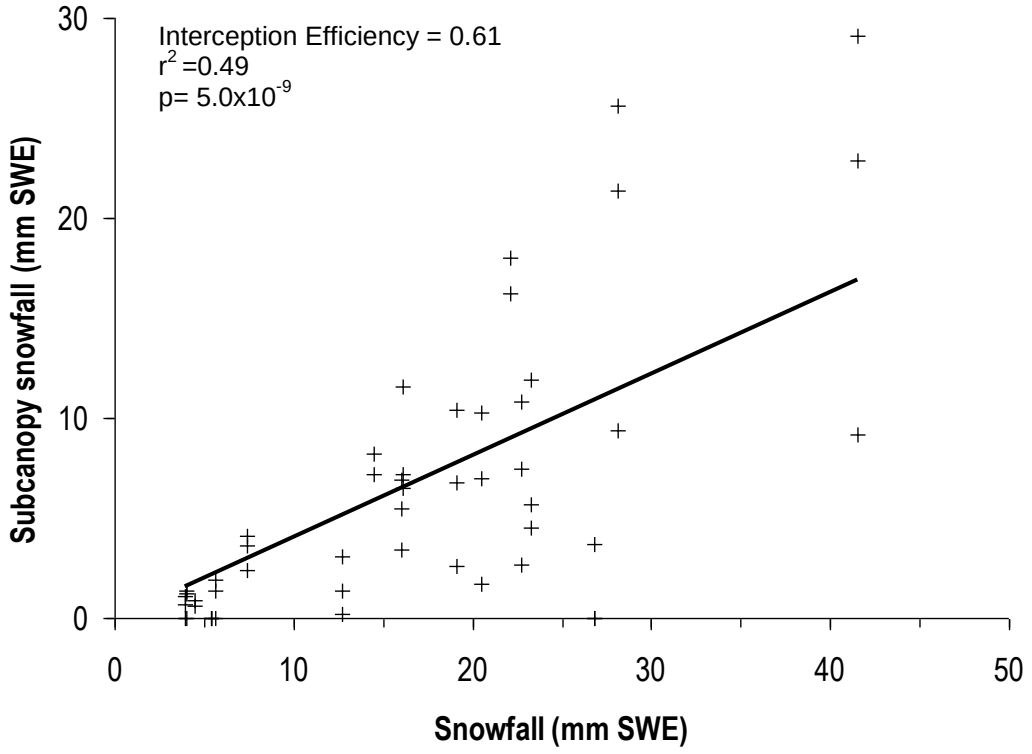

Figure 5.4. Sub-canopy snowfall and snowfall at Marmot Creek Research Basin.

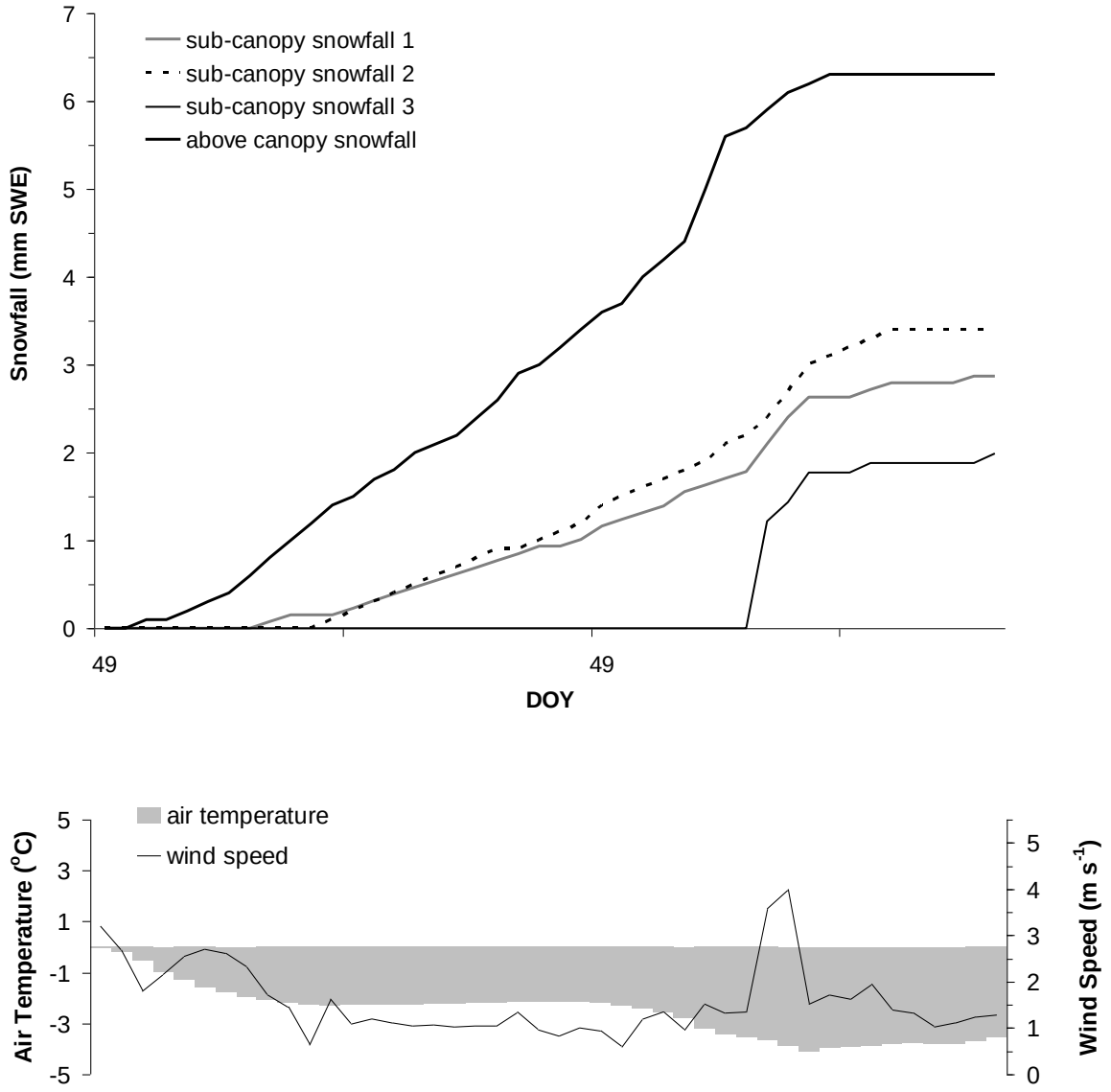

Figure 5.5. Snowfall interception event February 18, 2007. Geonor is recording above canopy, the hanging-trough lysimeters depict sub-canopy snowfall. Sub-canopy snowfall 2 is the least dense site and sub-canopy snowfall 3 is the most dense. Wind speeds (mid-canopy = 13 m) are from 15 min data and air temperatures are hourly averages. The event begins at 000 hrs on DOY 49 and continues until 1200 hrs on DOY 49 (3 hr intervals on axis).

5.2 Unloading Events

Unloading occurred during 11 of the 15 interception events where canopy load was > 1 mm SWE (Table 5.1). Each event considered for analysis was deemed significant based on the magnitude of interception (canopy load >1 mm SWE), and the percentage of the canopy that unloaded (>10%). Unloading was responsible for an average reduction in canopy load of 42%. Air temperature during unloading ranged from -12 ^{o}C to 2 ^{o}C, with an average of -4.4 ^{o}C. Mid-canopy wind speeds of up to 12 m s^{-1} were observed during unloading events. The average gust factor during unloading events was 4.6 with a range from 1 to 10 (Table 5.1).

The residence time of intercepted snow in the canopy ranged from as short as 8 hrs to as long as 9 days (216 hr) for all intercepted snow to be released. The residence time was measured from the completion of snowfall to either the time when unloading ceased to continue, or when snowfall resumed.

A typical example of unloading by mass release occurred on March 20th, 2007 (Fig. 5.6). This snowfall interception event saw 22.0 mm SWE of snow recorded by the Geonor and 10.5 mm SWE intercepted. Following snowfall, air temperature decreased overnight to a low of -8 ^{o}C. Air temperature then increased through the next day and small turbulent bursts of wind appeared in the afternoon. Unloading occurred at mid-day (1200 hrs) when air temperature was -5 ^{o}C average mid-canopy wind speed was 2 m s^{-1}. The gust factor increased to 6 during time of unloading. An unloading event of 9.5 mm SWE was recorded at 1200 hrs; approximately 14 hrs after snowfall had ceased (Fig. 5.6). Unloading in this event reduced the interception loss by 90%, increasing the sub-canopy snowpack by 9.5 mm SWE (Table 5.1).

Table 5.1. Winter 06/07 and 07/08 snowfall and unloading event data.

DATE	Snowfall mm SWE	Canopy Load mm SWE	Unloading mm SWE	Unloading % of load	Net Interception mm SWE	Residence Time	Unloading Conditions air temperature °C	Unloading Conditions mid canopy wind speed m s^{-1}	Unloading Conditions gust factor
Winter 06/07									
February 18	6.3	3.7	0.4	39	3.3	8 hr	-4	2	1
February 18	1.0	0.8	0.3	37	0.5	36 hr	-8	3	1
February 20	13.0	6.3	0.8	64	5.5	8 hr	-6	5	5
February 20	3.0	1.5	0.5	18	1.0	48 hr	-6	3	1
February 20	1.0	0.7	0.5	21	0.2	48 hr	-3	1	3
March 21	22.0	10.5	9.5	27	0.8	14 hr	-5	2	6
April 18	17.3	7.2	4.6	39	2.6	10 hr	2	3	3
Winter 07/08									
December 3	15.0	13.0	5.1	11	7.9	12 hr	0	12	10
December 12	9.0	8.3	3.1	38	5.2	7 day	-5	12	7
January 4	4.5	2.8	1.8	13	1.0	36 hr	-3	8	5
January 20	29.0	19.0	3.5	33	15.5	4 day	-6	4	6
January 29	15.0	14.0	2.9	71	11.1	9 day	-12	5	6
February 8	12.8	11.0	3.0	90	8.0	36 hr	-2	12	7
February 13	6.9	5.6	2.2	64	3.4	40 hr	-5	8	8

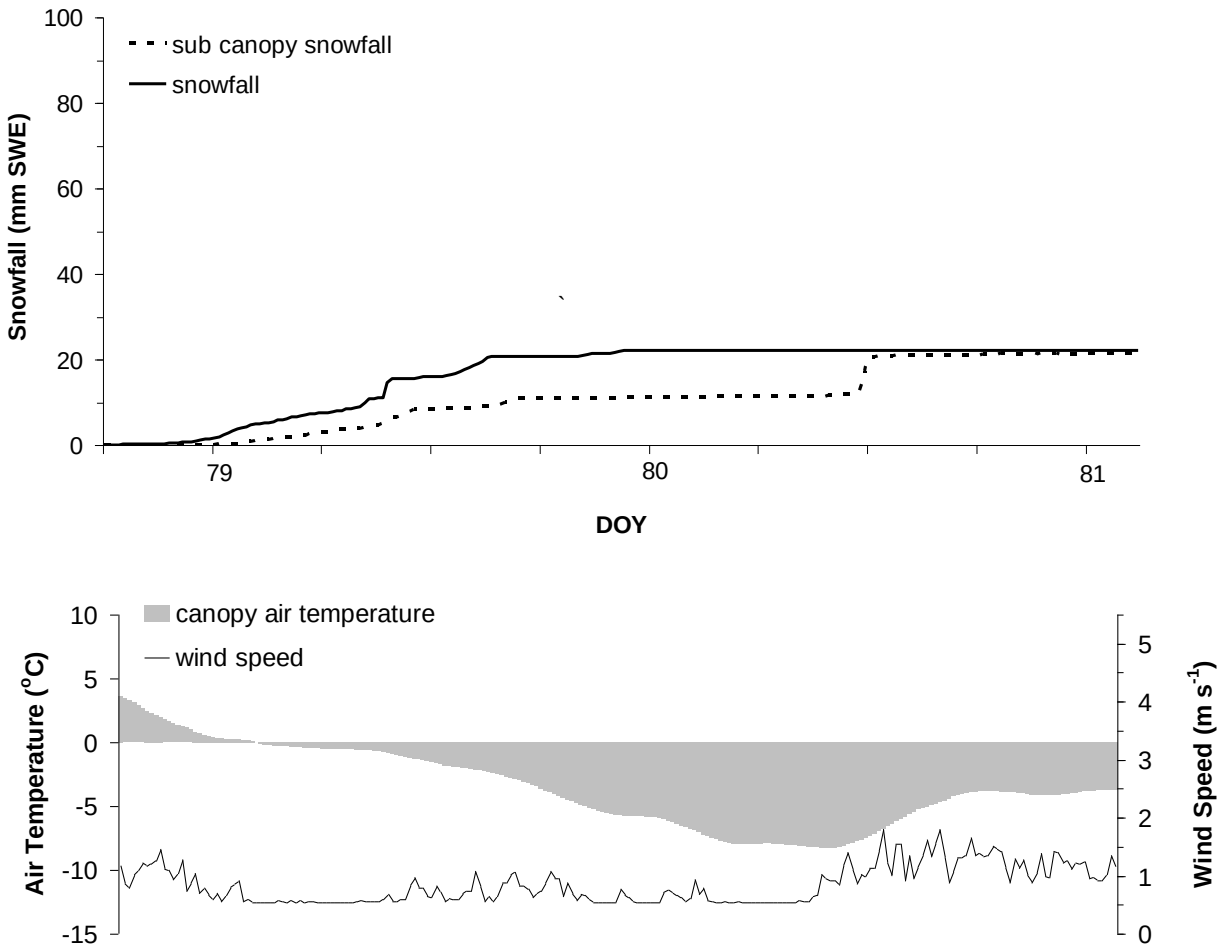

Figure 5.6. Unloading of intercepted snow: March 20-22, 2007. Mid-canopy wind speeds and air temperatures are shown.

CHAPTER 6

ANALYSIS

6.1 Interception evaluation

The forest intercepted 60% of the snow that fell during the study period of winters 06/07 and 07/08 (Fig. 6.1a). The average interception efficiency (%) was determined by the slope of the line in Figure 6.1. The average residence time of the canopy load was 53 hr (Table 5.1). Unloading of the canopy load decreased the interception loss by 40% (Fig. 6.2). Net interception (interception-unloading), the total loss of snowfall due to sublimation, for MCRB is therefore 41% of snowfall (Fig 6.1b). The relationship between forest density and subcanopy snow accumulation is shown in Figure 6.3. No direct relationship can be seen between forest density and snow accumulation throughout the winters of 06/07 and 07/08.

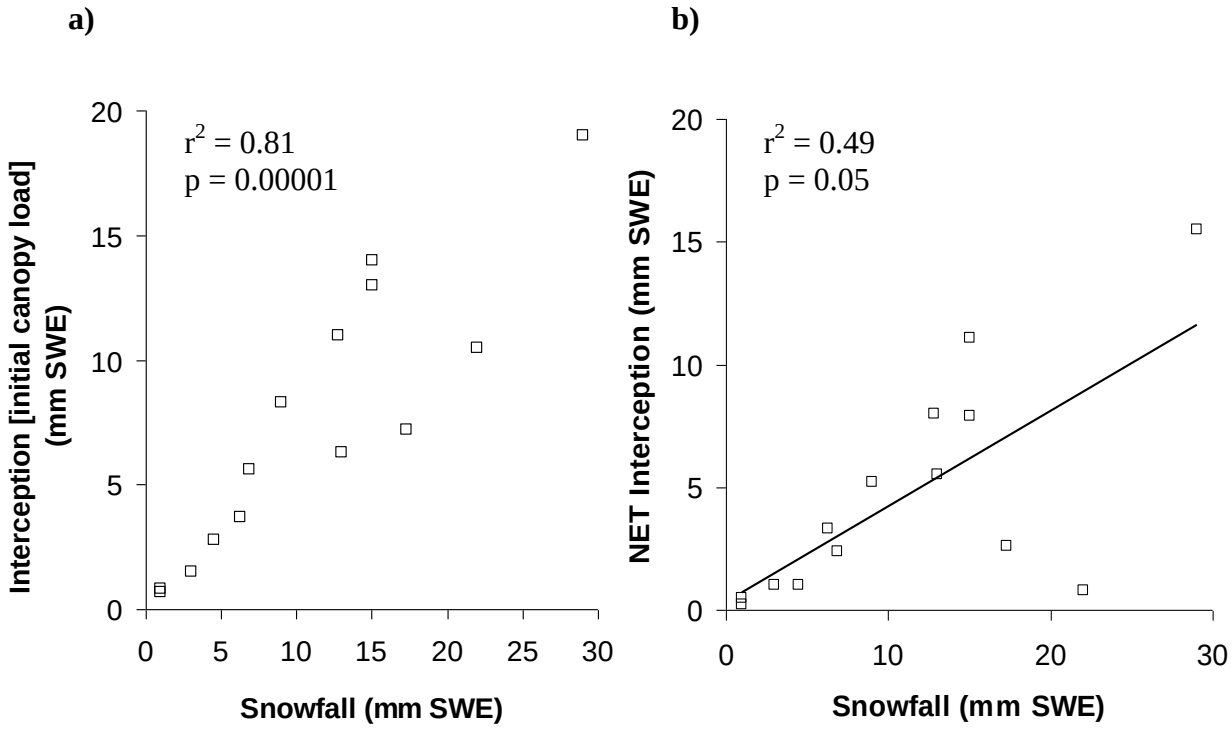

Figure 6.1. Interception (a) and net interception (interception-unloading) (b) compared to snowfall during the winters of 06/07 and 07/08.

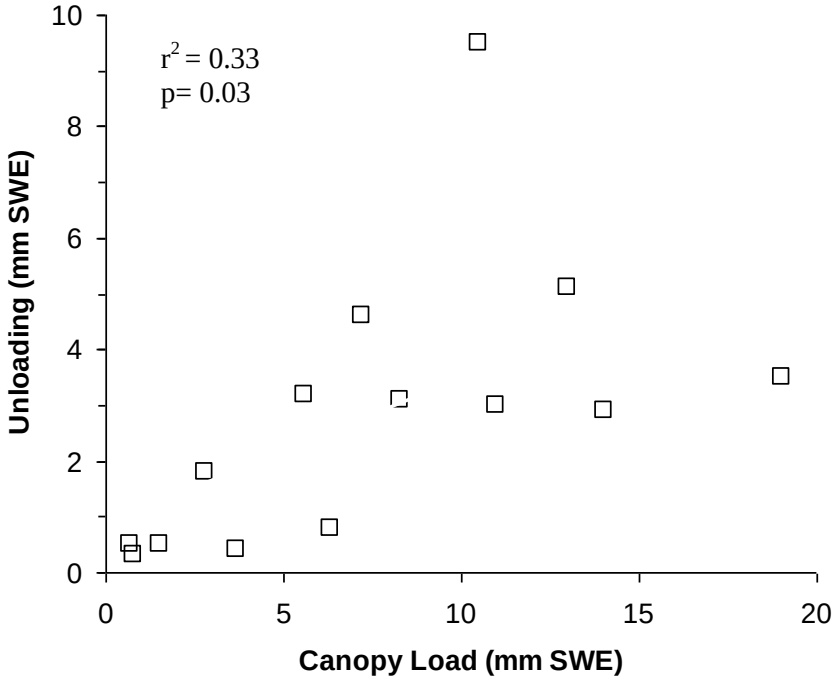

Figure 6.2. Unloading versus canopy load in MCRB.

a)

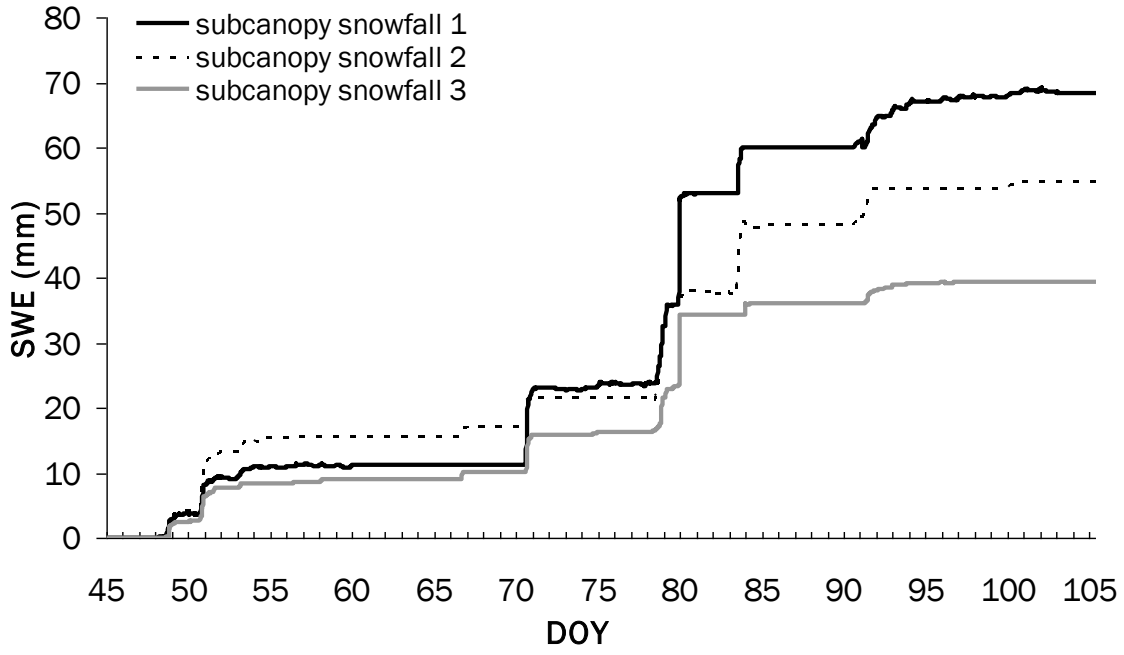

b)

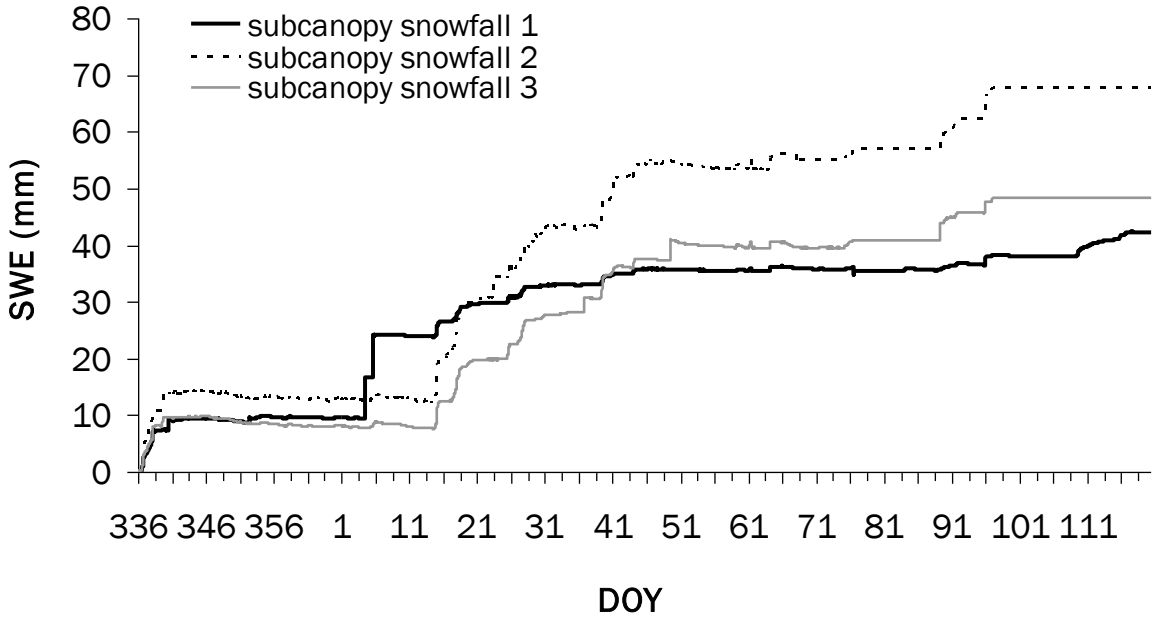

Fi

Figure 6.3. Subcanopy snow accumulation at the three subcanopy hanging-lysimeters in MCRB winter 06/07 (a) and 07/08 (b).

6.2 Unloading Model Intercomparison

The most common unloading models available and used in hydrological models are the Hedstrom-Pomeroy function used by Gelfan *et al.* (2004), the Bartlett adaptation on the H-P model (Bartlett *et al.*, 2006) found in CLASS, the Storck ratio (Stork *et al*., 2002) found in MOSES2c (Essery *et al*., 2003), and the Roesch *et al*. (2001) model found in ECHAM4. This section presents each of these models applied to the MCRB study site and evaluates model performance.

6.2.1 Hedstrom-Pomeroy model

The application of the McNay *et al.* (1988) linear relationship and the Hedstrom-Pomeroy exponential function is shown in Figure 6.4. The McNay *et al.* model had a model bias of 0.86 and a standard error of 30.3% (RMSE=3.04 mm SWE). The Hedstrom-Pomeroy model had a bias of 0.78 and a standard error of 7.6% (RMSE=3.21 mm SWE). There is considerable variation in over and under-estimation of interception by the Hedstrom-Pomeroy model which creates a misleading standard error value. Errors in model estimation offset each other and therefore it must be applied cautiously to hydrological models.

The Hedstrom-Pomeroy interception model is a physically based model as it includes parameters of maximum canopy load and storage capacity in the canopy. The improvement on McNay *et al.* (1988) is that the model is no longer a simple linear function. Canopy storage capacity in MCRB was observed to be as high as 19 mm SWE. The Hedstrom-Pomeroy model estimates L^* = 14.7 mm SWE when using a species loading coefficient for spruce, given by Schmidt and Gluns (1991). Because there was a discrepancy between the modeled and observed L^*, the species loading coefficients may not apply to the tree species and canopy structure of the Rocky Mountains.

An attempt to increase the accuracy of the Hedstrom-Pomeroy model with this dataset used observed value of L^* at MCRB. L^* was calibrated to the study site by taking the maximum snow interception event measured by the hanging-tree lysimeter. Substitution of the observed value for L^* (24 mm SWE) allowed for a model bias =1.01 and a standard error of (19.4%) (RMSE=2.4 mm SWE). Though the model bias and RMSE are improved, the standard error increases when the Hedstrom-Pomeroy interception model is calibrated with the observed L^*.

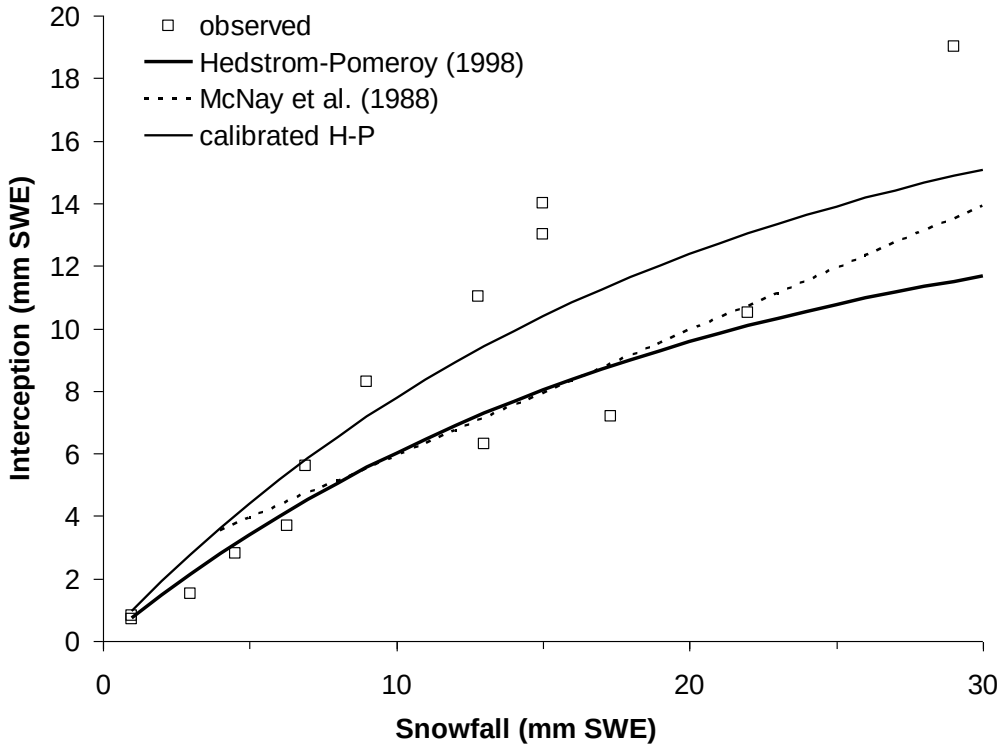

Figure 6.4. Interception model comparison to observations. The McNay *et al.* (1988) and Hedstrom and Pomeroy (1998) models are compared to observations at MCRB

The exponential decay function of the Hedstrom-Pomeroy unloading model (Hedstrom and Pomeroy, 1998) is shown in Appendix B (Figure B.1). Model bias was 0.59 for estimation of unloading (Table 6.1). The model has an accuracy of 84% but contains a high degree of underestimation (RMSE = 3.43 mm SWE). The Hedstrom-Pomeroy model lacks the ability to vary the rate of unloading with changing meteorological conditions.

The Gelfan *et al.* (2004) model (Eq. 2.17) integrates the Hedstrom-Pomeroy model (Eq. 2.16) with the decreases in canopy load due to sublimation losses. Unloading occurs only from the snow in the canopy which has not already been sublimated. An additional mechanism for unloading is included in the Gelfan *et al.* model which dumps the remaining canopy load as unloading under conditions that favour melt. In this situation, all remaining snow in the forest canopy is unloaded. Unloading rates are known to increase in isothermal snow conditions (Pomeroy and Gray, 1995). Furthermore, the dumping mechanism is not unlike the unloading model by Storck *et al.* (2002).

Table 6.1 Hedstrom and Pomeroy (1998) modeled output for unloading events.

Canopy Load mm SWE	Calculated Unloading mm SWE	Modelled Unloading mm SWE
3.7	0.9	0.5
6.3	0.7	0.4
1.5	0.3	0.3
0.7	0.4	0.3
10.5	9.7	0.6
7.2	4.4	0.3
13.0	2.3	0.5
8.3	2.4	4.0
2.8	2.8	0.1
14.0	2.8	8.1
11.0	2.1	1.5
5.6	0.5	0.8
	MODEL BIAS	**0.59**

The Pomeroy et al. (1998) and Gelfan *et al.* (2004) model could not be tested on the MCRB data. Without a direct measurement of sublimation rates, and sublimation estimations derived from observed unloading, the model cannot function.

6.2.2 CLASS Unloading algorithm

The unloading algorithm used in CLASS is the basic Hedstrom-Pomeroy model with a different coefficient of unloading. Bartlett *et al*. (2006) looked at unloading of intercepted snow on a canopy scale through changes in forest albedo. Data from the boreal forest depicted a faster rate of unloading than the 0.0969 day^{-1} that was initially proposed by Hedstrom and Pomeroy (1998). Albedo changes in the forest canopy were linked temporally to changes in canopy load by Bartlett *et al.* (2006). Bartlett *et al*., suggest the unloading coefficient from the Hedstrom-Pomeroy model be applied on an interval of 2 days as opposed to 7 days. The new unloading coefficient is therefore 0.339 day^{-1} (Bartlett *et al.*, 2006). These coefficients of unloading are based on a half-life decay function and the observations of unloading in event data.

Intercepted load in the MCRB was poorly associated with the daily albedo of the forest (Fig. 6.5). Correlation between forest albedo and canopy load had an $r^2 = 0.34$. Studies by Pomeroy and Dion (1996) show no relationship between canopy load and forest albedo, while Yamazaki *et al*., (1996) have seen a positive correlation. Radiometers that are snow-covered can cause spuriously high albedo readings that can be misinterpreted as due to real albedo variations. Fundamentally, changes in albedo are controlled by changes in canopy load, which may be from sublimation or unloading. Differentiating between these two processes is impossible using albedo changes; therefore the Bartlett *et al*. model is more appropriate to modeling canopy snow losses (sublimation and unloading).

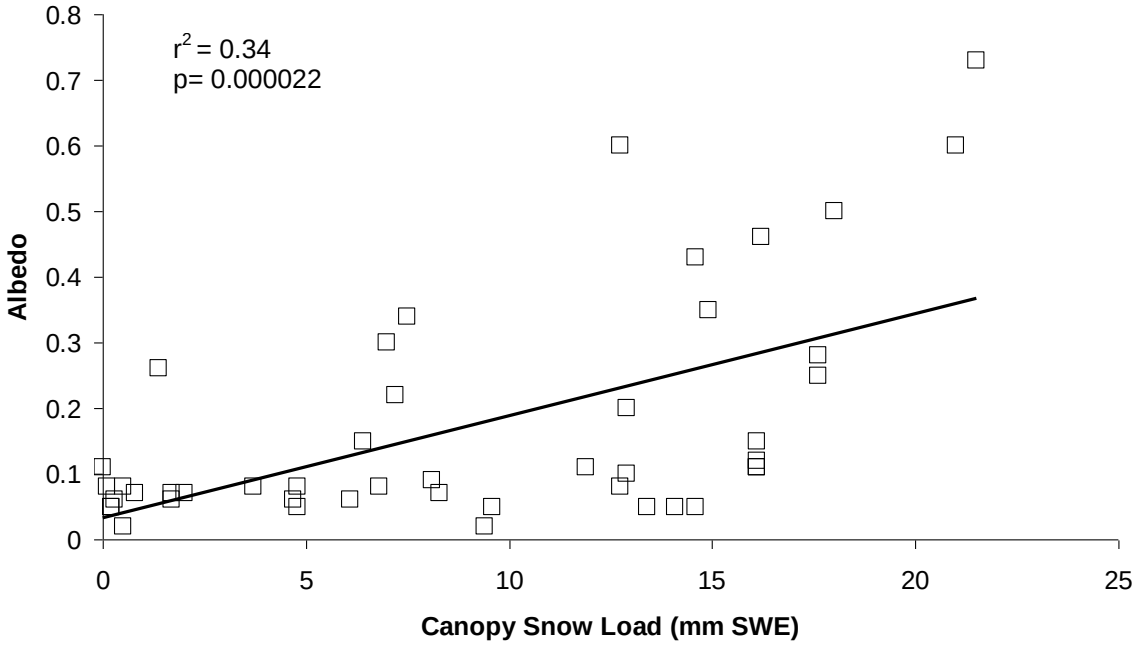

Figure 6.5. Relationship of forest albedo to canopy load at MCRB (SWE).

When the Barlett *et al*. (2006) model is used to calculate unloading during the study period, it overestimates unloading by 52% on an event basis (Table 6.2). The model output has a 51.7% error and a RMSE = 4.8 mm SWE. Time series of observed unloading versus modeled unloading depict the relationship between model output and canopy snow loss in two separate unloading events with different characteristics (Fig. 6.6). The February 10th, 2008, unloading event (Fig. 6.6.a) shows an initial period of unloading while the December 12th, 2007, unloading

event (Fig 6.6.b) shows an event where unloading occurs over a longer time period and of a steady rate.

Table 6.2 Bartlett *et al.* (2006) modeled unloading.

Canopy Load mm SWE	Calculated Unloading mm SWE	Modelled Unloading mm SWE
13.0	5.1	2.1
8.3	3.1	7.6
2.8	1.8	1.2
19.0	3.5	14.4
14.0	2.9	13.4
11.0	3.0	4.5
5.6	3.2	2.6
3.7	0.4	0.6
0.8	0.3	0.3
6.3	0.8	1.0
1.5	0.5	0.8
0.7	0.5	0.4
10.5	9.5	2.4
7.2	4.6	1.2
	MODEL BIAS	**1.3**

a)

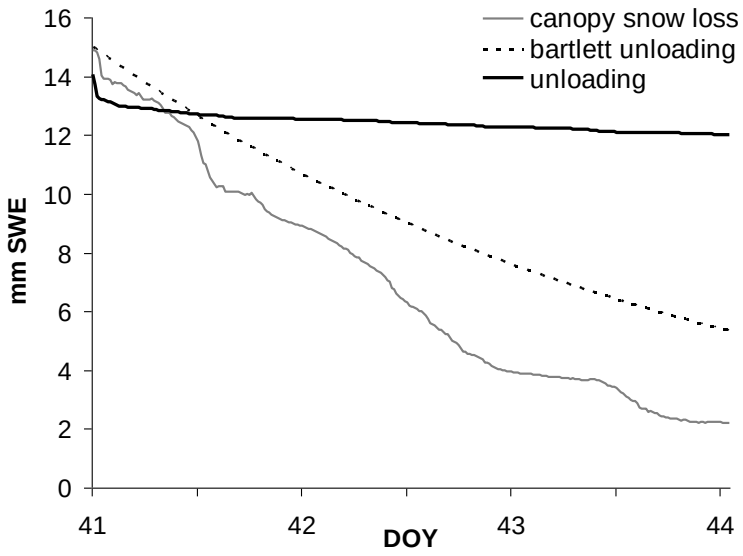

b)

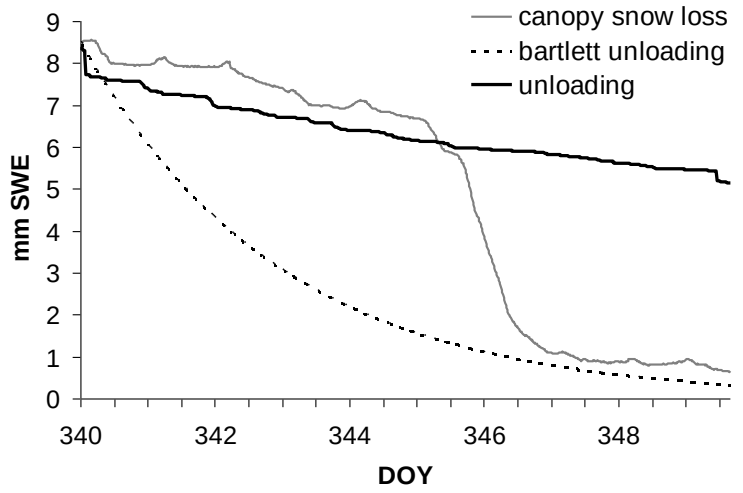

Figure 6.6. Bartlett *et al. (*2006) cumulative unloading model output for two separate 07/08 events.

6.2.3 Storck model

Storck *et al.* (2002) developed a model for interception/unloading in the maritime climate of the Coast Mountains in Oregon, USA. Here, unloading accounted for 30% of the canopy load and sublimation rates were as high as 4.3 mm in 7 hrs. Meltwater drip was observed

to be the trigger mechanism for mass release when the wind regime was not turbulent enough to unload snow. Unloading events which lacked melt conditions were not present; inhibiting the ability to model wind induced unloading or other mechanisms found in cold environments.

Modeling of the unloading process by Storck was limited to interception events when melt conditions are present. During these melt conditions; lysimeter data recorded 70% of unloading occurred as meltwater drip and 30% as mass release. Meteorological conditions prevalent in maritime climates such as rain on snow and mild air temperatures influenced the unloading process. Meltwater drip and mass release were recorded simultaneously in all unloading events. A ratio of mass release to meltwater drip (0.4) was developed for unloading events. In order for this ratio to be applied there must be melt conditions present in the canopy.

In MRCB meltwater drip was observed only once and was not able to be captured by the TBRG's due to equipment icing. Melt conditions ($T_a \geq 0\ ^oC$) were present only twice, while there were only three events which approached meltwater production ($T_a \geq -3\ ^oC$). Therefore, the Storck *et al.* ratio is not applicable to MCRB or continental climates. MOSES2c integrates the Storck model with a Hedstrom and Pomeroy model (1998) for the snow which is not sublimated when melt conditions occur.

6.2.4 Roesch model (ECHAM4)

The Roesch *et al.* (2002) model is the most complex algorithm for estimation of unloading (Eq. 2.19). Meteorological conditions of air temperature and canopy wind speed are included within the model making it applicable to all environments. A threshold renders unloading due to melt non-existent when air temperature < -3 ^oC. Model output was converted to the percentage of canopy load and applied to 15 min data.

A Roesch *et al.* model run of the MCRB unloading events is shown in Figure 6.7 as the dashed line versus the observed unloading (solid line). The model performs well at capturing the timing of unloading but has a tendency for over-estimation (Appendix B.3). Model bias was 0.93 and standard error was 0.20 (RMSE= 2.72 mm SWE). Over-prediction of unloading was greatest for events where unloading < 1.0 mm SWE, while underestimation occurred on the larger unloading events. Elimination of unloading events that are under 1.0 mm SWE increased the model accuracy to 80% (RMSE=2.89 mm SWE).

The Roesch *et al.* (2001) model is comprised of two separate functions which attempt to describe the unloading process. The increases in rates of unloading did match the observed unloading during periods of air temperatures approaching 0 ^{o}C. Deficiencies in the model output appeared to be related to the wind function. Increasing the wind speed constant (1.57 x 10^{5} s^{-1}) in the unloading function did not result in an increase in model performance. The wind regime in MCRB is turbulent and unloading oscillation of the trees is dominated by turbulent bursts (Fig. 5.4). Wind gusts are not accommodated in the Roesch *et al.* model.

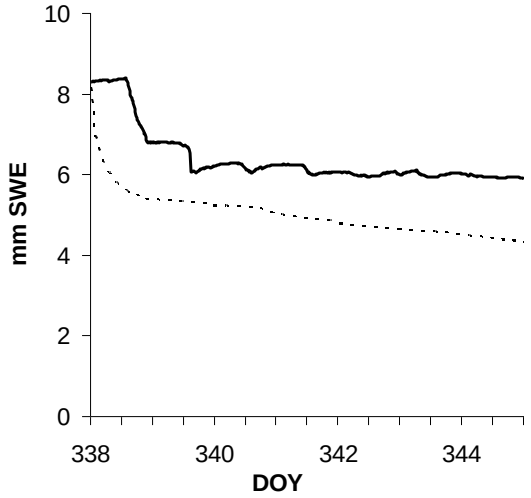

Figure 6.7. Unloading time series using the Roesch et al. model for a 07/08 event. Modelled $\sum$**U** is shown as the dashed line and observed $\sum$**U** as the solid line.

6.3 Unloading in Marmot Creek Research Basin

6.3.1 Unloading trends

The relationship between canopy load and unloading was weak in MCRB (p value = 0.03 and r^2 = 0.33) (Fig. 6.2). It would seem that atmospheric conditions such as mid-canopy wind speed and air temperature are considered the most important data to model rates of unloading.

There was no discernable trend between the rate of unloading and meteorological conditions. A graph comparing unloading, as a percentage of canopy load to average-daily canopy air temperature during unloading is shown in Figure 6.8. No relationship is apparent

between unloading and average-daily air temperature (r^2=0.07), and can been seen by the large amounts of scatter in the data.

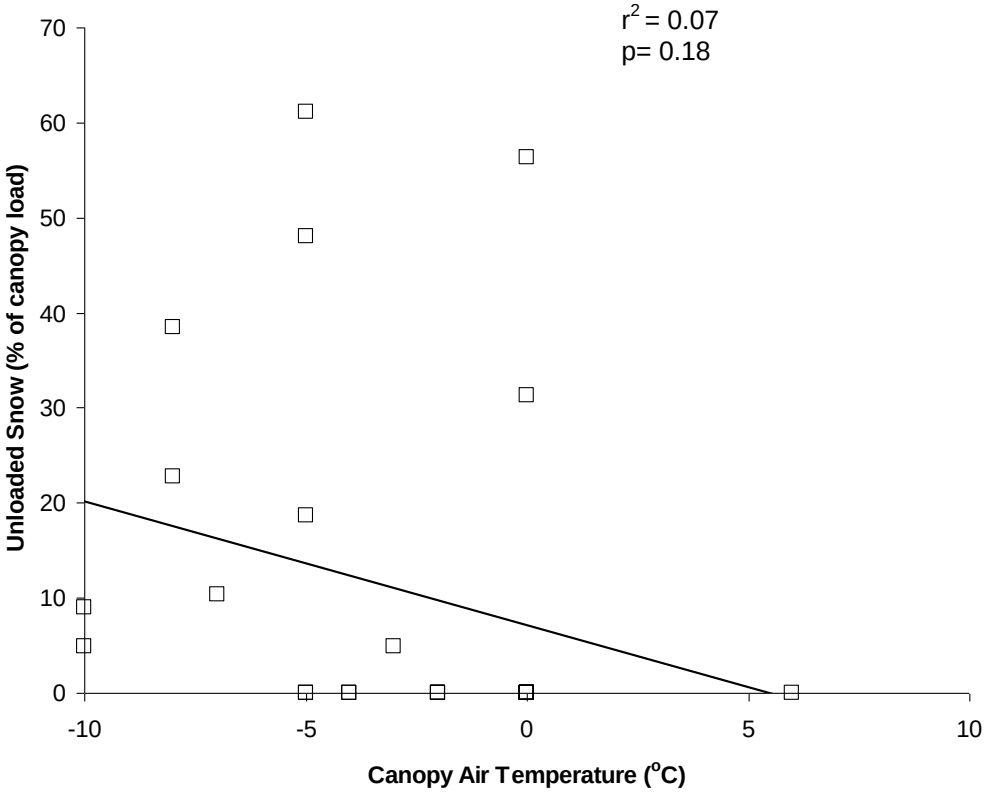

Figure 6.8. Unloading as a function of average-daily canopy air temperature.

The relationships between unloading and other measures of temperature are shown in Figure 6.9. The high degree of scatter shows that unloading is unpredictable when related to air temperature within the forest canopy. The relationship between maximum-daily air temperature and unloading has an r^2= 0.07 (Fig. 6.9.a). Changes in canopy air temperature prior to unloading also lacks correlation (r^2=0.11) (Fig. 6.9.b.). A wide range of temperature conditions are present where unloading rates are negligible. Therefore, unloading rates cannot be predicted from temperature conditions in the forest canopy.

Relationships between unloading and mid-canopy wind speed were non-existent as depicted in Figure 6.10. Parameters of maximum mid-canopy wind speed during the unloading event and the mean gust factor during the event had r^2 values less than 0.01. There is no trend in unloading rates based on mid-canopy wind speeds depicted in the data.

Residence time of canopy load was looked at for a relationship to rates of unloading. No relationship was found. The results of this analysis show a very poor link between time since snowfall interception to unloading and therefore no trend can be found (r^2=0.05) (Fig. 6.11). The spread of large and small unloading events at very low time intervals suggests a trigger mechanism has greater control on unloading then the storage time period.

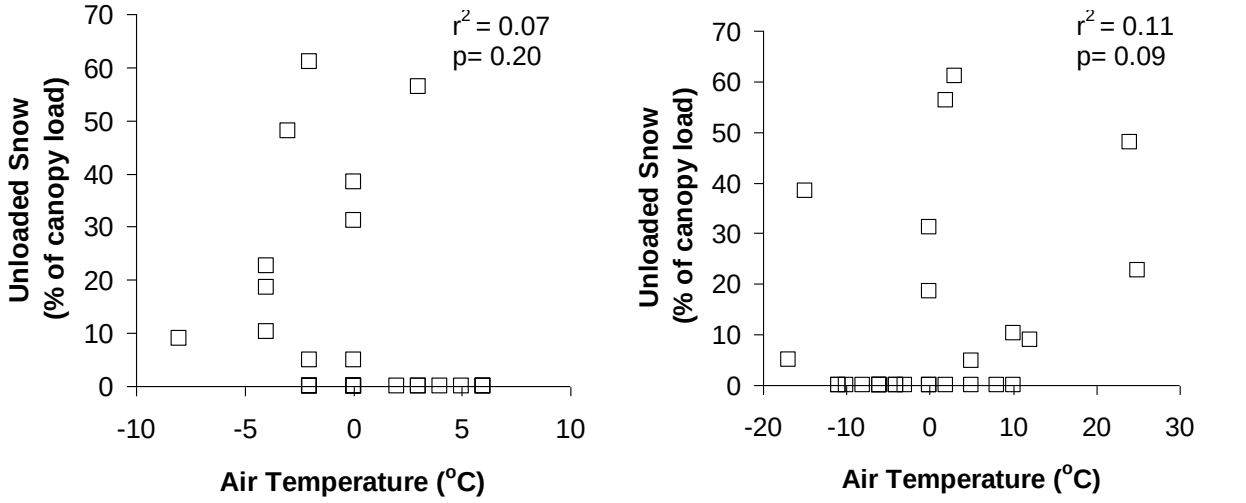

a) maximum-daily temperature **b) change in temperature during unloading**

Figure 6.9. Relationship between unloading and canopy air temperature.

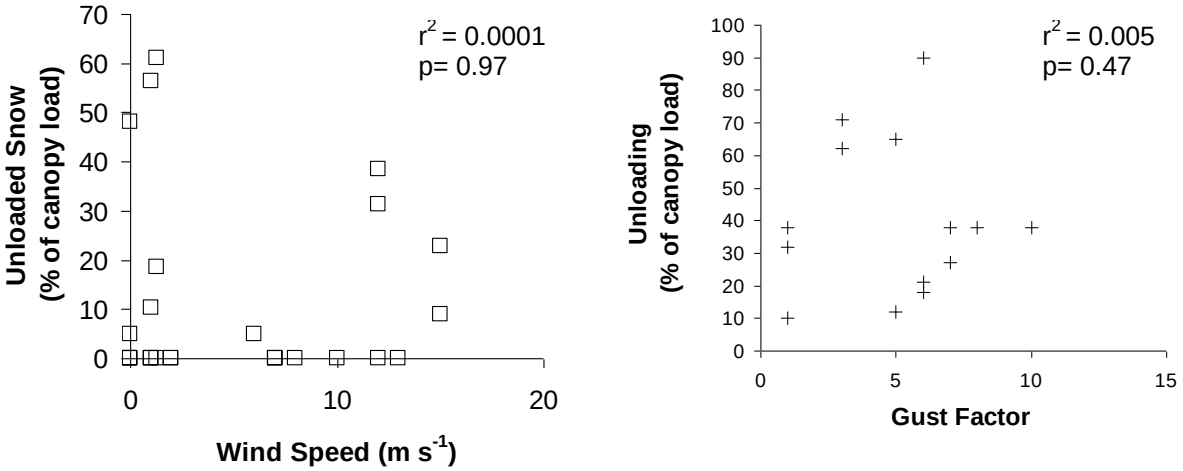

a) maximum event mid-canopy wind speed

b) event gust factor

Figure 6.10. Relationship between unloading and wind speeds.

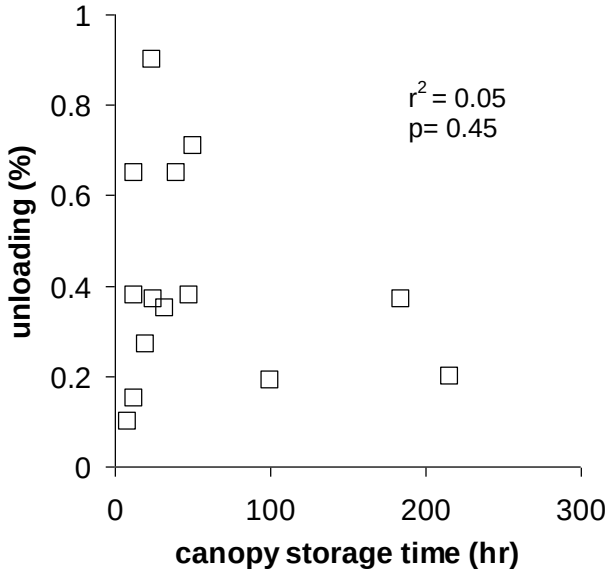

Figure 6.11. Relationship between unloading and storage time in canopy.

6.3.2 Unloading to Sublimation Ratios

Sublimation was calculated, by a mass balance approach, as the difference in the change in canopy snow load less the unloading which was measured as an average of the three hanging-trough lysimeters (Fig. 6.12). It was assumed that the entire canopy snow loss is partitioned into either sublimation or unloading. Some uncertainty is inherent in the estimation of sublimation due to spatial variability and scaling of the unloading process from a tree (point) to a forest (area). The second assumption made is that the tree weight gives an accurate representation of the change in canopy load for the whole forest. Sublimation was calculated from a mass balance approach whereby the canopy snow loss, which includes unloading and sublimation losses from the canopy snow load, was obtained from the hanging-tree lysimeter.

Unloading was directly measured at the three hanging-trough lysimeters which provide an average unloading value for the Upper Forest site. Any change in canopy snow load which was not recorded by the hanging-trough lysimeters was due to sublimation. Validating the accuracy of the hanging-tree lysimeter and its representation of the Upper Forest was done by comparing the residual of snowfall recorded by the Geonor and the hanging-troughs. The fact that unloading rates are an average value and the hanging-tree data is from a single point will introduce some error to calculating sublimation by the mass balance approach.

A limited number of events were possible for this analysis because of the necessity for the hanging-tree and hanging-trough lysimeters to all be operational. The hanging-tree lysimeter was the only measure of sublimation losses and it was only operational during the 07/08 winter. It was necessary for unloading events to be large enough to have confidence in the measurements and all events where unloading was < 1.0 mm SWE were eliminated for analysis.

Cumulative sublimation (ΣS) for each interception event displays a trend with cumulative unloading (ΣU) (Fig. 6.13). The average $\Sigma U / \Sigma S$ ratio for each unloading event which had sublimation data available is shown along with the r^2 of a simple linear relationship in Table 6.3.

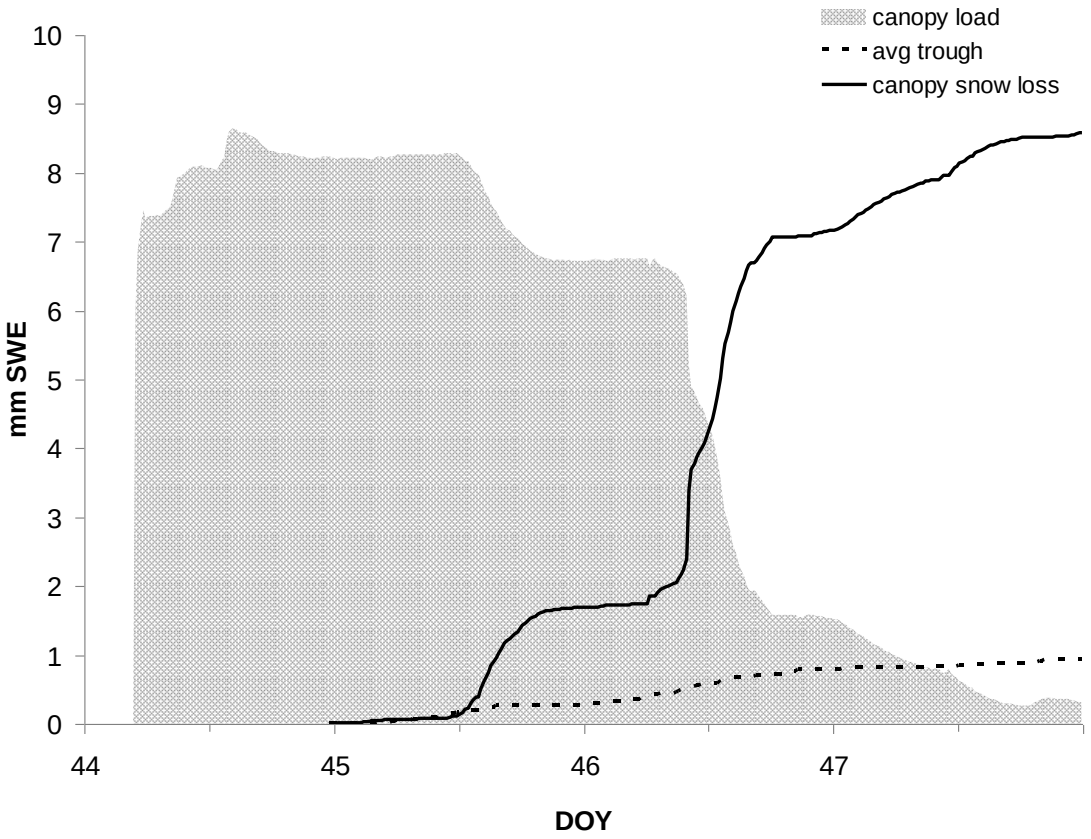

Figure 6.12. Estimation of sublimation loss in MCRB during 07/08 unloading event. Canopy snow loss is observed by decreases in the hanging-tree mass, unloading is what registered in the trough. Sublimation loss is calculated using a mass balance approach to be the change in canopy load not observed as unloading.

The ratio of ΣU/ΣS was established for each of the unloading events where data was available from both the hanging-trough and the hanging-tree lysimeters. The ratio of ΣU to ΣS for each of the unloading events used in the analysis is listed in Table 6.3 with their respective r^2. Cumulative sublimation and unloading were chosen because they eliminated the errors associate with small-scale time data. The high spatial variability in the unloading process meant that cumulative data would have a higher ability to quantify all unloading that occurred.

The ratio which describes the partitioning of canopy load to either unloading (if large, >1) or sublimation (if small, <1) in a forest environment was evaluated for variation with wind speed and temperature conditions, and time since interception. Air temperature and wind speed were chosen due to their known association with sublimation rates and as possible trigger mechanisms for unloading, determined from the literature.

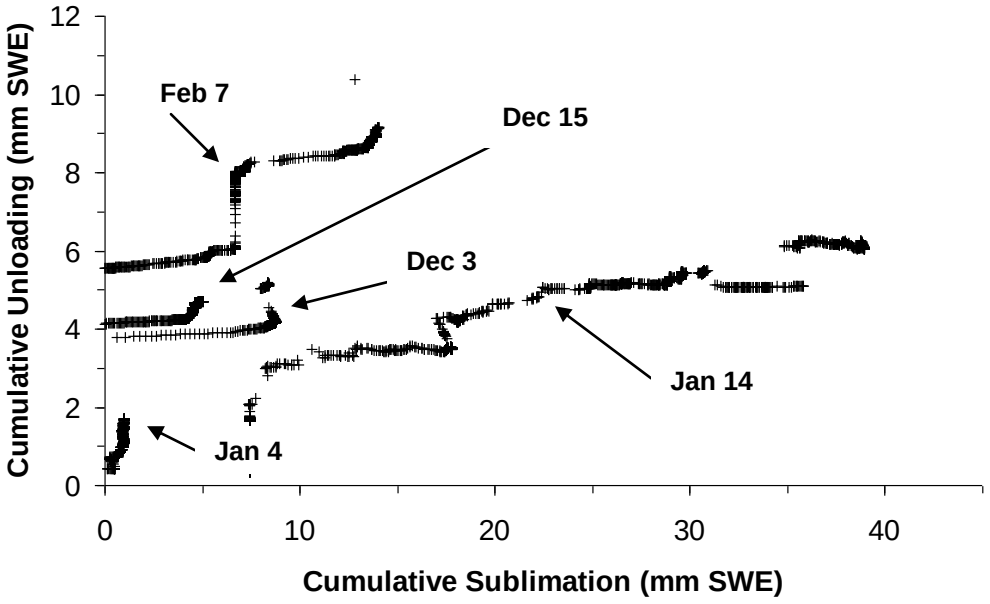

Figure 6.13. Cumulative unloading versus cumulative sublimation. Daily ratio of cumulative unloading to cumulative sublimation for unloading events.

Table 6.3. Linear relationship between ΣU and ΣS for unloading events.

DATE	∑U/∑S	r^2	p
December 3	0.044	0.91	0
December 15	0.12	0.54	0
January 4	1.30	0.60	0.27
January 14	0.24	0.78	0
February 7	0.16	0.41	0

ΣU/ΣS from each of the unloading events is depicted as an exponential decay function of time in Figure 6.14. Exponential decay functions are commonly used for their representation of natural process. A correlation was seen between time and ΣU/ΣS (r^2= 0.49). A simpler linear function was tested as well but did not increase the goodness of fit.

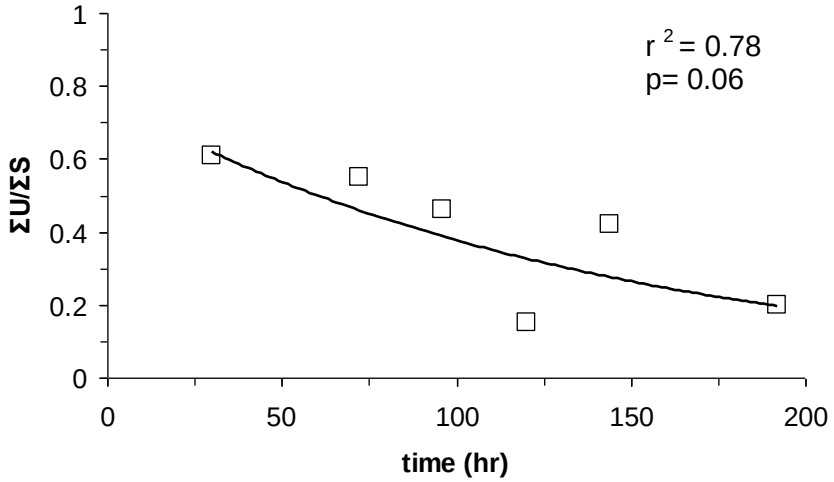

Figure 6.14. ΣU/ΣS as a function of time since interception has occurred.

The relationship between mid-canopy wind speed and ΣU/ΣS, during unloading events, showed good correlation (r^2 = 0.84) (Fig. 6.15). A limited number of data points means that there is a high degree of variation for wind speeds greater than 10 m s^{-1}.

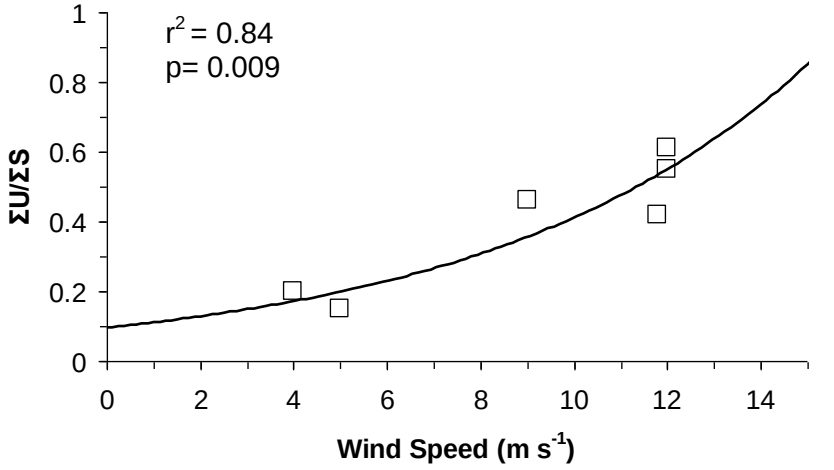

Figure 6.15. ΣU/ΣS as a function of mid-canopy wind speed.

The relationship between ΣU/ΣS during unloading events and air temperature was represented by an exponential function (Eq. 6.6) and had a correlation coefficient (r^2 = 0.88) (Fig. 6.16). The exponential function was chosen because the portion which is unloaded increases

dramatically as temperature approaches 0 ^{o}C. Unloading is negligible at temperatures < -20 ^{o}C and accounts for most canopy snow removal when the air temperature exceeds 3 ^{o}C.

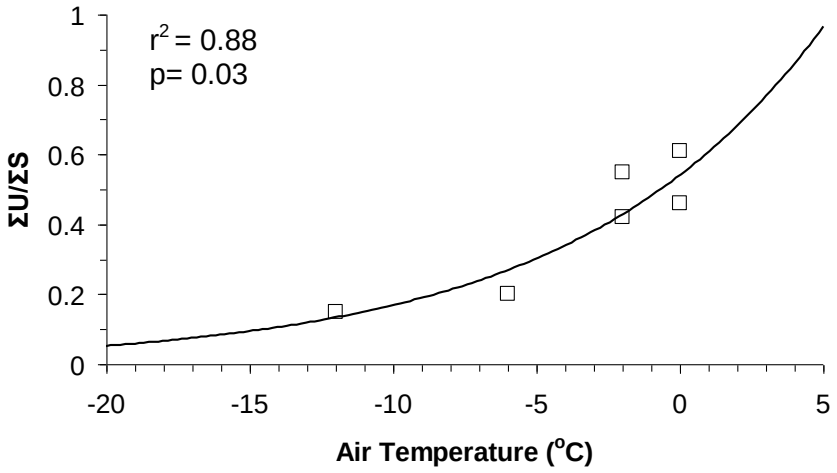

Figure 6.16. Relationship between ΣU/ΣS and canopy air temperature.

$$\frac{\Sigma U}{\Sigma S} = 0.541\ e^{0.116 T_a} \qquad \text{(Eq. 6.6)}$$

The rates of unloading and sublimation both increase during periods of high air temperatures (Storck *et al.*, 2002). As melt conditions are reached within the canopy snow load, unloading rates increase. The Gelfan *et al.* (2004) model calculates the rate of unloading based on the canopy load which has not already sublimated. The presence of unloading during periods of rapid sublimation controls the sublimation loss (Storck *et al.*, 2002).

Air temperature, mid-canopy wind speed, and time since snowfall are all related to the ratio of ΣU to ΣS, suggesting ΣU/ΣS may be estimated by multiple variables. Multiple step-wise regressions were conducted on the data to determine the correlations between the variables and ΣU/ΣS (Haan, 1977). Exponential values were chosen for the analysis to reflect the data because unloading responds as a time-decay function (Hedstrom and Pomeroy, 1998). The resulting equation for ΣU/ΣS based on wind speed (m s^{1}), temperature (^{o}C) and time (hr).

$$\frac{\sum U}{\sum S} = 0.19 + 0.326\, e^{T_a} + 2.22x10^{-6} e^{v} + 8.5x10^{-86} e^{t} \qquad \text{(Eq. 6.7)}$$

The equation has an r^2= 0.81 and a p value = 0.11. The effect of mid-canopy wind speed and time on the estimation was very small as can be seen by the regression coefficients (Eq. 6.7). Time since snowfall had a negligible effect on ΣU/ΣS, and can be eliminated from the analysis. The significance value increases to 0.02 when time was removed from the regression. Air temperature had the greatest control on the ratio of ΣU to ΣS. The low degree of control which mid-canopy wind speed and time since snowfall have on ΣU/ΣS can be explained by the presence of correlation between the independent variables. Wind speed, air temperature and time were found to be correlated and therefore not independent, meaning a multiple regression is not suitable for the data (Fig. 6.17).

Air temperature (r^2 = 0.23) and mid-canopy wind speed (r^2 = 0.45) were found to be correlated to time since snowfall. The relationship between mid-canopy wind speed and air temperature proved to be stronger (r^2=0.60), which explains why both mid-canopy wind speed and temperature displayed high correlation to ΣU/ΣS (Figs. 6.15 and 6.16). This suggests that mid-canopy wind speed and air temperature are related and are not independent.

Unloading was hypothesized to be a function of sublimation where changes in unloading rates are a function of sublimation rates and proportionality constant (K) (Eq. 6.8). The proportionality constant is represented by a function of air temperature based on air temperature having the strongest correlation to the ΣU to ΣS ratio. This integrates into the form of the equation (Eq. 6.9) which is used to represent the relationship of ΣU/ΣS and air temperature seen in Figure 6.16.

$$\frac{dU}{dt} = \frac{dS}{dt} K \qquad \text{(Eq. 6.8)}$$

$$\frac{dU}{dS} = K \qquad \text{(Eq. 6.9)}$$

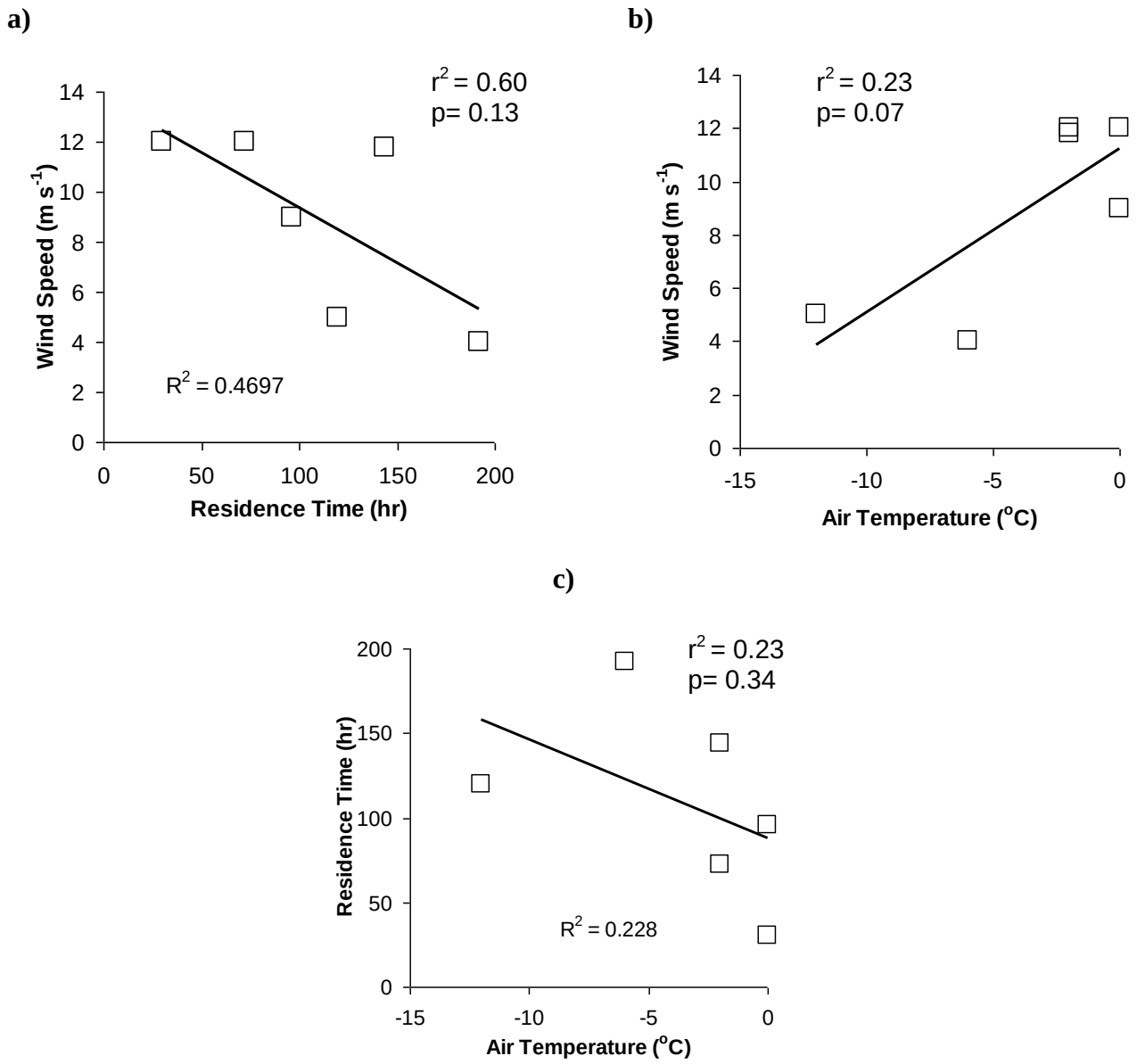

Figure 6.17. Correlation between the 'independent' variables.

A linear relationship may have been chosen for the temperature function due to its simplicity. The linear function had a lower degree of correlation (r^2= 0.75) to the ΣU to ΣS ratio. An exponential function was chosen to represent air temperature as it showed a stronger correlation (r^2= 0.88) than that of a linear relationship. Unloading processes such as branch

bending, act exponentially within the forest (Schmidt and Pomeroy, 1990). Application of a linear relationship would also mean no unloading at cold air temperatures (< -20 ^{o}C), whereas Hedstrom and Pomeroy (1998) observed unloading rates even at low air temperatures. Therefore, an exponential equation better represents the unloading process as seen by field observations and past research.

MCRB is frequented by Chinook winds which are associated with a strong warming trend, high wind speeds and lack of snowfall. In addition, heating of the canopy by solar radiation creates instability, meso-scale winds and gusty conditions. The Chinook conditions therefore are likely to be associated with substantial time since snowfall and high wind speeds as well as warm air temperatures. Inclusion of wind speed and time since snowfall in addition to air temperature increases the complexity of the model without adding to the predictive power of the function. A simple exponential function of temperature can then be applied for calculating ΣU as a percentage of ΣS. This model is attractive due to its simplicity as a low order equation with an adequate r^2.

Cumulative sublimation is a function of wind speed, temperature, humidity, canopy load and time since snowfall (Pomeroy and Gray, 1995). It can also be calculated as initial canopy load, L_i, less that which subsequently unloads (Eq. 6.10). By assuming that all canopy snow loss is partitioned into sublimation or unloading and temperature and time are inconsequential to this partitioning we can insert Equation 6.6 and 6.10 into Equation 6.9. Therefore, ΣU is calculated as a function of initial canopy load and subsequent air temperature, which allows unloading to be calculated on an event basis (Eq. 6.11).

$$\Sigma S = L_i - \Sigma U \qquad \text{(Eq. 6.10)}$$

$$\Sigma U = \frac{L_i e^{0.116 T_a}}{1.85 + e^{0.116 T_a}} \qquad \text{(Eq. 6.11)}$$

Sublimation losses within the intercepted snow act to weaken the snow structure. Snowpack metamorphism and the desiccation of bonds between snow crystals develop a granular structure to the intercepted snowpack under isothermal conditions. The result of these

mechanisms is a decrease in adhesion between the canopy snow and the branch structure and cohesion within the canopy snow load. Unloading of intercepted snow is then attributed to the decreased canopy snow structure and can be triggered by melt conditions or wind disturbances.

6.4 Model performance of the ΣU/ΣS ratio

The ΣU/ΣS model (Eq. 6.11) performs with 94.6% accuracy (RMSE = 2.13 mm SWE) on unloading events > 1.0 mm SWE. This level of accuracy was much higher than the other models. The Hedstrom-Pomeroy, Roesch *et al.,* and Bartlett models have accuracies of 84%, 80%, and <50% respectively. ΣU/ΣS model bias was 0.73 and is shown with respect to a 1:1 line (Fig. 6.18).

The largest discrepancy in modeled unloading was the snowfall event of March 18, 2007 where 90% of 10 mm SWE unloaded within 14 hr (Fig. 6.18). The air temperature during the unloading event averaged -5^{o}C (max = -3^{o}C), while mid-canopy wind speeds and incoming radiation were high.

The following are some limitations of the model: sublimation measurement; measurement techniques of changes in canopy load compared to unloading, and; scaling of the hanging-tree lysimeter. Sublimation was measured using a mass balance approach as the difference between canopy snow loss and unloading. The hanging-tree measured changes in canopy load at a single point, whereas unloading was observed in three hanging-lysimeters. Unloading is a much more spatially variable process than interception, meaning that the tree was not as representative of the former as the latter. A single event acting as an outlier may be a result of the location of the hanging-troughs in relation to sites where clumps of snow slide off the branches. It would require a high density of instrumentation in order to fully accommodate the variability in the unloading process.

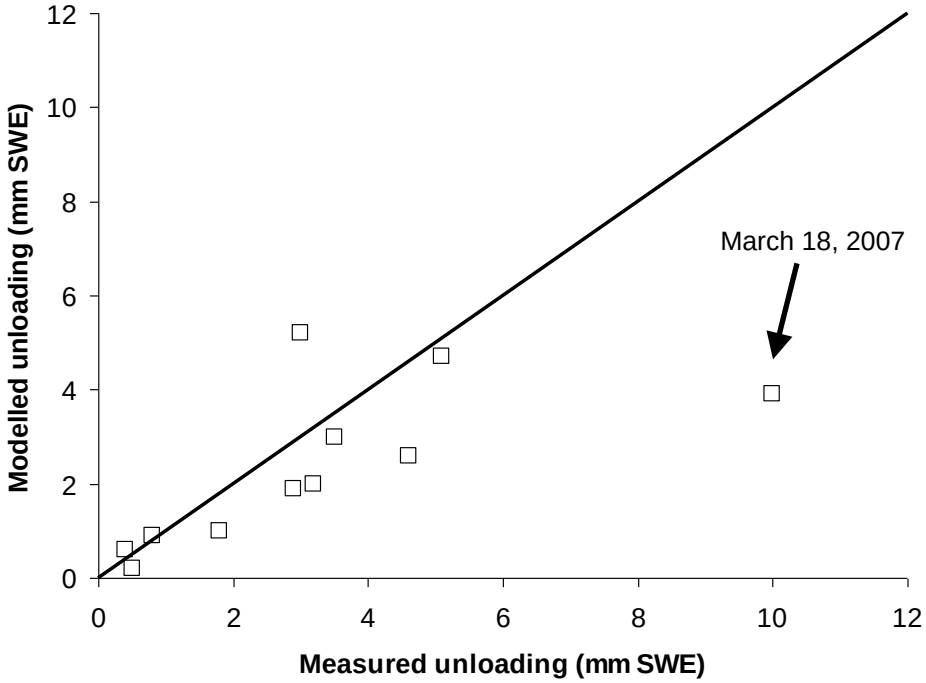

Figure 6.18. Performance of the ΣU/ΣS ratio for event based unloading estimates. The modelled results are shown with respect to a 1:1 line, and the March 18th, 2007 outlier is labelled.

The ΣU/ΣS model is different from other unloading models because it estimates unloading based on sublimation. The Hedstrom-Pomeroy model (1998) is based on a time decay function and initial canopy load, while the Roesch *et al.* model (2001) integrates meteorological variables. A comparison of the model performance statistics of standard error, RMSE and model bias is shown in Table 6.4. Statistically, the ΣU/ΣS model has the lowest standard error and lowest scatter of all the models, and has a lower model bias then the Roesch *et al.* model, but not the Hedstrom-Pomeroy model (Fig. 6.19). Although no direct relationship was found between unloading and wind, temperature, or time in MCRB, the relation to sublimation rates is very promising and integrates the cumulative energy status of the intercepted snow load.

Implementing the ΣU/ΣS model is very simple in hydrological models by using sublimation rates which are already being calculated. This method also follows the basic principles of the Gelfan *et al.* (2004) model whereby intercepted snow is first available to sublimation. After sublimation has occurred, what remains may unload. This supports the

hypothesis that sublimation has a role in the unloading process as it weakens the snow structure within the canopy load, although does not link sublimation to unloading rates directly. The influence of time was found to be negligible through non-linear multiple-regression. In an environment such as the Kananaskis Valley in the Rocky Mountains, Chinook events have a strong control on unloading because of coincidental fluctuations in air temperature and wind speed. Environments such as the boreal forest would not be expected to behave similarly.

Table 6.4. Unloading model output comparative statistics.

Unloading Model	Standard Error (%)	RMSE (mm SWE)	Model Bias
∑U/∑S	5	2.13	0.73
Hedstrom-Pomeroy	16	3.40	0.59
Roesch	20	2.72	0.93
Bartlett	52	4.80	1.33

Advantages of the ΣU/ΣS model are its simplicity and physical basis. A function describing ΣU/ΣS based on air temperature was created and is useful for estimating unloading due to its simplicity (Eq. 6.6). Describing ΣU/ΣS using the additional variables of wind speed and time since snowfall was not found to increase the predictive capacity of the model. The justification for eliminating wind speed and time since snowfall in the ΣU/ΣS model is based on the difficulty in obtaining data for these variables. Measurements of wind speed are usually taken in forest clearings and are not representative of the forest canopy. Measurements of winter precipitation are far less common than those of air temperature and difficult to extrapolate in mountain environments. Air temperature on the other hand, is easily measured and can be extrapolated using lapse rates.

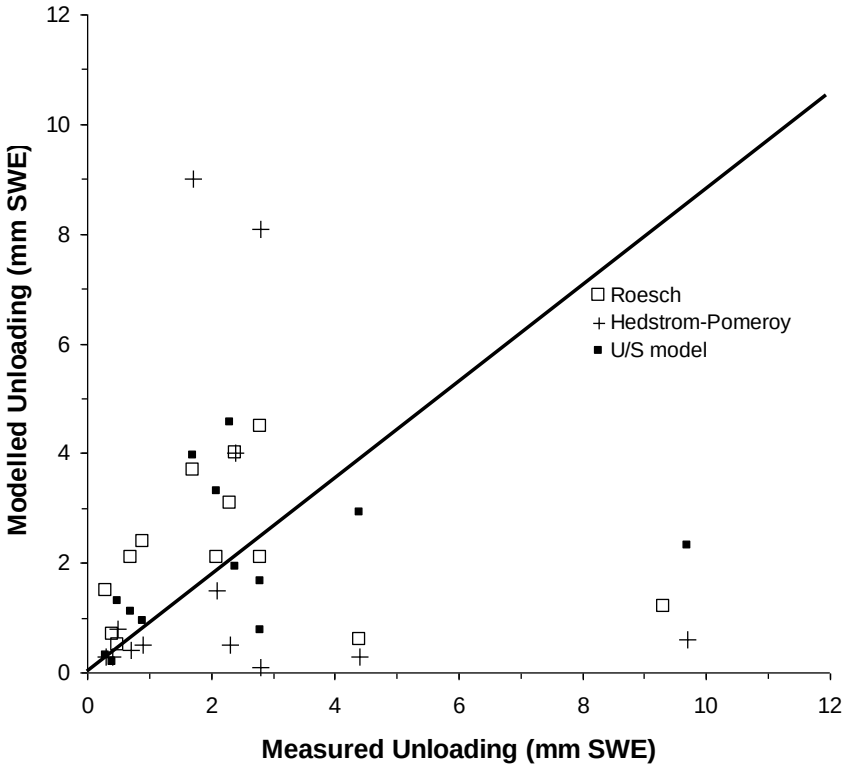

Figure 6.19. Comparison of unloading model performance.

CHAPTER 7

SUMMARY & CONCLUSIONS

Interception in Marmot Creek Research Basin dramatically affected snow accumulation processes by reducing the influx of snow to the forest floor by 60%. The forest canopy intercepted snowfall unloaded on approximately half of the snowfall events. The maximum canopy load observed on the hanging-tree lysimeter was 21.6 mm SWE, interception efficiency ranged from 29% to 71% with an average value of 60 %.

Unloading was observed on 11 of the 15 most significant interception events (>1 mm SWE), and decreased the canopy load by 42%. Unloading events limit the amount of snow available to sublimate while stored in the canopy. The net interception loss was 36% in MCRB once unloading had occurred. The largest magnitude unloading event was 90% of the canopy load and occurred in only 14 hr. Meteorological conditions during unloading events were characterized by average temperatures of approximately -4 ^{o}C and average gust factors of 5 (max= 10).

Meteorological conditions were distinct between the two winters of data collection. Winter 06/07 had an average daily wind speed of 3.9 m s^{-1} and an average daily temperature -5.4 ^{o}C. Winter 07/08 saw extremes in average daily temperatures (min= -31^{o}C) with an average daily temperature over the entire winter of -6.9 ^{o}C. Average daily wind speeds for winter 07/08 were 3.6 m s^{-1}. Melt conditions in the forest were present on 14 days in 06/07 and 10 days in 07/08. Residence times of intercepted snow ranged from the most rapid events where unloading occurred in <8 hr, to events which stored intercepted snow for as many as 9 days (216 hr).

Existing unloading models were unsuccessful at depicting the unloading process in MCRB (Fig. 6.19). The Hedstrom and Pomeroy (1998) model has a model bias of 0.60 (standard error 16%) and the Barlett *et al.* (2006) adaptation on the Hedstrom and Pomeroy model overestimated unloading (model bias =1.34, standard error = 52%). These models are based on an exponential decay function of time and cannot accommodate physical mechanisms which trigger unloading through mass release. The predominant method of transferring snow from the canopy to surface are melt conditions and turbulent wind bursts which trigger increased rates of unloading. Turbulent wind bursts operate on shorter time scales than those of existing

models. The Hedstrom and Pomeroy (1998) and Bartlett *et al.* do not incorporate air temperature or melt condition and therefore lack the ability to model unloading events which occur rapidly. The Roesch *et al.* (2001) model is the most complex and parameterized model and encompasses the effects of air temperature and wind speed. The model had a standard error of 20% and a model bias of 0.93 in MCRB. The Roesch et al. model does capture the timing of unloading well through the temperature function but the wind speed component is inadequate. Calibration of the Roesch et al. model did not increase accuracy of the model when the coefficients of wind and temperature were altered.

A relationship between canopy load and unloading rates in MCRB is supported by Equation 6.11, which depicts unloading (over a given time-step) as a function of inital canopy load and time. Hypothesis 1 is therefore accepted on the observations at MCRB.

Hypothesis 2 is supported by the data and therefore accepted. Analysis at MCRB did not show a direct link between unloading rates and meteorological conditions. There was in fact a link between meteorological conditions and the partitioning of canopy snow load to either sublimation or unloading. Relationships were present between the $\sum U/\sum S$ ratio and wind speed, storage time within the canopy and air temperature. The $\Sigma U/\Sigma S$ ratio was found best related to air temperatures through an exponential function in MCRB. Application of the $\Sigma U/\Sigma S$ model performed better than the other unloading models with a standard error of 5% (RMSE = 2.13 mm SWE) (Fig. 6.19). The $\Sigma U/\Sigma S$ ratio will allow for unloading to be better modelled in hydrological models for coupling of the unloading and sublimation process in hydrological models.

Association of unloading and sublimation as canopy snow loss processes has been suggested and used in models/studies of Gelfan *et al.* (2004) and Storck *et al*. (2002). Sublimation may act to destroy the adhesive and cohesive bonds within the intercepted snow, thus weakening overall snow structure. Trigger mechanisms such as wind gusts or melt conditions within the canopy would then be able to increase rates of unloading. Further studies would be needed in order to quantitatively support this statement.

These results agree with the study of Gelfan *et al.* (2004), which associates unloading and sublimation rate. Further research into the unloading process should focus on the role of relative humidity as it is the controlling factor of sublimation rate. It is known that atmospheric

water vapour pressure is an important term in the energy balance and it has been suggested that it influences the partitioning of energy from sublimation to unloading (Gelfan *et al.* 2004).

The ΣU/ΣS model should be carefully tested before being applied to other environments. The relationships found were dependent on sublimation rates and air temperatures, which are controlled primarily by the occurrence of Chinook events and therefore may not be applicable to environments where high air temperature events occur without high wind speeds. The strength of the ΣU/ΣS model is its simplicity and that it can be used within hydrological and land surface models by calculating unloading as a function of sublimation or in field based studies that focus on event-based data.

CHAPTER 8

REFERENCES

Andreadis A.M., Storck P. and Lettenmaier D.P. (2009) Modeling snow accumulation and ablation processes in forested environments. *Water Resources Research.* 45(5): W05429

Bailey W.G., Oke T.R., and Rouse W.R. (1997) *Surface Climates of Canada*. McGill Queens, Canada

Bartlett P.A., MacKay M.D., and Verseghy D.L. (2006) Modified snow algorithms in the Canadian Land Surface Scheme: model runs and sensitivity analysis at three boreal forest stands. *Atmosphere-Ocean*. 43(3): 207-222

Betts, A. K., and Ball J. H. (1997) Albedo over the boreal forest, *J. Geophys. Res.*, 102(D24), 28,901–28,909

Calder I.R. and Rosier P.T.W. (1976) The design of large plastic-sheet net-rainfall gauges. *Journal of Hydrology*. 30:403-405

Chen J.M. (1996) Optically-based methods for measuring seasonal variation of leaf area index in boreal conifer stands. *Agricultural and Forest Meteorology.* 80: 135-163

Chen J.M. and Black T.A. (1992) Determining leaf area index for non-flat leaves. *Plant, Cell and Environment.* 15: 412-429

Essery R., Pomeroy J., Parviainen J., Storck P. (2003) Sublimation of snow from coniferous forests in a climate model. *Journal of Climate.* 16:1855-1864

Frazer, G. W., Canham, C. D. and K. P. Lertzman. (2000) Gap Light Analyzer (GLA), Version 2.0. Technical Tools. Bulletin of the Ecological Society of America, pp. 191-197.

Gelfan A.N., Pomeroy J.W. and Kuchment L.S. (2004) Modelling forest cover influences on snow accumulation, sublimation and melt. *Journal of Hydrometeorology*. 5:785-803

Goodison B.E., Louie P.Y.T. and Yang D. (1998) WMO Solid Precipitation Measurement Intercomparison: Final Report. WMO/TD no 872.

Haan C.T. (1977) *Statistical methods in hydrology.* The Iowa State Press. Iowa, U.S.A.

Hancock N.H. and Crowther J.M. (1979) A technique for the direct measurement of water storage on a forest canopy. *Journal of Hydrology*. 41:105-122

Harding R.J. and Pomeroy J.W. (1996) The energy balance of the winter boreal landscape. *Jounral of Climate.* 9: 2778-2787

Hedstrom N. and Pomeroy J. (1998) Measurements and modelling of snow interception in the boreal forest. *Hydrological Processes.* 12:1611-1625

Holst T., Hauser S., Kirchgabner A., Matzarakis A., Mayer H., and Schindler D. (2004) Measuring and modelling plant area index in beech stands. *International Journal of Biometeorology.* 48: 192-201

Hoover M.D. and Leaf C.F. (1967) Process and significance of interception in Colorado subalpine forest in *Forest Hydrology.* Sopper W.E. and Lull H.W. (eds), Pergamon Press, New York. 213-223

Hsu S.A. and Blanchard B.W. (2004) Estimating overwater turbulence intensity from routine gust-factor measurements. *Journal of Applied Meteorology*. 43: 1911-1916

Liston G.E. and Elder K. (2006) A distributed snow-evolution modelling system (SnowModel). *Journal of Hydrometeorology.* 7: 1259-1276

Lundberg A. (1993) Evaporation of intercepted snow- review of existing and new measurement methods. *Journal of Hydrology.* 151: 267-290

Lundberg A. and Halldin S. (1999) Snow measurement techniques for land-surface atmosphere exchange studies in boreal landscapes. *Theoretical and Applied Climatology.* 20: 215-230

Lundberg A. and Koivusalo H. (2003) Estimating winter evaporation in boreal forests with operational snow course data. *Hydrological Processes.* 17: 1479-1493

Lundberg A., Nakai Y., Thunehed H. and Halldin S. (2004) Snow accumulation in forests from ground and remote-sensing data. *Hydrological Processes.* 18:1941-1955

MacDonald J.P. and Pomeroy J.W. (2007) Gauge undercatch of two common snowfall gauges in a prairie environment. *Proceedings of the 54th Eastern Snow Conference. 119-126*

McKay M.D. and Bartlett P.A. (2006) Estimating canopy snow unloading timescales from daily observations of albedo and precipitation. *Geophysical Research Letters.* 33: L19405

McNay R.S., Peterson L.D. and Nyberg J.B. (1988) The influence of forest stand characteristics on snow interception in the coastal forests of British Columbia. *Canadian Journal of Forest Research.* 18: 566-573

Miller (1962) Snow in the trees – where does it go? *Proceedings of the 62nd Western Snow Conference.* 21-27

Montesi J., Elder K., Schmidt R.A. and Davis R.E. (2004) Sublimation of intercepted snow within a subalpine forest canopy at two elevations. *Journal of Hydrometeorology – special section*. 5: 763-773

Nakai Y., Sakamoto T., Terajima T., Kitahara H., Saito T. (1994) Snow interception by forest canopies: weighing a conifer tree, meteorological observation and analysis by the Penman-Monteith formula. IAHS Publication 223:227-236

Perla R.I. and Martinelli J. (1976) Avalanche Handbook. Agricultural Handbook 489 Rocky mountain forest and range experiment station, USDA Forest Service, Fort Collins.

Pomeroy J.W. and Brun E. Physical Properties of Snow in Jones *et al.* (2001) *Snow Ecology: an interdisciplinary examination of snow-covered ecosystems*. Cambridge Press, USA

Pomeroy J.W. and Dion K. (1996) Winter radiation extinction and reflection in a boreal pine canopy: measurements and modeling. *Hydrological Processes.* 10: 1591-1608

Pomeroy J.W. and Gray D.M. (1995) Snowcover: accumulation, relocation and management. National Hydrology Research Institute, Science Report no. 7. Saskatoon, Environment Canada.

Pomeroy J.W., Gray D.M., Brown T., Hedstrom N.R., Quinton W.L., Granger R.J., and Carey S.K. (2007) *Hydrological Processes*. 21: 2650-2667

Pomeroy J.W., Gray D.M., Hedstrom N.R., and Janowicz R. J. (2002) *Prediction of seasonal snow accumulation in cold climate forests.* Hydrological Processes. 16: 3543-3558

Pomeroy J.W., Parviainen J., Hedstrom N. and Gray D.M. (1998) Coupled modeling of forest snow interception and sublimation. *Hydrological Processes.* 12:2317-2337

Pomeroy J.W. and Schmidt R.A. (1993) The use of fractal geometry in modelling intercepted snow accumulation and sublimation. *Proceedings of the 61st Western Snow Conference.* 1-10

Roesch A., Wild M., Gilgen H. and Ohmura A. (2001) A new snow cover fraction parameterization for the ECHAM4 GCM. *Climate Dynamics*. 17: 933-946

Rutter N., Essery R., Pomeroy J., and 48 others (2009) Evaluation of forest snow processes models (SnowMIP2). *Journal of Geophysical Research.* 114: DO6111

Schmidt R.A. (1990) Sublimation of snow intercepted by an artificial conifer. *Agricultural and Forest Meteorology.* 54:1-27

Schmidt R.A. and Gluns D.R. (1991) Snowfall interception on branches of three conifer species. Canadian Journal of Forest Research. 21:1262-1269

Schmidt R.A., Jairell and Pomeroy J.W. (1988) Measuring snow interception and loss from an artificial conifer. *Proceedings of the 56th Western Snow Conference.* 166-169

Schmidt R.A. and Pomeroy J.W. (1990) Bending of a conifer branch at subfreezing temperatures: implications for snow interception. *Canadian Journal for Forest Research.* 20:250-1253

Schmidt R.A. and Troendle C.A. (1989) Snowfall into a forest and clearing. *Journal of Hydrology*. 110: 335-348

Sellier D., Brunet Y., and Fourcaud T. (2008) A numerical model of tree aerodynamic response to a turbulent airflow. *Forestry* 81(3): 279-297

Storck P., Lettenmaier D., and Bolton S. (2002) Measurement of snow interception and canopy effects on snow accumulation and melt in a mountainous maritime climate, Oregon, United States. *Water Resources Research*. 38(11):1223

Suzuki K. and Nakai Y. (2008) Canopy snow influence on water and energy balances in a coniferous forest plantation in northern Japan. *Journal of Hydrology.* 352: 126-138

Swanson R.H. (1977) The Alberta watershed research program 1959-1977. In Swanson R.H. and Logan P.A. *Proceedings from the Symposium for the Alberta Watershed Research Program.* Fisheries and Environment Canada, Forestry Service Report NOR-X-176

Troendle C.A. (1987) Effect of clearcutting on streamflow generating processes from a subalpine forest slope. *Forest Hydrology and Watershed Management*. 167: 545-552

Troendle C.A., Schmidt R.A. and Martinez M.H. (1988) Snow deposition processes in a forest stand with a clearing. *Proceedings of the 56th Western Snow Conference.* 78-86

U.S. Army Corps of Engineers. (1956) Snow Hydrology: Summary Report of the Snow Investigations. North Pacific Division, USACE. Oregon, U.S.A.

Woods S.W., Ahl R., Sappington J. and McCaughey W. (2006) Snow accumulation in thinned lodgepole pine stands, Montana, USA. *Forest Ecology and Management*. 235:202-211

Yamazaki T., Fukabori K. and Kondo J. (1996) Albedo of forest with crown snow. *Journal of the Japanese Society for Snow and Ice.* 58:11-18

APPENDIX A – Instrument calibrations

Figure A.1. Geonor T-200B catch efficiency curve.

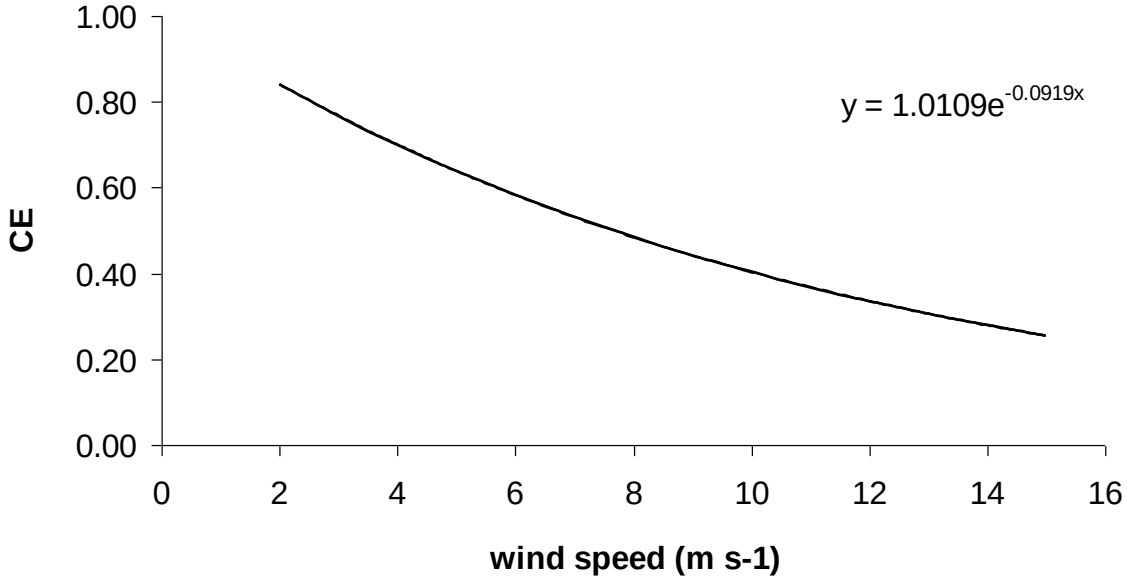

Figure A.2. Load cell calibration coefficients.

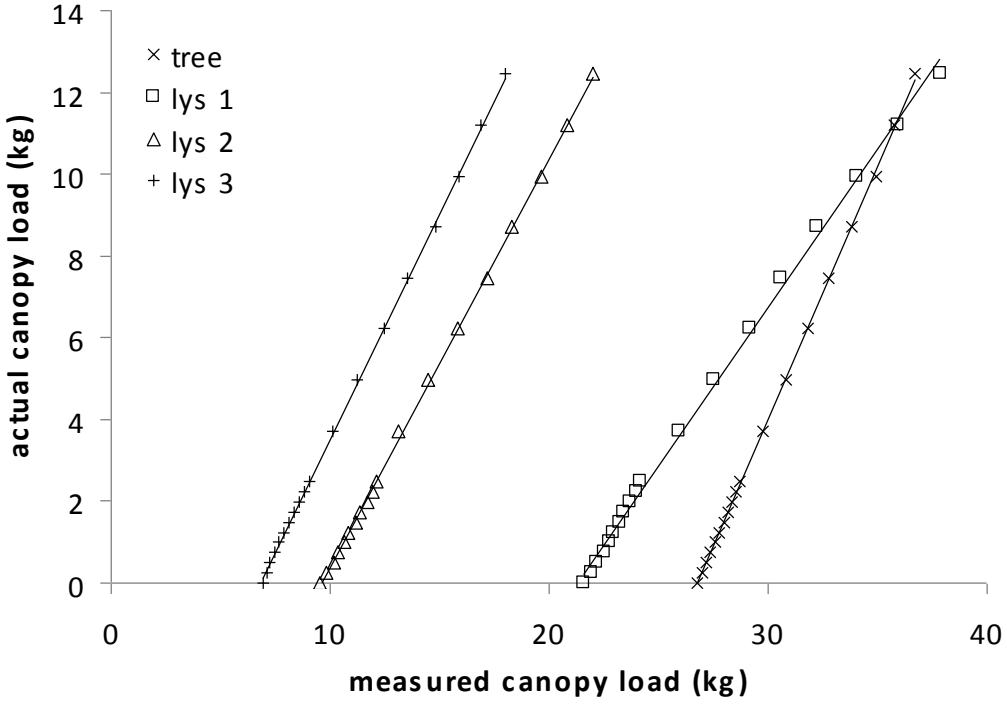

Trough 1
multiplier = 1.078
offset (tare weight) = 7.55 kg

Trough 2
multiplier = 0.999
offset (tare weight) 9.61 kg

Trough 3
multiplier = 0.775
offset (tare weight) = 16.53 kg

Tree
multiplier = 1.239
offset (tare weight) = 233.18 kg

Figure A.3. Upper Forest synthetic wind speed generation based on 06/07 values.

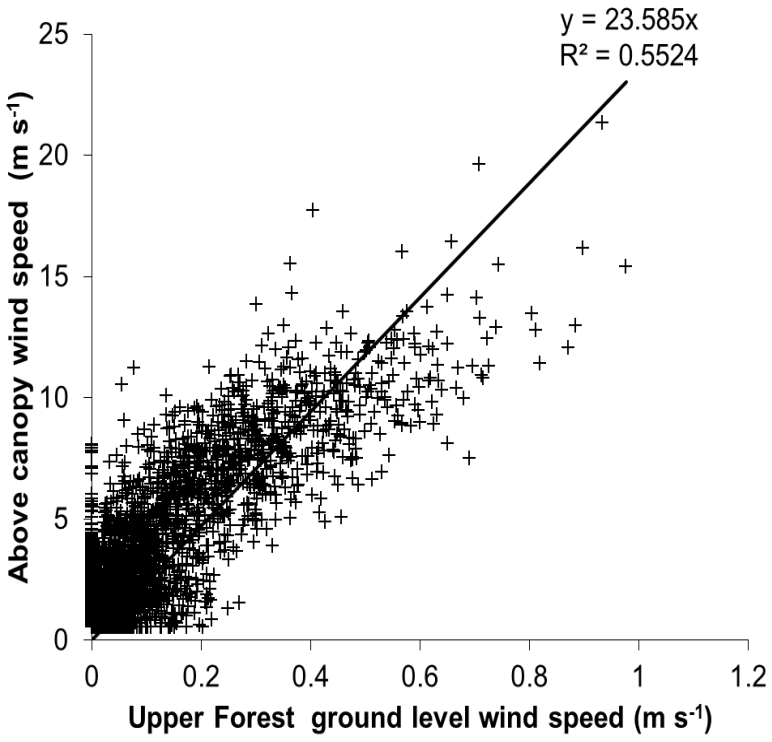

APPENDIX B – Unloading model intercomparison data

B.1. Hedstrom and Pomeroy (1998) unloading model.

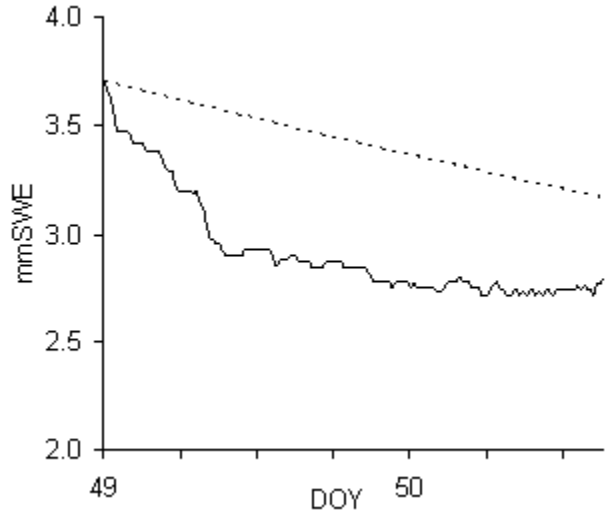

a) February 18, 2007

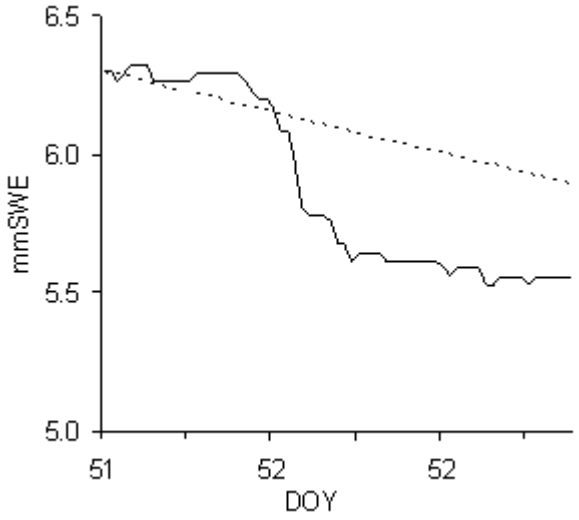

b) February 20(a)

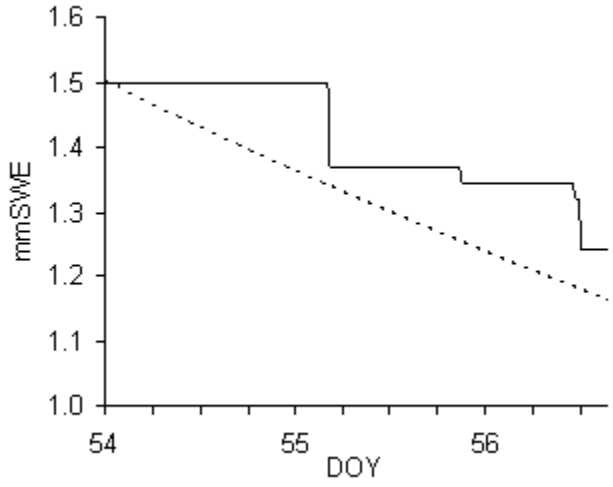

c) February 20(b)

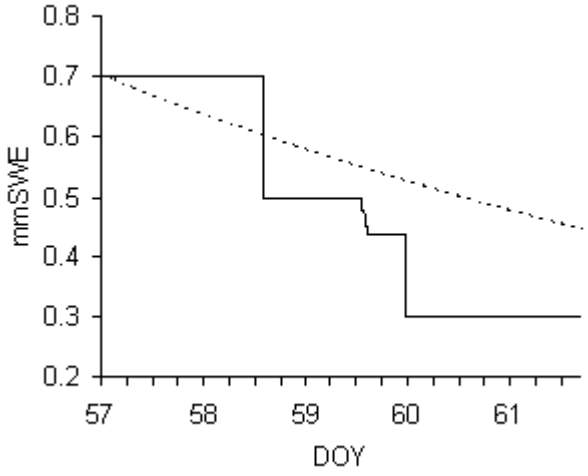

d) February 20(c)

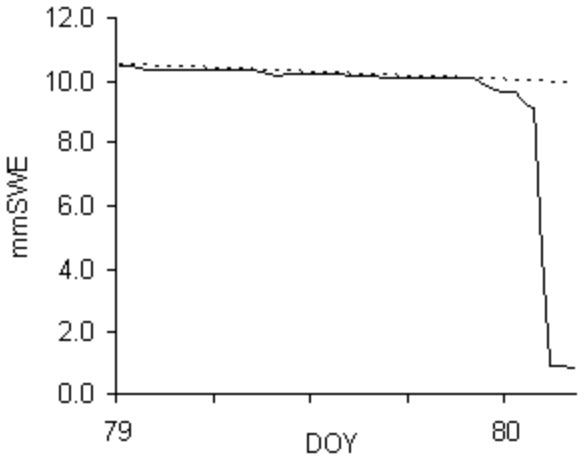

e) March 21, 2007

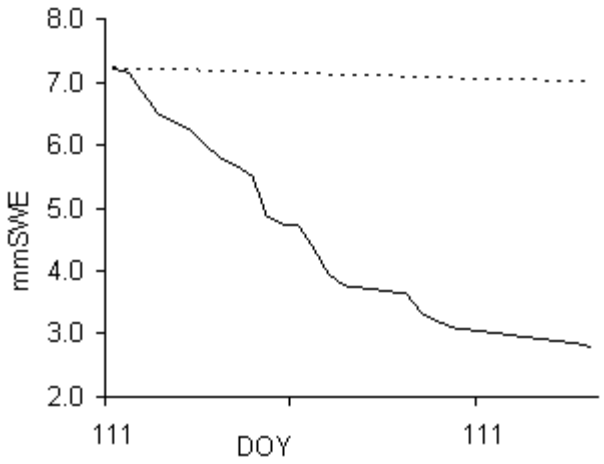

g) April 18, 2007

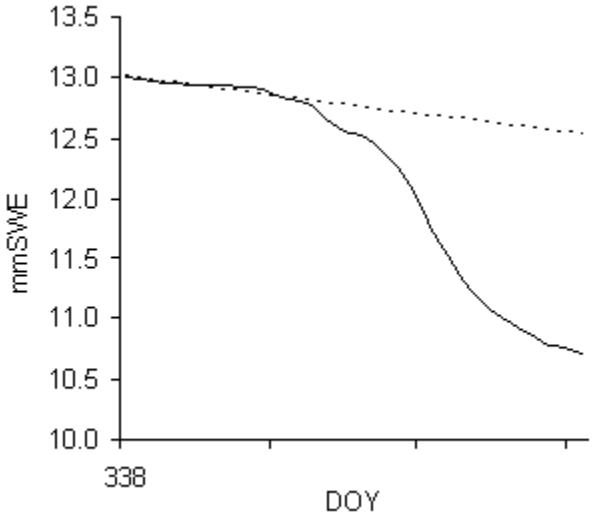

f) December 3, 2007

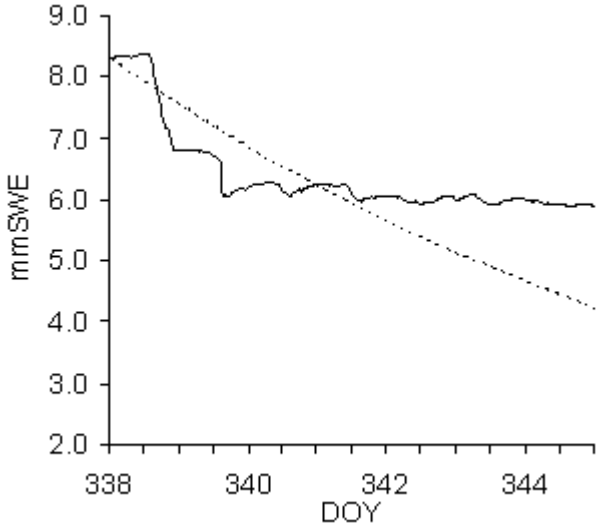

h) December 12, 2007

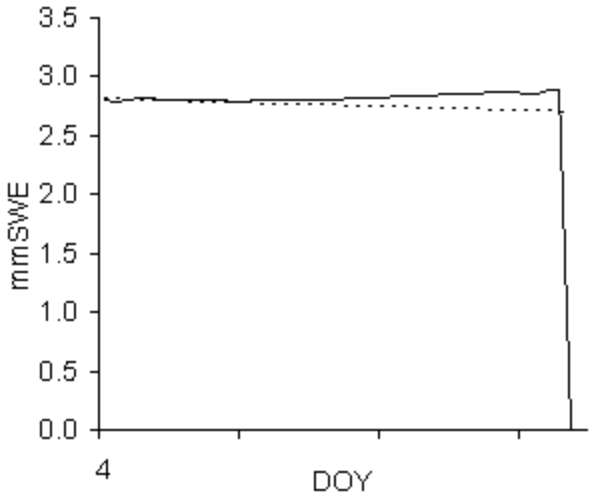

i) January 4, 2008

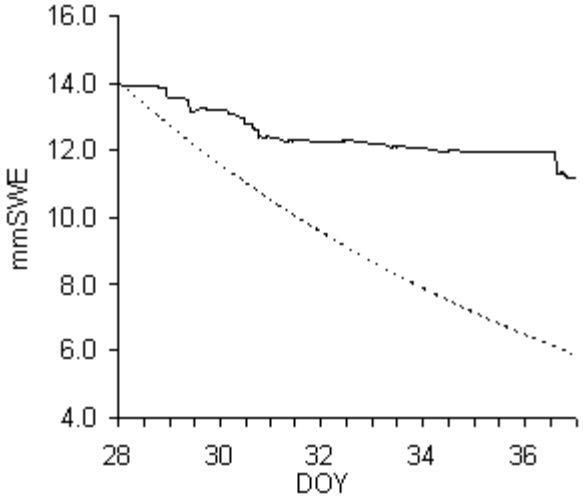

j) January 20, 2008

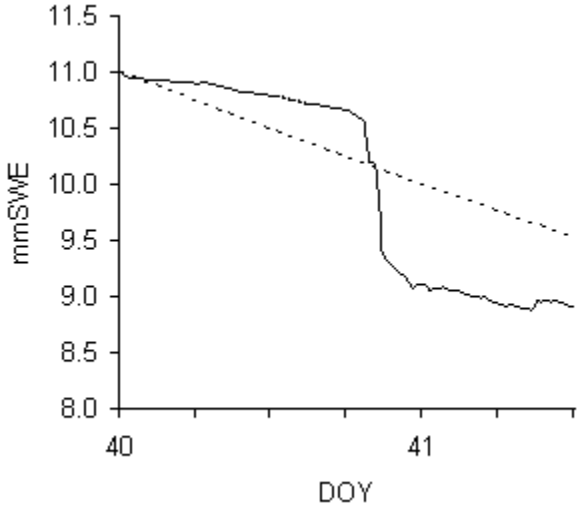

k) January 29, 2008

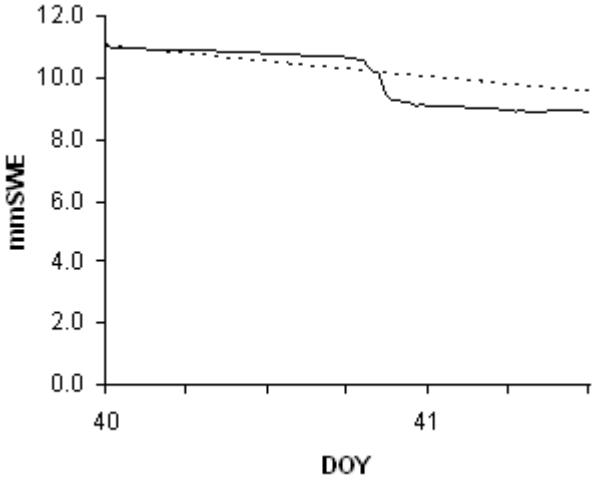

l) February 8, 2008

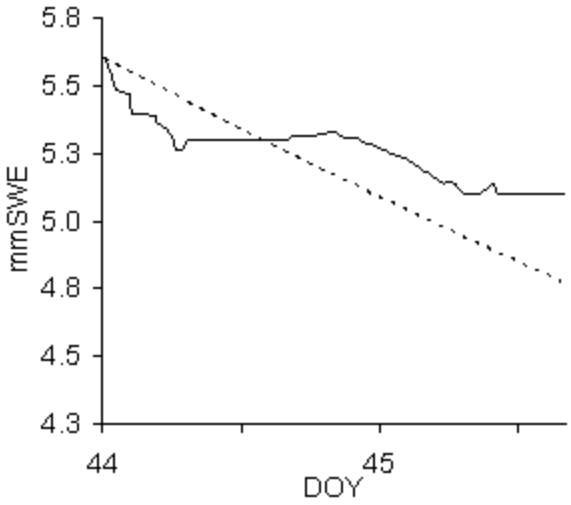

m) February 13, 2008

Figure B.1. Hedstrom and Pomeroy (1998) modeled unloading time series. Modelled output is shown as a dashed line and observed unloading as the solid line.

B.2. Roesch *et al.* (2002) model output

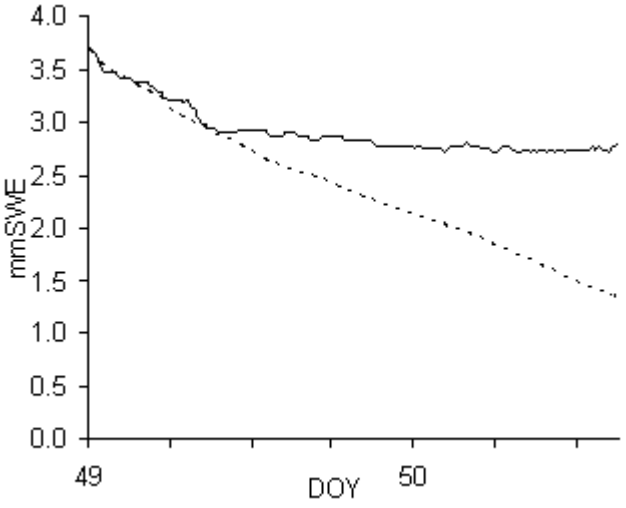

a) February 18, 2007

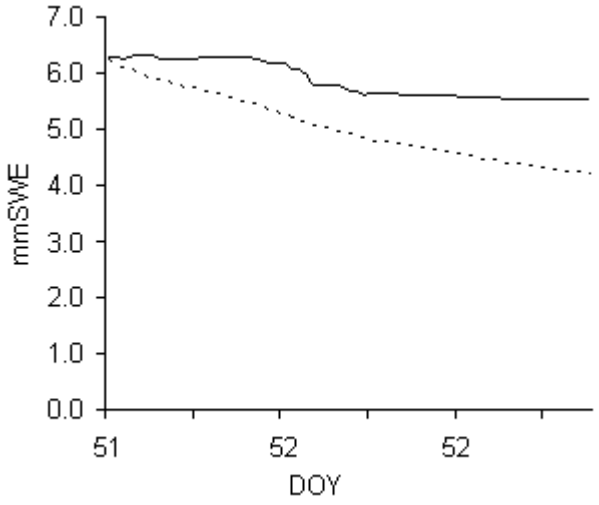

b) February 20(a)

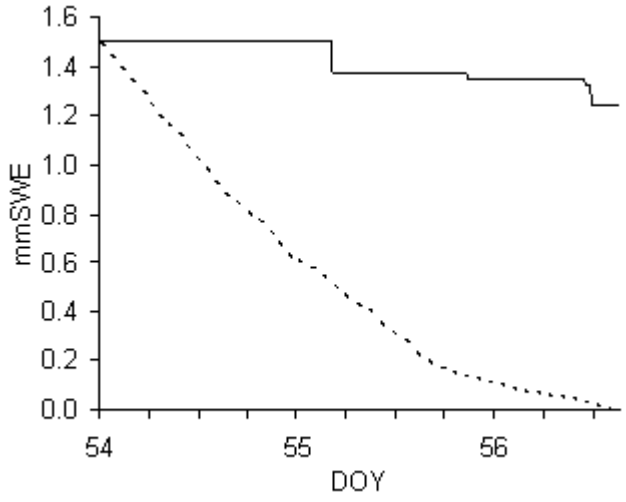

c) February 20(b)

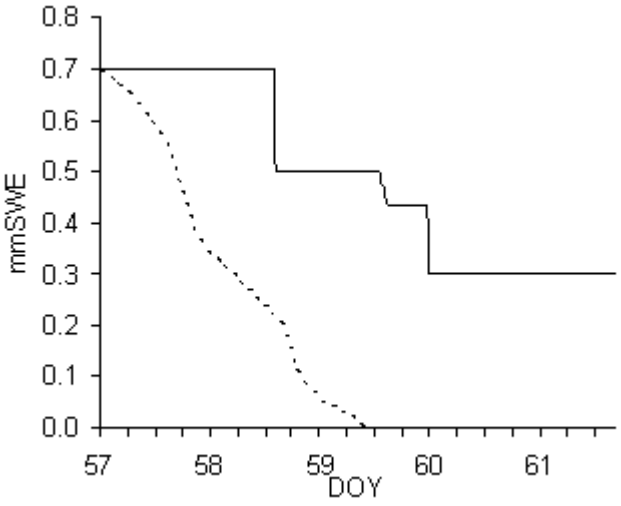

d) February 20(c)

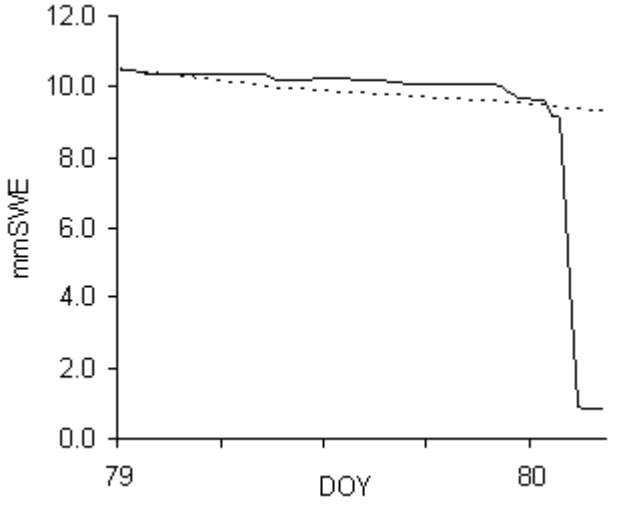

e) March 21, 2007

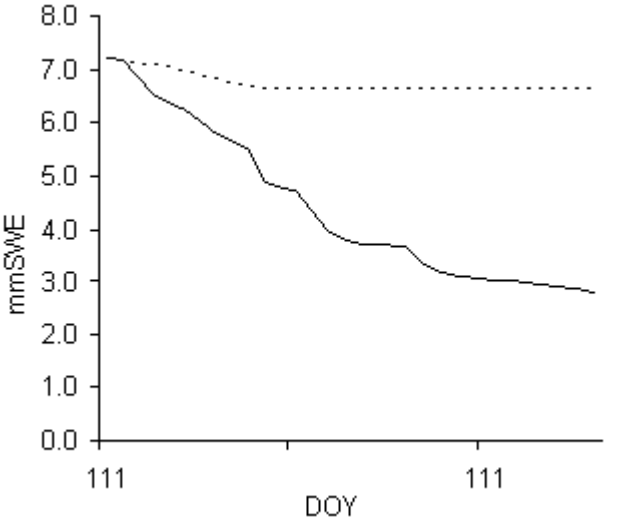

f) April 18, 2007

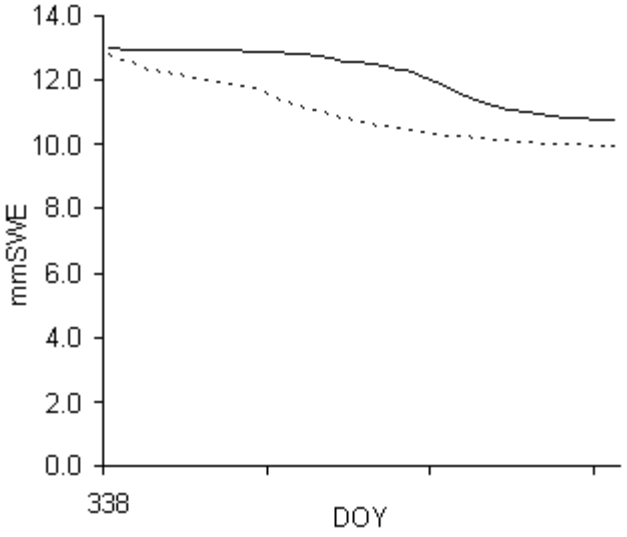

g) December 3, 2007

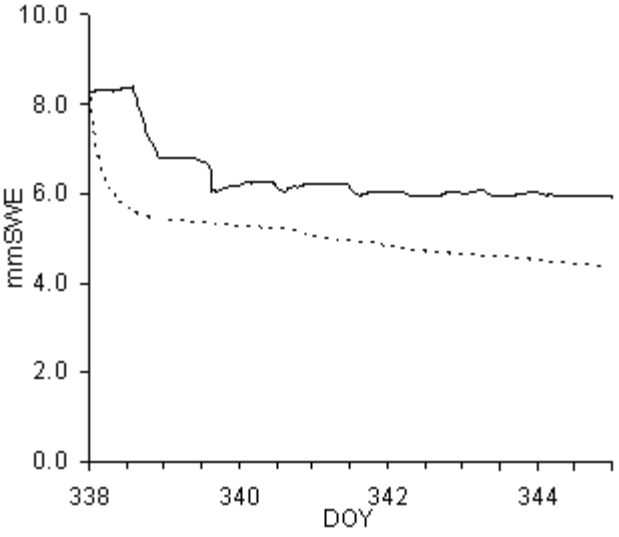

h) December 12, 2007

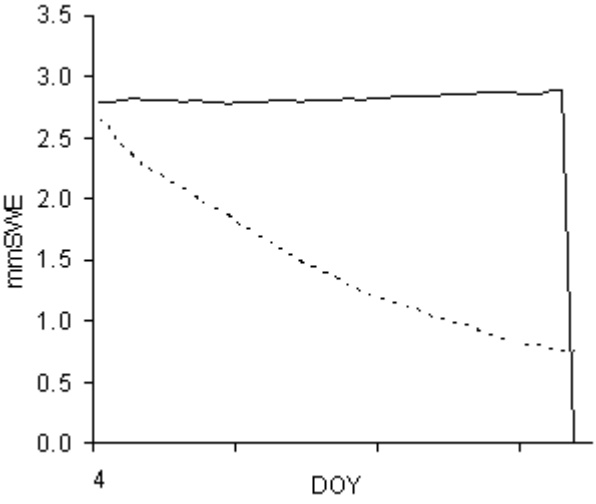

i) January 4, 2008

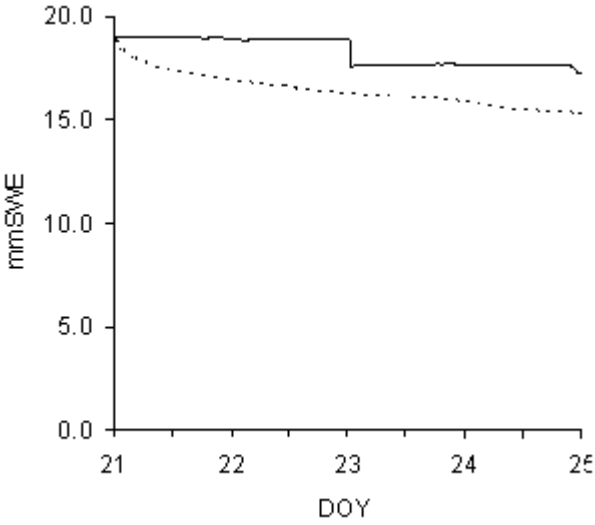

j) January 20, 2008

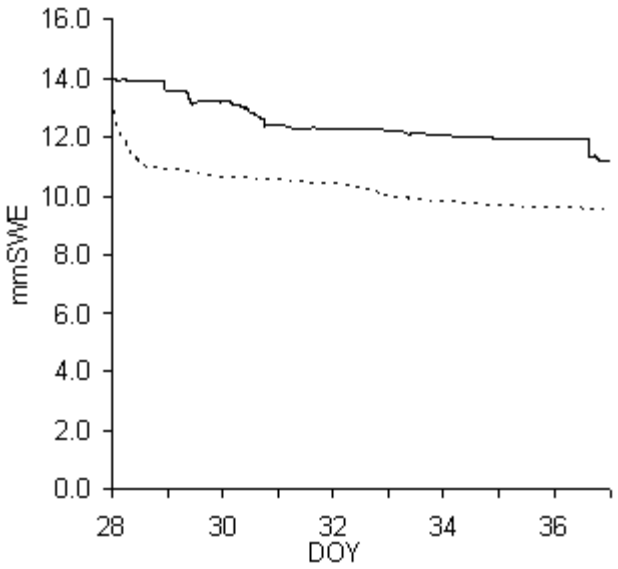

k) January 29, 2008

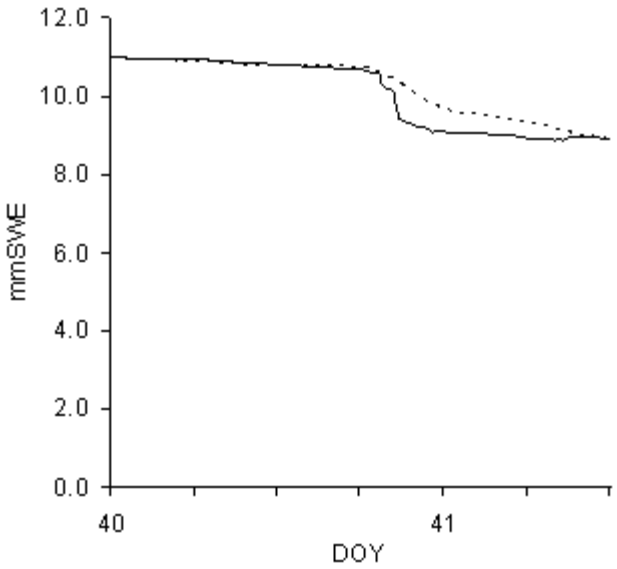

l) February 8, 2008

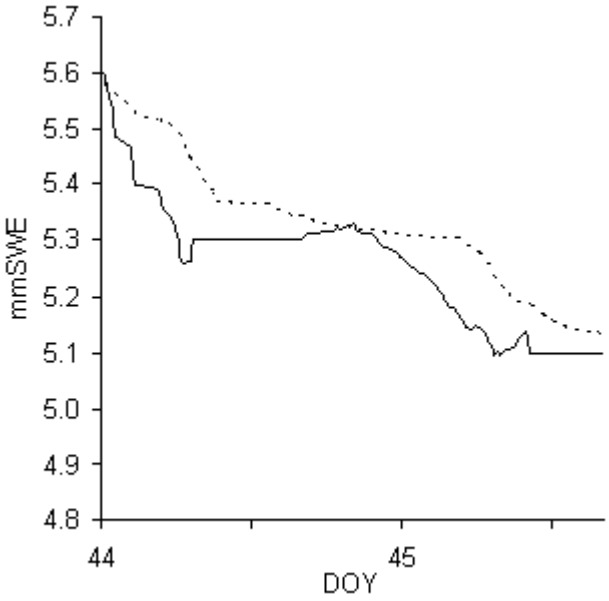

m) **February 13, 2008**

Figure B.2. Roesch et al. modeled unloading time series. Modelled output is shown as a dashed line and observed unloading as the solid line.